Center for Medical Physics and Biomedical Engineering
Medical University of Vienna

Austrian Society for Biomedical Engineering (ÖGBMT)

12th VIENNA INTERNATIONAL WORKSHOP ON FUNCTIONAL ELECTRICAL STIMULATION

Vienna, Austria, September 8th - 9th, 2016

Van Swieten Saal, Medical University, Vienna

PROCEEDINGS

ISBN 978-3-900928-12-4

Proceedings

of the

12*th* Vienna International Workshop on Functional Electrical Stimulation

Vienna, Austria
September 8th-9th, 2016

Edited by

Manfred Bijak
Winfried Mayr
Melitta Pichler

Published by

Center for Medical Physics and Biomedical Engineering
Medical University of Vienna, Vienna Medical School
AKH 4L
Waehringer Guertel 18-20
A-1090 Vienna
Austria

Tel.: +43-1-40400-19840
Fax: +43-1-40400-39880

http://www.fesworkshop.org
ISBN 978-3-900928-12-4

Scientific Committee

ALON Gad
AZEVEDO COSTE Christine
BERSCH Ines
CARRARO Ugo
CIUPA Radu
CLIQUET Jr Alberto
CRETU Mihaela
CREVENNA Richard
DANNER Simon
DAVIS Glen
FERRANTE Simona
FROTZLER Angela
GARGIULO Paolo
HELGASON Thordur
JARVIS Jonathan
KELLER Thierry
KNEISZ Lukas
KOCH Klaus Peter
KRENN Matthias
LINDENTHALER Werner
MANDL Thomas
MARTINEK Johannes
MEKJAVIC Igor
POPOVIĆ Dejan
QUITTAN Michael
RATTAY Frank
RUPP Ruediger
RUSSOLD Michael
SAUERMANN Stefan
SCHAUER Thomas
SCHMOLL Martin
SPAICH Erika G.
VARGAS LUNA José Luis
VELTINK Peter
WILLAND Michael

Table of Contents

MED-EL *Workshop:*
Functional Rejuvenation in Aging

MED-EL *Workshop:*
Electrical Stimulation in Neuromuscular Disorders

RETRAINER *Workshop with Hands on*

Session1: Basic Research

Session 2: Neuromodulation, Rehabilitation strategies

Session 3: FES Exercise

Session 4: Technologies, Engineering, Sensors

MED-EL *Workshop: Functional Rejuvenation in Aging*

The aging muscle: Changes in muscle morphology – A summary of the current knowledge

U. Carraro[1], H. Kern[2,3]

[1]Fondazione Ospedale San Camillo, Venezia-Lido, Italy
[2]Ludwig Boltzmann Institute of Electrical Stimulation and Physical Rehabilitation, Vienna, Austria
[3]Institute of Physical Medicine and Rehabilitation, Wilhelminenspital, Vienna, Austria

Abstract: *In a detailed review of literature, Mitchel et al.[1] state that "Changing demographics make it ever more important to understand the modifiable risk factors for disability and loss of independence with advancing age. For more than two decades there has been increasing interest in the role of sarcopenia, the age-related loss of muscle or lean mass, in curtailing active and healthy aging. There is now evidence to suggest that lack of strength, or dynapenia, is a more constant factor in compromised wellbeing in old age and it is apparent that the decline in muscle mass and the decline in strength can take quite different trajectories . This demands recognition of the concept of muscle quality, that is the force generating capacity per unit cross-sectional area (CSA). An understanding of the impact of aging on skeletal muscle will require attention to both the changes in muscle size and the changes in muscle quality. The aim of this review is to present current knowledge of the decline in human muscle mass and strength with advancing age and the associated risk to health and survival and to review the underlying changes in muscle characteristics and the etiology of sarcopenia. Cross-sectional studies comparing young (18–45 years) and old (>65 years) samples show dramatic variation based on the technique used and population studied. The median of values of rate of loss reported across studies is 0.47% per year in men and 0.37% per year in women. Longitudinal studies show that in people aged 75 years, muscle mass is lost at a rate of 0.64–0.70% per year in women and 0.80–00.98% per year in men. Strength is lost more rapidly. Longitudinal studies show that at age 75 years, strength is lost at a rate of 3–4% per year in men and 2.5–3% per year in women. Studies that assessed changes in mass and strength in the same sample report a loss of strength 2–5 times faster than loss of mass. Loss of strength is a more consistent risk for disability and death than is loss of muscle mass".*

Though authors spend several thousand of words to understand the cellular mechanisms of dynapenia, that is the decreased strength of aged muscle, three hypotheses are still to be proved or disproved (or weighted for the relative contribution): i) Intramuscular molecular and ultrastructural properties; ii) Muscle fibre adaptation/change in fibre type or number; iii) ratio of myofiber to extracellular connective tissues (including fascia and tendon properties). Surprisingly, the most obvious factor, the dependence of muscle fibre size and characteristics from innervating motor units is under looked. I will discuss all these factors (detailed described in the attached abstracts of relevant publications, in particular those of the Helmut Kern's group) with particular attention to neuro-muscular interactions as potential target for effects of Functional Electrical Stimulation (FES) on aged muscles. I would like to outline current understanding of the changes that occur in human skeletal muscles with age, describing changes in structure size and thus in function and then describe causes and potential interventions. The complex etiology and physio-pathology of mobility impairments due to aging ask for a multifactorial approach to delay this unavoidable process.[2] Beside volitional physical activity,[3-10] including Total-Body In-Bed Gym,[11] Functional Electrical Stimulation may be applied in case elderly persons are unable or reluctant to do them.[12]

Keywords: *skeletal muscle, aging, aging, muscle quality, strength, impact of denervation, FES and other interventions*

References

1. *Mitchell WK1, Williams J, Atherton P, Larvin M, Lund J, Narici M. Sarcopenia, dynapenia, and the impact of advancing age on human skeletal muscle size and strength; a quantitative review. Front Physiol. 2012 Jul 11;3:260. doi: 10.3389/fphys.2012.00260. eCollection 2012.*
2. *Gava P, Kern H, Carraro U. Age-associated power decline from running, jumping, and throwing male masters world records. Exp Aging Res. 2015;41(2):115-35. doi: 10.1080/0361073X.2015.1001648.*
3. *Frontera WR, Hughes VA, Fielding RA, Fiatarone MA, Evans WJ, Roubenoff R. Aging of skeletal muscle: a 12-yr longitudinal study. Appl Physiol 2000;88:1321-6.*
4. *Hepple RT, Rice CL. Innervation and neuromuscular control in ageing skeletal muscle. J Physiol. 2016 Apr 15;594(8):1965-78. doi: 10.1113/JP270561. Epub 2015 Dec 21.*
5. *Flack KD, Davy BM, DeBerardinis M, Boutagy NE, McMillan RP, Hulver MW, Frisard MI, Anderson AS, Savla J, Davy KP. Resistance exercise training and in vitro skeletal muscle oxidative capacity in older adults. Physiol Rep. 2016 Jul;4(13). pii: e12849. doi: 10.14814/phy2.12849.*
6. *Boncompagni S1, d'Amelio L, Fulle S, Fanò G, Protasi F. Progressive disorganization of the excitation-contraction coupling apparatus in aging human skeletal muscle as revealed by electron microscopy: a possible role in the decline of muscle performance. J Gerontol A Biol Sci Med Sci. 2006;61:995-1008.*
7. *Zampieri S, Pietrangelo L, Loefler S, Fruhmann H, Vogelauer M, Burggraf S, Pond A, Grim-Stieger M, Cvecka J, Sedliak M, Tirpáková V, Mayr W, Sarabon N, Rossini K, Barberi L, De Rossi M, Romanello V, Boncompagni S, Musarò A, Sandri M, Protasi F, Carraro U, Kern H. Lifelong physical exercise delays age-associated skeletal muscle decline. J Gerontol A Biol Sci Med Sci. 2015 Feb;70(2):163-73. doi: 10.1093/gerona/glu006. Epub 2014 Feb 18.*
8. *Mosole S, Carraro U, Kern H, Loefler S, Fruhmann H, Vogelauer M, Burggraf S, Mayr W, Krenn M, Paternostro-Sluga T, Hamar D, Cvecka J, Sedliak M, Tirpakova V, Sarabon N, Musarò A, Sandri M, Protasi F, Nori A, Pond A, Zampieri S. Long-term high-level exercise promotes muscle reinnervation with age. J Neuropathol Exp Neurol. 2014 Apr;73(4):284-94. doi: 10.1097/NEN.0000000000000032.*
9. *Kern H, Barberi L, Löfler S, Sbardella S, Burggraf S, Fruhmann H, Carraro U, Mosole S, Sarabon N, Vogelauer M, Mayr W, Krenn M, Cvecka J, Romanello V, Pietrangelo L, Protasi F, Sandri M, Zampieri S, Musaro A. Electrical stimulation counteracts muscle decline in seniors. Front Aging Neurosci. 2014 Jul 24;6:189. doi: 10.3389/fnagi.2014.00189. eCollection 2014.*
10. *Nishida MM, Tsuboyama T, Moritani T, Arai T. Review of the evidence on the use of electrical muscle stimulation to treat sarcopenia. Eur Geron 2016; doi:10.1016/j.eurger 2015.11.010.*
11. *Carraro U, Marcante A, Baba A, Piccione F Home-based Bed-Gym and FES in borderline mobility impairments: Fighting permanent or progressive muscle weakness by do-it- yourself, take-home strategy. Eur J Transl Myol - Basic Appl Myol 2016;26:27-8.*
12. *Carraro U, Kern H, Gava P, Hofer C, Loefler S, Gargiulo P, Mosole S, Zampieri S, Gobbo V, Ravara B, Piccione F, Marcante A, Baba A, Schils S, Pond A, Gava F. Biology of Muscle Atrophy and of its Recovery by FES in Aging and Mobility Impairments: Roots and By-Products. Eur J Transl Myol. 2015 Aug 25;25(4):221-30. doi: 10.4081/ejtm.2015.5272. eCollection 2015.*

Chronic neurostimulation for treatment of age related laryngeal muscular atrophy

M. Gugatschka[1], M. Karbiener[1], J. Perkins[2], C. Gerstenberger[1], J. Jarvis[3], G. Friedrich[1]

[1]ENT University Hospital Graz, Department of Phoniatrics, Medical University of Graz, Austria
[2]The Royal Veterinary College, Department of Clinical Sciences and Services, London, UK,'
[3]Faculty of Science, John Moores University, Liverpool, UK

Abstract: *Muscle atrophy as part of the ageing process also affects the larynx, where it constitutes the major cause of presbyphonia. Current treatment options are mainly conservative or phonosurgically based and are far from being satisfactory. Electrical stimulation of motor neurons constitutes a promising strategy.*
Materials and Methods: Using aged sheep as an animal model electrical chronic stimulation of laryngeal muscles was achieved via a mini-electrode that targeted the right recurrent laryngeal nerve (RLN; unilateral stimulation). Functional electrical stimulation (FES) implants were programmed to deliver a pattern able to evoke supramaximal muscle stimulation over a period of 29 days. At the end of the study, vocalis and posterior crico-arytenoid muscles were excised and analyzed molecularly and histologically. To quantify the expression levels of genes related to distinct muscle fiber types, a real-time PCR (RT-qPCR) analysis pipeline was newly established.
Results: First results showed a shift towards larger muscle fiber diameters of the stimulated side, compared to the unstimulated control side. Based on this, chronic electrical stimulation of the RLN can induce hypertrophy of the vocalis muscle even after a relatively short stimulation period of 29 days. Upcoming trials will focus on longer stimulation periods as well as more intense stimulation algorithms.

Keywords: *Ageing, muscle atrophy, larynx, electrical stimulation, animal model*

Studying the Effects of Functional Electrical Stimulation on the Thyro-arytenoid Muscle in Rats

M. Karbiener

ENT University Hospital Graz, Department of Phoniatrics, Medical University of Graz, Austria

Abstract: *Aim of the study was to induce muscular hypertrophy of the thyroarytenoid muscle (TAM) by functional electrical stimulation (FES) of the recurrent laryngeal nerve (RLN) in rats to counteract age related muscular atrophy. This can be a new treatment option for reversing the glottic gap as main feature of the presbylarynx. Conditioning patterns were determined in acute trials by exploring fatigue parameters of the TAM. For chronical trials, a cuff electrode was sutured unilaterally around the RLN and connected to a radio-frequency controlled implant fixated subcutaneously in the back region. A preliminary trial in younger rats (age: 5 months) was pursued to establish surgical and methodological procedures. Another trial employing older rats (age: 21 months) was done subsequently. Training patterns were delivered once daily without additional anaesthesia required for a period of 6 weeks. Myosin heavy chain analysis was performed by qPCR. After a short training period of six weeks we identified significant increases of mean feret diameter and TAM area when compared to an untreated age-matched control group. There was no change in the number of fibers and additionally no undesired fast-to-slow fibers twitch detectable. FES induced increases of muscle fibre diameters and can be a new treatment strategy to reverse the effects of laryngeal muscle atrophy.*

Keywords: *age related laryngeal muscle atrophy, glottic gap, dysphonia, functional electrical stimulation*

MED-EL *Workshop: Electrical Stimulation in Neuromuscular Disorders*

Optimization of waveform shapes for electrical neuromuscular stimulation based on conductive and displacement membrane currents

Kaniusas E, Kampusch S, Thürk F, Krenn M.
[1]Institute of Electrodynamics, Microwave and Circuit Analysis, Vienna University of Technology, Austria
kaniusas@tuwien.ac.at

Abstract: *Neuromuscular stimulation requires energy-efficient waveforms. An external stimulus is needed, which produces a dynamic conductive current above a certain threshold across the membrane of an excitable cell. Since the membrane acts also as a capacitor, a displacement current across the membrane necessarily associates this conductive current. The sum of both the displacement and conductive currents yields the external current stimulus. Thus the displacement current composes the reactive power of this stimulus, which does not contribute to neuromuscular excitation but does disadvantageously increase the total power/energy costs of the external stimulus. In order to render energy-efficient waveforms of the external stimulus, which is usually done on empirical basis, the conductive and displacement currents and their specific temporal behaviour are considered here within the scope of a simple membrane model to describe the membrane depolarization just before a subsequent action potential. The proposed methodology offers a simple theoretical basis and optimization guidelines for the design of energy-efficient waveform shapes of the external current stimulus.*

Keywords: *Neuromuscular stimulation, stimulation waveform, energy efficiency, displacement current*

Introduction

The energy-efficiency of the electrical neuromuscular stimulation, i.e., the excitation of nerve or muscle cells, is a crucial issue with respect to the size of neuromuscular wearable and implantable stimulators, and stimulation-induced local tissue damage. The size and operation duration of such stimulators are largely determined by the battery size which, in turn, is proportional to the total power and energy of electrical stimuli delivered via the stimulating electrodes. Thus, the better is the energy-efficiency of the stimulation, the longer is the stimulator's lifetime up to its expensive and invasive replacement after battery depletion. On the other hand, the tissue damage is determined by the total charge delivered during each stimulus [1] so that minimal energy but still excitatory parameters of the stimulus waveform are required.

Spatial and temporal parameters of the electrical stimulation waveforms determine neuromuscular excitation. In terms of space, for instance, transversal currents across the axon of an excitable cell are less likely to excite this cell than longitudinal currents of the same magnitude along the axon [2]. In terms of time, the shape of the stimulation waveform and especially its temporal dynamics govern the cell excitation and its threshold. The excitation requires a certain dynamics which is not too slow in order to override accommodation effects and not too fast to avoid both the refractory behaviour and non-depolarizing displacement currents draining the stimulators battery [3]. For instance, the excitatory depolarizing stimulus should be fast enough to open the relatively fast voltage-gated Na^+ channels depolarizing the cell membrane but not the relatively slow voltage-gated K^+ channels repolarising the membrane [3].

While the accessibility of spatial parameters for their energy-efficient optimization is hardly given, temporal parameters of the stimulation waveform are determined by engineers and thus are readily available for their

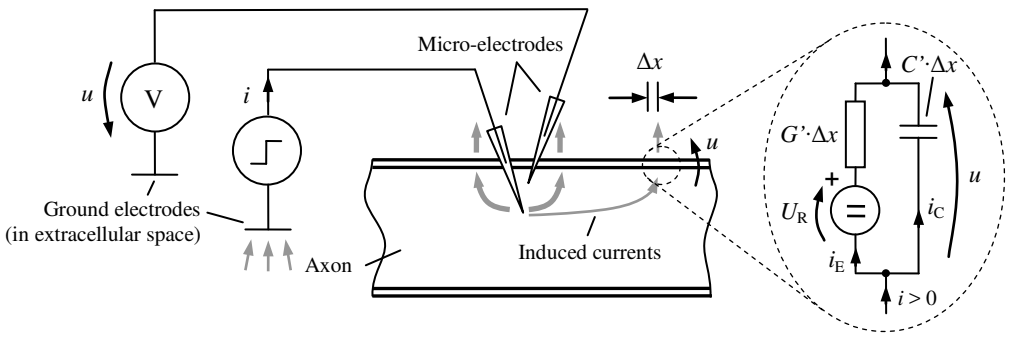

Figure 1: Stimulation set-up with the injected current i ($= i_E + i_C$) and the resulting voltage u across the cell membrane. The equivalent electrical circuit model for the passive membrane response denotes the conductive current i_E in parallel to the displacement current i_C.

arbitrary optimization.
Empirical settings, quite complex computational and analytical models are used for the charge-related, power-related, or energy-related optimization of waveform shapes [1,2,4]. Controversial results are frequent because of varying experimental settings and complex models [1,4].
In the present work, a simple model and a few simple optimization guidelines will be derived for an energy-efficient optimization of temporal parameters, i.e., of the waveform shape of the electrical current stimulus. In particular, the effective and reactive components of the stimulus will be separated for the latter optimization based on the strength-duration curve. The model considers a single spatially-limited membrane with the associated simple closed-form mathematical expressions for underlying electrical processes and the resulting subthreshold relationships. This is because even large-scale macroscopic excitations are a result of individual excitable cells, so that the following consideration of a single isolated membrane of a single excitable cell provides a useful and clear basis.

Methods

Basics

A passive response of the membrane voltage u of an excitable cell to an external current i as well as the membrane's pre-excitation state (subthreshold behaviour) can be modelled with a simple linear equivalent electrical circuit model, as shown in Fig. 1. It includes the resting membrane voltage U_R, the electrical conductance $G'\cdot\Delta x$ of the membrane (with G' as the conductance related to axon's axial length x) determined mainly by the number of passive K^+ resting channels in the membrane, and the capacitance $C = C'\cdot\Delta x$ determined by the lipid double layer of the membrane. Typically, U_R is around -70mV, $G'' = G'/(\pi D)$ is about 1mS/cm^2, and $C'' = C'/(\pi D)$ is about 1µF/cm^2, with D as the axon diameter in the typical range of 0.5-20µm [3].
The resting state of the membrane is denoted by $u = U_R$ with $i = 0$. An external current $i < 0$ perturbation (i.e., positive i inwards through the membrane) yields a graded hyperpolarization of the membrane with the associated $u < U_R$. In contrast, a perturbation $i > 0$ (i.e., positive i outwards through the membrane) yields a graded depolarization with $u > U_R$. The extent of this depolarization determines if the membrane becomes finally excited or not in the non-graded all-or-none fashion and generates an action potential. Typically, Δu of about 20mV [3] is needed to reach the excitation threshold level of $u = U_R + \Delta u = u_T \approx$ -50mV ($> U_R$).

Proposed optimization

It is important to recognise that not the external i is primarily responsible for the membrane's u depolarization towards u_T but, to be more precise, only its conductive component i_E, which passes the leakage resistance $R = 1/G'\cdot\Delta x$ (Fig. 1). In fact, real conductive currents (across mainly passive K^+ resting channels) are needed for the membrane depolarization so that i_E can be considered as an effective component of i in terms of the depolarization. Another component of i, the displacement current i_C, crosses the membrane capacitor (with its C) in order to discharge it during the depolarization (i.e., the capacitor charge $|C\cdot u_T| < |C\cdot U_R|$). This component i_C can be considered as a reactive component of i, which does not directly contribute to the depolarization but increases the level of i and thus the energy costs of the stimulation.
In other words, not only the temporal dynamics of the applied $i = i_E + i_C$ govern the depolarization but also the RC behaviour of the membrane, since only the partial current i_E determines the depolarization-relevant $\Delta u = i_E \cdot R$ (Fig. 1). Likewise, the relationship between Δu and the waveform parameters of i (e.g., its pulse duration) should be instructive in the design of energy-efficient waveform shapes. Such resulting parameters would prevent both under-depolarization ($u < u_T$) and over-depolarization ($u > u_T$) and thus make sure that these optimised waveform shapes have just the necessary but minimum energy for a successful excitation (right at $u = u_T$).
To start with, we assume step current pulses of $i(t)$, i.e., a simple rectangular waveform shape over time t, and derive the aforementioned relationship. The transfer function between $i(t)$ with its magnitude I and $i_E(t)$ with its magnitude I_E for the angular frequency $\omega = 2\pi f$ is

$$I_E = \frac{I}{1 + j\omega RC} \tag{1}$$

The associated $i_E(t)$ for the step current pulse $i(t)$ with its magnitude I (Heaviside step function) can be readily

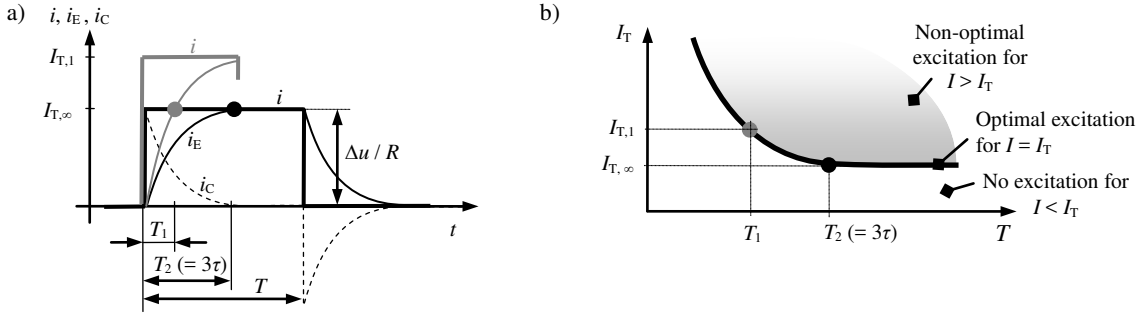

Figure 2: a) Rectangular current i ($= i_E + i_C$) stimulus with its duration T and the associated conductive i_E and displacement i_C components. b) The current strength-duration curve (Eq. 3), quantified as the threshold current magnitude I_T in relation to T.

solved as

$$i_E(t) = I \cdot (1 - e^{-t/\tau}) \quad (2)$$

with $\tau = RC$. That is, the necessary threshold magnitude $I = I_T$ of the now rectangular $i(t)$ with its pulse duration T (Fig. 2a) in order to reach $\Delta u = i_E \cdot R$ follows from Eq. 2 as

$$I_T = \frac{\Delta u / R}{1 - e^{-T/\tau}} \quad (3)$$

In fact, Eq. 3 represents the well-known strength-duration curve, as shown in Fig. 2b. Please note as $T \to \infty$, $I_T \to I_{T,\infty} = \Delta u / R$. From a practical point of view, we can already approximate $I_T = 1.05 \cdot I_{T,\infty} \approx I_{T,\infty}$ for $T \geq 3\tau$.

As an approximation, the energy-efficient excitation can be expected along this curve for rectangular pulses $i(t)$ with their parameters $I = I_T$ and T from Eq. 3 (see limitations from the discussion). Likewise, $I > I_T$ corresponds to an energetically unfavourable over-depolarization at a given T, with $i(t)$ then having too high I (grey area in Fig. 2b), whereas $I < I_T$ implies under-depolarization without a subsequent action potential.

In practical terms, Eq. 3 yields an energy-efficient $I = I_T$ given a certain T, which can be considered as an optimization/design guideline. In analogy, an energy-efficient $T = T_T$ can be expressed from Eq. 3 as

$$T_T = \tau \cdot \ln\left(\frac{RI}{RI - \Delta u}\right) \quad (4)$$

given a certain I, which then composes another optimization guideline. Please note that since $RI > \Delta u$, $T_T > 0$ in Eq. 4. Likewise, $T > T_T$ corresponds to an energetically unfavourable over-depolarization at a given I (grey area in Fig. 2b), whereas $T < T_T$ implies under-depolarization.

Results

Fig. 2a demonstrates i_E (Eq. 2) and i_C ($= i - i_E$) for a rectangular i. Since the component i_E is crucial for the membrane depolarization, please note that a high momentary i_C indicates a relatively weak depolarization because of the associated low i_E ($< i_C$). Likewise, a relatively high $I = I_T$ would be needed to reach Δu at this particular moment. In contrast, a disappearing i_C ($< i_E$) indicates the maximum possible depolarization by i_E and thus a relatively low $I = I_T$ required to reach u_T.

The associated strength-duration curve (Eq. 3) in Fig. 2b indicates two threshold magnitudes $I_{T,\infty}$ and $I_{T,1}$ ($> I_{T,\infty}$) with the respective T_2 ($\approx 3\tau$) and T_1 ($< T_2$). These parameters are also depicted in the time courses of Fig. 2a to illustrate the mutual relationship between Fig. 2a and Fig. 2b.

Proposed energy-efficient optimization of the rectangular waveform shapes of i is illustrated in Fig. 3, with the relevant stimulation set-up from Fig. 1. Fig. 3a facilitates the guideline from Eq. 4 in finding the optimum T_T ($\approx 3\tau$) for an arbitrary selected $I = I_{T,\infty}$ of a depolarizing monophasic stimulation impulse. As an alternative, T_T can be found by numerically tracing i_E up to the threshold level $\Delta u / R$.

Another typical stimulation waveform, the biphasic pulse, is considered in Fig. 3b along the guideline from Eq. 3. While the first negative impulse leads to the aforementioned graded hyperpolarization and the associated decrease of i_E, the second depolarizing impulse leads to the graded depolarization with increasing i_E (Eq. 2). The magnitude I of the second impulse is optimised based on Eq. 3 for a constant T (Fig. 3b). An increasing I shows the transition from under-depolarization without excitation ($I < I_T$), to the optimal excitation ($I = I_T$), and then to over-depolarization with excitation but with wasted impulse energy ($I > I_T$).

In analogy to Fig. 3a, the numerical tracing of i_E (but not of the total i) up to the threshold $\Delta u / R$ leads to an optimum $I = I_T$. This possibility of tracing highlights the applicability of the proposed optimization procedure to any waveform shape needed.

Discussion

The present work provides a simple methodological basis for optimization and design of energy-efficient waveform shapes for electrical neuromuscular stimulation. The major clue is that not the waveform of the applied

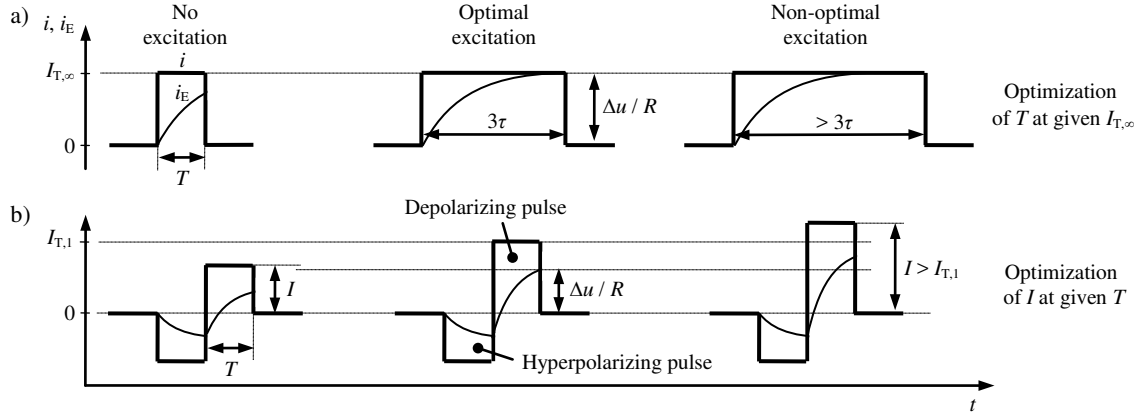

Figure 3: Proposed optimization of the current $i(t)$ waveform shapes based on the strength-duration curve (Fig. 2b). (a) Optimization of monophasic stimulation impulses in terms of varying T (Eq. 4). b) Optimization of biphasic impulses in terms of varying amplitude I (Eq. 3) of the second depolarizing pulse.

external current i through the membrane of an excitable cell is primarily responsible for the excitation of the cell but the associated conductive current i_E across this membrane. The additive displacement current i_C can be considered as a reactive component which does not directly contribute to the depolarization but increases the total i and thus the energy budget of the stimulation procedure.

Likewise, a simple RC model for the pre-excitation state of the membrane (subthreshold behaviour) is consulted to estimate i_E out of i ($= i_E + i_C$). As soon as the excitation condition ($\Delta u = i_E \cdot R$) is met by the rather inert course of i_E over time, the momentary waveform of i (or the momentary parameters of i) can be considered as being already excitatory and energy-efficient (in line with the strength-duration curve). If this condition is surpassed, the excitation still takes place but the energy budget is not optimal.

As a simple example, the case of a stimulating rectangular pulse i - with its parameters such as the magnitude I and T to be optimised - is considered here. Theoretical considerations in Eqs. 3,4 and a schematic illustration in Fig. 3 illustrate the proposed energy-efficient optimization of I and T. A transition is clearly shown from under-depolarization without excitation, to the optimal energy-efficient depolarization with the subsequent excitation, and up to over-depolarization with excitation but also with wasted stimulation energy.

The considered monophasic and biphasic pulses are quite common in neuromuscular stimulation. The presented method is also applicable to any shape of stimulating waveforms, such as saw-tooth, exponential, or sinusoidal waveforms. However, the solution of the differential equation (Eq. 1) would differ from Eq. 2 because i_E and i_C have then different time courses, which affects the fulfilment of the excitation condition from above. In addition, a numerical tracing of i_E in the time domain (based on the RC model) could also be applied for any stimulating waveform in order to figure out waveform parameters at which the latter excitation condition is just fulfilled.

Derived optimization guidelines refer to current as the used external stimulus. However, waveforms of voltage stimuli could also be energetically optimised but with a different transfer function (different from Eq. 1).

An optimization of waveform shapes may focus not only on the strength-duration curve (as used in this work) but also on the minimization of the total delivered charge $i(t) \cdot t$ (to minimize tissue damage) or of the total energy of the stimulating waveform $\propto i^2(t) \cdot t$ (to maximize battery lifetime), as applied in [1]. Obviously, different optimization criteria yield different optimization results: shorter T of rectangular pulses tend to yield a greater charge efficiency, longer T a greater power efficiency, and medium T (around chronaxie) a greater energy efficiency [1,2].

It should be noted that the proposed optimization guidelines require either RC model parameters or the relevant strength-duration curve. Another limitation of the procedure is that it is designed for the simplest set-up with implanted electrodes and transversal depolarizing currents across the membrane of a single excitable cell (Fig. 1). Longitudinal currents along axons as well as surface electrodes require consideration of many more model parameters, which should account, for instance, for the (non-linear) contact impedance of (polarizable or non-polarizable) electrodes and heterogeneous tissue properties with embedded excitable cells.

Another limitation is that the accommodation behaviour of the membrane is ignored, i.e., an increase in Δu during extended subthreshold stimulation. Furthermore, the leakage resistance R (Fig. 1) is a non-linear function of u. In the resting state and during sub-threshold stimulation R is determined by passive K^+ resting channels in the membrane and stays constant only up to about 80% of the action potential threshold u_T [2]. For supra-threshold stimulation, R decreases and is now mainly governed by voltage-gated Na^+ and K^+ channels.

Obviously, the relevance of the proposed methodology should be validated with respect to numerical modelling and/or experimental data using a more realistic membrane model.

However, the present work offers a possibility to step from an empirical or complex analytical optimization of stimulating waveforms with respect to their energy-efficiency towards a tangible, instructive, and rather simple theoretical approach. This may speed up, render transparent, and simplify the design of energy-efficient stimulating waveforms in future.

Acknowledgement

The corresponding author thanks Prof. Helmut Pfützner from Vienna University of Technology for valuable discussions.

References

[1] A. Wongsarnpigoon, J.P. Woock, W.M. Grill: Efficiency analysis of waveform shape for electrical excitation of nerve fibers. *IEEE Trans. Neural. Syst. Rehabil. Eng.*, vol. 18(3), pp. 319-328, 2010.

[2] J.P. Reilly, Applied Bioelectricity: From Electrical Stimulation to Electropythology, Springer, 1998.

[3] E. Kaniusas, *Biomedical Signals and Sensors I: Linking physiological phenomena and biosignals*, Springer, 2012.

[4] M. Schmoll, J.C. Jarvis: Investigating energy efficiency for different pulse shapes and electrode arrangements to activate motor neurones, *European Journal of Translational Myology - Basic and Applied Myology*, vol. 26(1), pp. 54-55, 2016.

Author's Address

Ao.Univ.Prof. Eugenijus Kaniusas
Head of "Biomedical Sensing" research group, Institute of Electrodynamics, Microwave and Circuit Engineering, Vienna University of Technology
kaniusas@tuwien.ac.at
www.emce.tuwien.ac.at

Method for selective surface stimulation of denervated muscles in the larynx

B. Schneider-Stickler[1], M. Leonhard[1], L. Kneisz[2], M. Ladurner[2], W. Mayr[3], M. Krenn[3]

[1]Division of Phoniatrics and Logopedics, Medical University of Vienna, Austria
[2]MED-EL Innsbruck, Austria
[3] Center for Medical Physics and Biomedical Engineering, Medical University of Vienna, Austria

Abstract: *Vocal fold paralysis is a pathological motion impairment of one vocal fold, mostly caused by laryngeal nerve damage. If the vocal fold does not reinnervate a flaccid paralysis occurs due to denervation of the vocalis muscle and its atrophy. Patients with unilateral vocal cord paralysis suffer from hoarse and weak voice since there is always a remaining glottic gap during phonation. Today's standard treatment of unilateral paralysis includes surgical medialization through either injection augmentation or laryngoplastic framework surgery.*
We want to investigate whether it is possible to selectively stimulate the denervated muscle fibers of the vocalis without causing pain or excitation of sensory nerve fibers or activation of innervated muscles in the neck region. The goal is 1. a verivication of functionality for screening and 2. a strengthening and increase in total volume of the target muscle on order to improve voice quality in patients with unilateral paralysis.
In combination with voice therapy also electrical stimulation of laryngeal muscles has alraedy been used in order to achieve hypertrophy]. Furthermore research with functional electrical stimulation of patients with long time denervated limb muscles showed very promising results.
The selective stimulation of denervated muscles has been investigated in rabbits with unilateral paresis of the recurrent laryngeal nerve. It could be shown that with triangular ramping and very long pulses (> 200ms) the afferent nerve fibers where not stimulated but only denervated muscle, with change in muscle fibers confirmed through histology. It is to be investigated if these findings can be repeated with surface electrodes positioned in the neck area and successful stimulation of the denervated vocalis muscle can be performed without causing pain and excessive contraction of neighboring neck muscles rendering treatment impossible. The optimal stimulation parameters for this application and ideal position of the surface electrodes have yet to be investigated.

Keywords: *Ageing, muscle atrophy, larynx, electrical stimulation, denervated muscles*

Determining optimal settings for selective surface stimulation in order to recruit paralyzed facial muscles under non painful conditions

G.F. Volk[1], O. Guntinas-Lichius[1], T. Schmid[1], L. Kneisz[2], M. Ladurner[2], W. Mayr[3], M. Krenn[3]

[1]Facial-Nerve-Center, Universitätsklinikum Jena, Germany
[2]MED-EL Innsbruck, Austria
[3] Center for Medical Physics and Biomedical Engineering, Medical University of Vienna, Austria

Abstract:
Purpose:
Facial nerve paralysis as a peripheral nerve injury results in neuromuscular atrophy. The symptoms include significant aesthetic, functional and often life-altering consequences. Several procedures such as Nerve Grafting, Facial Reanimation and Rehabilitation have been developed to treat functional and cosmetic aspects of this disease. Nerve grafting is a sophisticated surgery, which requires experience but offers promising results. Although cable grafting is state of the art, the method suffers the disadvantage of long nerve regrowth time. Facial Pacing systems too show promising results to treat facial paralysis. Former research showed good results stimulating denervated extremity muscles using FES. Nevertheless this field of research is still lacking optimal stimulation settings to selectively recruit denervated atrophic or simply age-related atrophic facial muscles under non painful conditions.
Methods:
Several Devices are considered to investigate optimal stimulation settings. To encourage noninvasive screening methods for facial pacing, surface electrodes are used to estimate the optimal settings for stimulations. The use of surface electrodes causes the need for optimized electrode positioning, which is also investigated.
Results:
Martin et al. showed that recruitment of denervated muscles requires exponentially shaped pulses with long phase durations(>200ms). The outcome of our investigation confirms these findings as well, showing best performance when recruiting paralyzed facial human muscles with biphasic long-duration impulses. It is crucial to position the surface electrodes appropriately in order to avoid stimulation of innervated muscles, for instance the masseter muscle.
Conclusions:
Surface electrodes, combined with the optimal stimulation settings, offer a screening possibility for facial pacing. Since muscles affected by age-related atrophy could be recruited too, further research is necessary to show effectiveness of training using the determined exponential patterns.

Keywords: *Facial nerve paralysis, surface electrodes, electrical stimulation*

Reaching and grasping training based on robotic hybrid assistance for neurological patients

Bulgheroni M[1], d'Amico E[1],

Ferrante S[2], Ambrosini E[2], Pedrocchi A[2], Ferrigno G[2],

Schauer T[3], Wiesener C[3],

Becker S[4] , Weber M[4], Epperlein M[4],

Gfoehler M[5], Puchinger M[5,]

Crema A[6], Raschellà F[6], Furfaro I[6], Micera S[6],

Rossini M[7], Palumbo G[7], Gasperini G[7], Molteni F[7],

Krakow K[8], Fischer N[8,]

Zajc J[9,] Russold M[9]

[1] Ab.Acus , Milan, Italy

[2]NEARLAB, Politecnico di Milano, Milan, Italy

[3]Control Systems Group, Technische Universität Berlin, Germany

[4]Hasomed GmbH, Magdeburg, German

[5] Technische Universität Wien, Wien, Austria

[6]Translational Neural Engineering Laboratory, EPFL, Switzerland

[7] Centro di Riabilitazione Villa Beretta, Costamasnaga, Italy

[8] Asklepios Neurologische Klinik Falkenstein, Königstein, Germany

[9] Ottobock Health Products GmbH, Vienna, Austria

Abstract: *The aim of the RETRAINER project is to tune and validate advanced, robot-based technologies to facilitate recovery of arm and hand function in stroke survivors and to verify extensively the use of the system by end-users. RETRAINER allows the users to use their own arm and hand as much and as soon as possible after the trauma so to achieve the best outcomes in rehabilitation. RETRAINER makes available two systems that could be used either combined or stand-alone. RETRAINER S1 provides the end-user with a robot that does not completely take over the user's tasks and substitute the functionality of the body, but specifically supports the user only whenever he/she really needs support. Residual functionality is trained and improved on rather than replaced by the robotic device. Arm movements is supported by the combined action of a passive exoskeleton for weight relief and Neuromuscular Electrical stimulation (NMES)delivered to several arm muscles in a controlled manner. RETRAINER S2 exploits a wearable NMES system with multiple arrays of electrodes for hand rehabilitation facilitating the grasping function. Both systems benefit from use of interactive objects, i.e. daily-life objects able to supply information about themselves to drive usage.*
The systems will undergo a thorough randomized control clinical trial with end users to assess their efficacy in rehabilitation.

Keywords: *Hybrid robotic rehabilitation system, stroke survivors, upper limb rehab, exoskeleton, wearable functional electrical stimulation, myocontrol neuroprosthesis, randomized control clinical trial*

Introduction

Stroke is the main cause of permanent and complex long-term disability in adults and has implications for patients, caregivers, health professionals and society in general [1]. Stroke is the second most common cause of death in Europe, in 2008, there were approximately 1.3 million deaths from stroke in Europe, accounting for almost 14% of all deaths [2]. There are currently approximately 8 million stroke survivors in the European Union (EU). Stroke costs the EU over 62 billion euros a year including the cost of health care services, medications to treat stroke, and missed days of work. Stroke is a leading cause of serious long-term disability.

At present there is no routinely available curative treatment for stroke patients and therefore rehabilitation interventions are relied upon to maximize patient outcomes. Upper limb (arm) hemiparesis is widely reported in the literature as one of the primary impairments following stroke. While many patients recover ambulatory function after dense hemiplegia, restoration of arm motor skills is often incomplete.

Rehabilitation's outcomes often conclude in incomplete motor recovery and over 60% of patients cannot use their paretic hands in functional activities [3]. Nevertheless, the recovery of voluntary arm movements is one of the most important goals during stroke rehabilitation in order to avoid long- term disability in activities of daily living (ADL), social and occupational activities, and depression. The aim of rehabilitation is to reduce impairment and minimize disability and a number of interventions to achieve these aims and improve arm function after stroke have been suggested.

The aim of RETRAINER Project is to tune and validate advanced robot-based technologies to facilitate the recovery of the arm and hand functions in post-stroke patients, and to extensively verify the use of the system by end-users under three perspectives: 1) the usability of the system in clinical and in home settings; 2) the perceived benefits by the end-users and the informal and formal caregivers; 3) the impact of the use of the system on the rehabilitative outcomes.

RETRAINER system overview

RETRAINER makes available two systems which could be either combined or used stand-alone according to users' needs.

RETRAINER S1 - Training of arm movements: S1 provides the end-user with a robot that does not completely take over the user's tasks and substitute the body's functionality, but specifically supports the user only wherever he/she really needs support. Residual functionality is trained and improved rather than replaced by the robotic device. Arm movements are supported by a combined action of a passive exoskeleton for weight relief and Neuromuscular Electrical stimulation (NMES) delivered to arm muscles in a controlled manner (Fig.1). The lightweight exoskeleton provides the user with an adjustable amount of weight support to reduce necessary muscular effort for movements and at the same time NMES increases muscle activation and strengthen the muscles. Stimulation amplitudes is controlled based on the residual EMG activities of the same stimulated muscles since the combination of NMES with the voluntary effort of the patients seems to maximize the therapeutic effects of NMES, thus having the highest potential to increase the rehabilitative outcomes.

From a rehabilitative point of view, RETRAINER S1 has the major advantage of being intrinsically controlled by the subject himself/herself and stimulating the use of the arm in a context of real life activities, it indeed ensures the active participation of the users while keeping a good level of assistance to the user, depending on the condition.

RETRAINER S2 - Training of hand functions: Electric stimulation as restorative or assistive technology is among the best available practices, though not necessarily widespread in clinical environment. In the framework of RETRAINER, a novel wearable NMES system with multiple arrays, which could be a modular tool usable as a platform for grasp rehabilitation potentially improving the clinical applicability of NMES is being developed. The device is designed for providing electrical stimulation on extrinsic and intrinsic grasp muscles. It is composed of independent electrode arrays, customizable to user needs and anthropometric characteristics, which can be donned on the user forearm and hand, and can deliver NMES provided by an external stimulator with demultiplexers. The actual implementation offers a scalable anthropometric based design, which takes advantage of a priori knowledge of human anatomy. The aim is to have a device, with modular components that can be adapted to single patient needs (Fig.2). The stimulation patterns can be manually tuned to elicit functional grasp, to obtain whole muscle conditioning, and to produce open-loop or closed-loop grasp control.

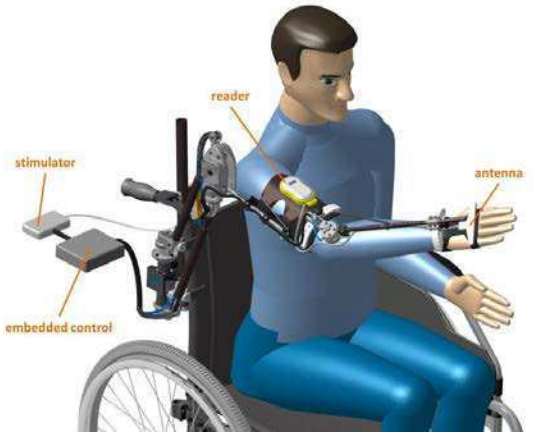

Figure 1: Digital mock-up of the complete RETRAINER S1 system

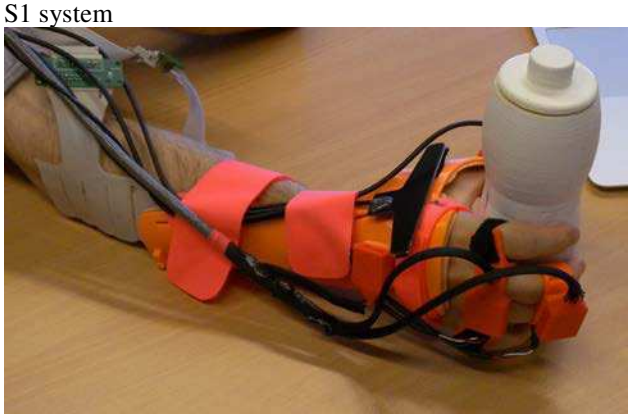
Figure 2: RETRAINR S2 system: electrode arrays, hand orthosis, interactive object.

RETRAINER interactive objects: Both systems will benefit from the use of interactive objects. Interactive objects are daily life objects able to supply the robotic system with some information on themselves (e.g. physical characteristics, expected sequence of use) to drive their usage. The objects are equipped with RFID (Radio

Frequency IDentification) tags and a suitable reader embedded in the robotic system. A devoted processing of Received Signal Strength Indication (RSSI) from the RFID tags and environmental constraints allow the recognition of the selected objects among several ones. The system identifies the proximity of an object to start grasping, the size and weight of an object to modulate grasp, the proximity of the table to return an object and to relax the hand [4]. The developed algorithms allow repeated selections of "target objects" aimed at driving a sequence of tasks in a known environment while the user is interacting with them. As soon as the sequence of tasks develops the system plans next task to be performed.

RETRAINER clinical trial

Potential end users will be selected among stroke patients. A subject will be considered eligible if his/her brain hemispheric lesion is unilateral, if s/he has no history or evidence of previous neurological and/or psychiatric disorders, if s/he is vigilant, collaborative and without global cognitive impairment. This last feature will assure the possibility for the potential participant subject to accept and sign by him/herself the informed consent.

The primary endpoint is the pre- and post-treatment difference in the ARAT Test, as well as in the other clinical scales that measure the effectiveness of the treatment. Sample size will be defined on the basis of ability to detect a Minimally Clinically Important Difference for primary outcome measure. It is calculated that a sample size of 68 patients would be capable of detecting a between-group difference of 5.67 points in the primary endpoint, this is the value indicated like Minimally Clinically Important Difference in Chronic Stroke population with a standard deviation of 12.5, a type I error of 5%, and a power of 80%78. Since ARAT is the reference scale for the upper limb functions, we consider it as the primary outcome measure of either the clinical trial with S1 and the one with S2. 68 end users will then be recruited for each clinical center.

NMES treatments literature suggests that effective treatments have prolonged duration and frequent sessions [5]. In this study, we will have not less than 30 minutes of effective NMES per session. Each session will last one hour considering the don on and off time, setup and calibration. The treatment will include three sessions a week for nine weeks for each end-user. The clinicians will choose a subset of exercises according to patient's condition and needs and will define the set of exercises to be performed at the beginning of the training session. The composition of each training session could be changed by the clinicians before starting according to the clinical situation of the patient. The RETRAINER software running on the tablet provides an interface for the therapist to setup the system for the patient, including configuration and calibration of all attached modules as well as teaching of reference positions if needed. The exercise subset includes arm and hand dedicated exercises. See in the tale below some examples.

ARM exercises	HAND exercises
Anterior Reaching Exercise on plane	Flexion and extension of fingers
Anterior Reaching Exercise in the space	Grasp and release objects
Moving Object on a plane	Grasp, move and release object on a plane
Moving Object on a plane in the space	Grasp, move and release object in the space
Moving Object in space	Flex Extension of wrist and fingers
Lateral elevation on frontal plane	
Hand to Mouth	
Hand to Mouth with an object in the hand	

Additionally to the main outcome measure, other specific outcomes will be measured to best evaluate the effects of the trials. Some of these clinical and quality of life outcome measurements are: Mini-Mental State Examination (MMSE), motricity index, Motor Activity Log (MAL), Box & Blocks Test (BB), System Usability Scale (SUS), Stroke Specific Quality Of Life scale (SS-QOL). During the training session some information on the treatment are shown on the GUI to let the therapist understand how the training is going on. The therapist for instance has a simple feedback on the actual involvement of the patient during training that can be used to give the patient proper instructions in order to stimulate his attention to the training. To evaluate the effectiveness of RETRAINER S1 and S2 will be used the Modified Ashworth Scale (MAS). The muscular assessment will be performed on different target muscles for each subsystem: on pectoralis major, deltoids, biceps and triceps for S1; wrist flexor and extensor, fingers and thumb flexor and extensor for S2. In both subsystems, kinematic data will be used to have an evaluation of the functional range of motion during the trial movements. The timeline for the application of the three evaluations is shown in Fig.3.

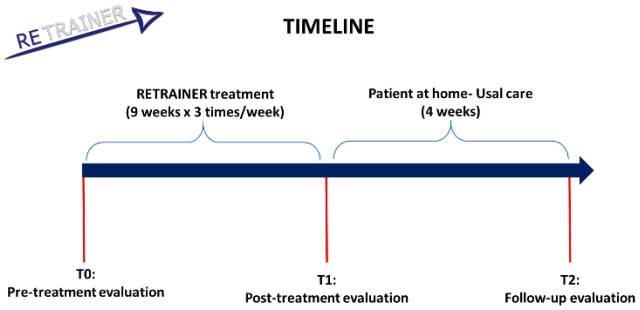

Figure 3: RETRAINER clinical trial design

Conclusions

The wide on the field validation of the RETRAINER system aims at objective assessment of robotic neurorehabilitation on stroke survivors. From a robotics point of view, the RETRAINER arm module is an innovative and original system where the actuation exploits

as much as possible the residual muscle functionality of the user himself/herself. This approach goes beyond the current classical rehabilitation robotics paradigms. Furthermore, the exoskeleton in S1 assures the gravity compensation and the control of the target motion using the contraction of the subjects own muscles. NMES controls the muscular activation until the user has achieved the desired task. The repetition of functional tasks with the participation of the user volition are key ingredients for re-learning and the additional proprioceptive feedback provided by the NMES has been recently proved in the literature as an additional element in favour of recovery and brain remapping [6] [7]. An effective clinical validation of this system is a key issues in supporting technological innovation in current rehabilitation practices. The concept and design of this clinical trial validation is another interesting output of this project. The personalized set of exercises selected by the clinician according to patient's functional conditions is a real benefit for the patient: thanks to this unique solution, the upper limb movement could be rehabilitated according the therapist clinical evaluation, using his/her expertise integrated with the technology facilities to get the feasible best rehabilitation outcome.
RETRAINER is a clear example of multidisciplinary cooperation aimed at the design and setup of a rehabilitation system including technology development as well as exercises design and clinical assessment.

Acknowledgement

This work has received funding from the European Union's Horizon 2020 research and innovation program under grant agreement No 644721.

References

[1] Coupar F, Pollock A, van Wijck F, Morris J, Langhorne P. Simultaneous bilateral training for improving arm function afterstroke. Cochrane Database of Systematic Reviews 2010, Issue 4. Art. No.: CD006432.
[2] Andreotti F et al. How Can We Avoid a Stroke Crisis in Europe? Oct 2012
[3] Fusco A, De Angelis D, Morone G, et al., "The ABC of tDCS: Effects of Anodal, Bilateral and Cathodal Montages of Transcranial Direct Current Stimulation in Patients with Stroke—A Pilot Study," Stroke Research and Treatment, vol. 2013, Article ID 837595, 6 pages, 2013
[4] Bulgheroni M, d'Amico E, Sartori L, RFID technology for objects recognition and their position estimation, in J.L. Pons et al (Eds): Converging Clinical & Engi. Research on NR, BIOSYSROB 1, 1165-1169, Springer-Verlag 2013
[5] Thrasher TA, Zivanovic V, McIlroy W, Popovic MR. Rehabilitation of reaching and grasping function in severe hemiplegic patients using functional electrical stimulation therapy. Neurorehabil Neural Repair. 2008 Nov-Dec;22(6):706-14.
[6] Iftime-Nielsen, S.D., Christensen, M.S., Vingborg, R.J., Sinkjaer, T., Roepstorff, A., Grey, M.J. Interaction of electrical stimulation and voluntary hand movement in SII and the cerebellum during simulated therapeutic functional electrical stimulation in healthy adults. Hum Brain Mapp. 2012; 33, 40–49.
[7] Gandolla M, Ferrante S, Molteni F, Guanziroli E, Frattini T, Martegani A, Ferrigno G, Friston K, Pedrocchi A, Ward NS. Re-thinking the role of motor cortex: Context-sensitive motor outputs? Neuroimage. 2014 May 1;91:366-74.

Author's Address

Maria Bulgheroni
Ab.Acus srl
mariabulgheroni@ab-acus.com
www.ab-acus.com

The ReTrainer arm exoskeleton - a modular lightweight device that combines adjustable gravity compensation, lockable joints and neuromuscular electrical stimulation.

Puchinger M[1], Wiesener C[2], Schauer T[2], Ferrante S[3], Ambrosini E[3], Pedrocchi A[3], Becker S[4], Weber M[4], Epperlein M[4], Zajc J[5], Russold M[5], Gfoehler M[1]

[1]Vienna University of Technology, Austria
[2]Control Systems Group, Technische Universität Berlin, Germany
[3]Politecnico di Milano, Italy
[4]Hasomed GmbH, Magdeburg, Germany
[5]Otto Bock Healthcare Products, Vienna, Austria

Abstract:
The recovery of voluntary arm movements is one of the most important goals during stroke rehabilitation in order to avoid long-term disability in activities of daily living. Devices that are currently used for rehabilitation and training in clinical settings are mostly bulky and stationary. One of the objectives of the European project RETRAINER is to develop a lightweight arm exoskeleton that can be used for clinical rehabilitation as well as home training and is suitable for movement control by means of neuromuscular electrical stimulation (NMES). The RETRAINER arm exoskeleton represents a passive, 3-degrees of freedom (DoFs), lightweight arm orthosis with gravity compensation at the shoulder and elbow joints to minimize muscular effort during arm movements. All DoFs can be locked via electromagnetic brakes to keep static postures without continuous muscle work. Main focus of the development was the modularity and easy adaption to a wide range of user's anthropometrics as well as increasing the user's comfort while wearing the exoskeleton. A universal mounting device allows to install the exoskeleton on both wheelchairs and normal chairs with different backrest shapes. The exoskeleton can be used together with NMES of a maximum of two arm muscles. NMES is triggered by means of the residual muscle activity of the subject, so as to enhance motor recovery. First tests of the prototype with healthy subjects showed promising results regarding functionality and wearing comfort. Further prototypes are currently in two rehabilitation centres for starting test series with stroke patients.

Keywords: *upper limb rehabilitation, neuromuscular electrical stimulation, exoskeleton, arm orthosis, gravity support*

Introduction

Upper limb hemiparesis is widely reported in the literature as one of the primary impairments following stroke. While many patients recover ambulatory function after dense hemiplegia, restoration of arm motor skills is often incomplete and over 60% of patients cannot use their paretic hand in functional activities [1]. The recovery of voluntary arm movements is one of the most important goals during stroke rehabilitation in order to avoid long-term disability in activities of daily living (ADL), social and occupational activities, and depression.

In the last years, numerous upper-limb exoskeletons for after stroke survivors have been developed but most of them did not succeed, especially clinically [2]. Momentary the only commercially available upper-limb exoskeleton is the motor-driven ArmeoPower© by Hocoma, based on the ARMin robot [3]. The structure does not allow an individual installing on a wheelchair or chair because of its dimensions and weight.

Recent neurophysiological studies [4-6] advocated the use of Neuro Muscular Electrical Stimulation (NMES) co-incidentally with the voluntary drive to enhance its beneficial effects on the motor re-learning process.

The RETRAINER arm exoskeleton is based on the MUNDUS exoskeleton [7]. Its aim is to facilitate the recovery of the arm function in stroke survivors with a lightweight and non-cumbersome passive device which provides weight relief at the shoulder and elbow joints so as to reduce the muscular effort required to perform arm movements. Residual muscle function will be used for actuation as far as possible, if needed, NMES will be used to provide additional support to the arm muscles.

Material and Methods

The RETRAINER arm exoskeleton

For developing the RETRAINER arm exoskeleton the following main requirements were defined:

1) three lockable degrees of freedom (DoF) that can also be actuated by NMES: *shoulder elevation, rotation of shoulder elevation plane and elbow flexion-extension*
2) two additional DoF that can be locked at customized positions if residual actuation is not available: *humeral rotation and prono-supination*
3) adjustable gravity compensation at the shoulder and elbow joints in order to reduce muscular effort
4) the possibility to provide additional external torque at the joints at any selected position, so that the user can keep a posture without continuous muscle activation
5) easy and stable mounting on both wheelchairs and normal chairs with different backrest shapes
6) mobility of the upper body with worn exoskeleton when seated without generation of constraining forces

Additional design requirements were light weight construction, modularity and easy adjustability to different body anthropometrics. For actuation by NMES contact surfaces with the users arm should be reduced to a minimum to leave space for placing the electrodes.

Figure 1 shows a scheme of the modular structure of the RETRAINER arm exoskeleton and degrees of freedom. For control of the training exercises all DoFs are equipped with integrated angular sensors and each DoF is equipped with an electromagnetic brake so that the user can keep anti-gravity postures without any muscle contractions.

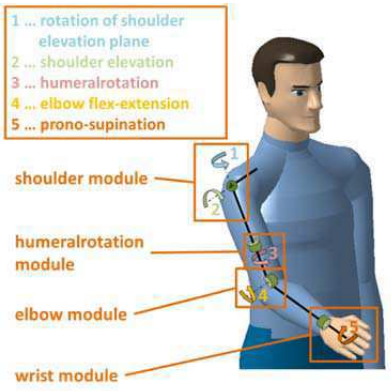

Figure 1: Schematic of the RETRAINER arm exoskeleton, degrees of freedom and module structure.

The 3D mechanical design was done in CATIA® V5 R20 (Dassaults Systèmes, France).

NeuroMuscular Electrical Stimulation

NMES is provided by means of the RehaMovePro (Hasomed GmbH) [8], a current-controlled stimulator with two channels of stimulation and two channels for EMG recordings. The control system uses the residual volitional EMG signal of the affected muscle to trigger the onset of a predetermined stimulation sequence applied to the same muscle. Up to two muscles, selected on the basis of the user's needs, can be stimulated simultaneously. More details on the control system can be found in [9].

Results

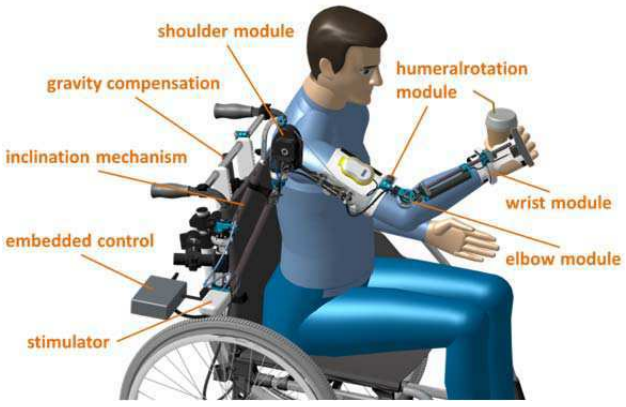

Figure 2: Digital mock-up of the complete RETRAINER arm exoskeleton

A digital mock-up of the complete RETRAINER arm exoskeleton mounted on a wheelchair is shown in Figure 2. Stimulator and control can either be mounted on the back of the wheelchair for maximum mobility or placed on a desk beside the wheelchair.

Gravity compensation

The gravity compensation module for the shoulder joint consists of a carbon-fibre tube at the backrest with two springs inside, linked with a cable pull guided through the inclination mechanism to the lever of the shoulder module. For users between 50th and 95th female/male percentile one spring is locked for higher weight compensation torques. These two modes (one spring mode, two spring mode) can be set manually. For fine tuning of the weight compensation, the level of the compensation is adjusted electronically by the operator at the beginning of each training session.

The weight relief for the forearm is instead realized by a spring linked with a cable pull and is manually adjusted by the operator at the beginning of the training session.

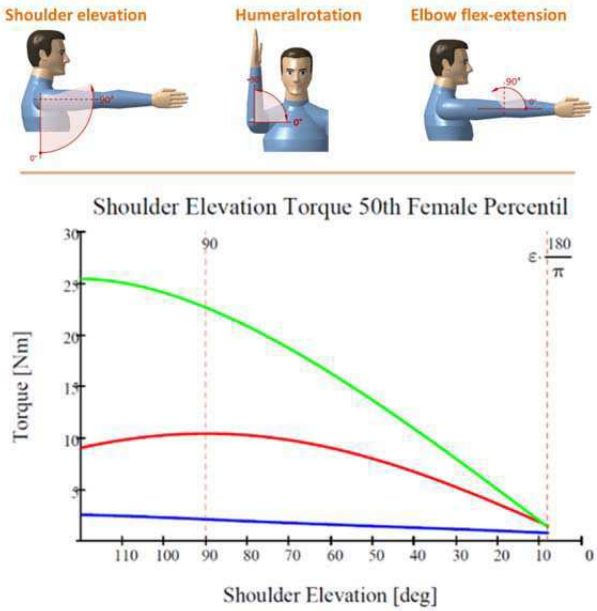

Figure 3: torque at the shoulder joint due to gravity of arm, exoskeleton plus 0.5 weight in hand (red); residual torque after gravity compensation (blue); maximum available compensation torque including electromagnetic brake (green). Elbow 90° flexed, humeral rotation 90°.

Figure 3 shows the generated torques due to gravity at the shoulder joint and the effectiveness of the gravity compensation. It can be seen that residual torques after gravity compensation are below 5 Nm. Additional torque from the electromagnetic brake is high enough for complete compensation for all body heights between 5th percentile female and 95th percentile male. The curves are shown for elbow joint flexed 90°, the results for elbow joint at 45° and 0° (elbow fully extended) are comparable.

Shoulder Module

Figure 4 shows the shoulder module which provides 2 DoFs: shoulder elevation and rotation of the shoulder elevation plane. The lever connects the shoulder module to the humeralrotation module and is linked to the gravity compensation springs with a rope. With the two bonnets on top and bottom the shoulder module is linked to the inclination mechanism. To lock the shoulder joint, an electromagnetic brake is integrated for each of the two DoFs. Angular sensors are integrated to provide information on the positions to the control. The housing of the shoulder head is split into two parts and produced of aluminium for optimal cooling of the brakes.

Figure 4: Shoulder module

Humeralrotation module

Central element of the humeralrotation module, shown in Figure 5, is an aluminium carrier, on which a circular guide is mounted. The two clamping blocks with rapid fasteners enable an easy way to setup the upper arm length of the patient. The slider on the circular guide is connected with a carbon-fibre rod to the elbow module. By pulling out the plunger and moving the slider a humeralrotation angle between 0° and 90° can be adjusted. The specific shape of the aluminium carrier allows the user to easily insert the appropriate size of the upper arm shell.

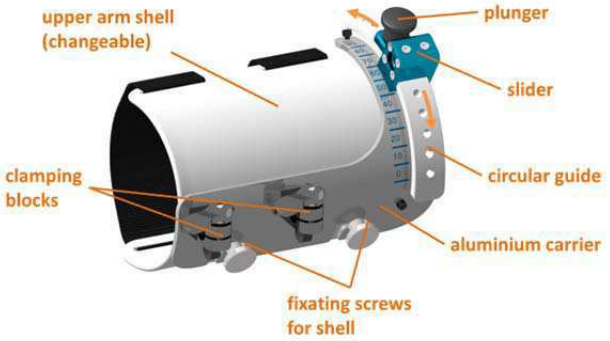

Figure 5: Humeralrotation module

Elbow module

The elbow module, shown in Figure 6, enables flex-extension of the elbow joint in the range of 0° to 110°. Main part is an electromagnetic brake that enables the locking of the joint. The sensor on the top measures the angular position of the elbow. The rope looped around the brake is linked to a spring, hidden in the tube, and enables the gravity compensation of the elbow joint.

Figure 6: Elbow module

Wrist Module

Figure 7 shows the wrist module. The wrist module is fixed on the patients forearm and hand with two velcro strips and hereby locks wrist flex-extension. The slider can be moved by pulling out the plunger on the circular guide and enables prono-supination of the forearm. A range of -50° to +50° can be set.
The whole module is clamped on the carbon-fibre rod of the elbow module with a rapid fastener at the adequate position depending on the forearm length of the individual end-user.

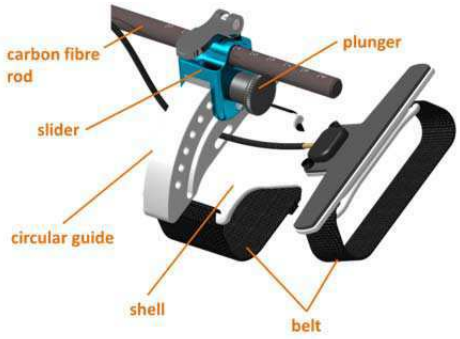

Figure 7: Wrist module

Universal fixation mechanism

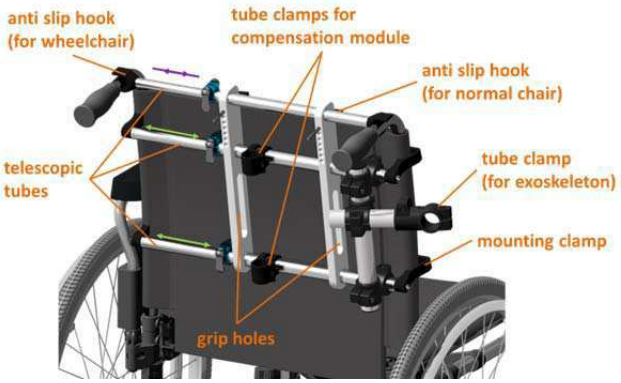

Figure 8: Universal fixation mechanism attached to a wheelchair

The exoskeleton can be mounted on the user's wheelchair or on normal chairs with different backrest shapes by means of a universal clamping mechanism (Figure 8), which assures easy and stable mounting with rapid fasteners.

Inclination module

With the inclination module, shown in Figure 9, the end-user is able to move the trunk when seated in the wheelchair or in a normal chair wearing the exoskeleton so that she/he is not restricted in using residual functionality. A 20° inclination of the trunk in the forward and sideward directions is possible.

The shoulder module is integrated into the four-bar linkage mechanism and remains in a vertical position aligned with the shoulder joint independent of the inclination angle of the mechanism. The rope for the gravity compensation mechanism is guided through the lower tube as well as all cables from the brakes and angular sensors to avoid damage and safety risks. The inclination module is linked to the fixation module by a tube clamp.

Figure 9: inclination module

NMES

Surface electrodes for NMES are attached to the upper arm when needed. Electrode cables are also guided through the exoskeleton tubes to avoid cable damages.

Discussion

A lightweight and non-cumbersome passive arm exoskeleton was developed, which provides weight relief at the shoulder and elbow joints and consequently reduces the muscular effort required to move the arm.

The combination with NMES allows effective assistance and rehabilitation depending on the user's residual muscle functions.

First tests on healthy users have shown that the exoskeleton fits well to different body anthropometrics and donning of the exoskeleton is quick and easy. The adjustable weight compensation adequately reduces the required muscle forces over the movement ranges of the DoFs and the inclination mechanism increases comfort especially during longer seating periods. Eight prototypes are currently available and test series with stroke patients are started in the rehabilitation centres Villa Beretta (Italy) and Asklepios Königstein (Germany).

Acknowledgement

This work was funded by the European Commission under grant 644721, H2020-ICT-2014-1

References

[1] A. Fusco, D. De Angelis, et al.: The ABC of tDCS: Effects of anodal, bilateral and cathodal montages of transcranial direct current stimulation in patients with stroke - A pilot study. *Stroke Res. Treat.*, vol. 2013, 2013.

[2] R. Riener, M. Guidali, et al.: Transferring armin to the clinics and industry, Top Spinal Cord Inj Rehabil, 17: 54–59, 2011

[3] Ho Shing Lo, Sheng Quan Xie: Exoskeleton robots for upper-limb rehabilitation: State of the art and future prospects, Medical Engineering & Physics 34, 261– 268, 2011.

[4] G. I. Barsi, D. B. Popovic, et al: Cortical excitability changes following grasping exercise augmented with electrical stimulation, *Exp. Brain Res.*, vol. 191, no. 1, pp. 57–66, 2008.

[5] S.D. Iftime-Nielsen, M.S. Christensen, et al: Interaction of electrical stimulation and voluntary hand movement in SII and the cerebellum during simulated therapeutic functional electrical stimulation in healthy adults. Hum Brain Mapp, 33:40–9, 2012.

[6] M. Gandolla, S. Ferrante, et al.: Re-thinking the role of motor cortex: Context-sensitive motor outputs?, *Neuroimage*, vol. 91, pp. 366–374, 2014.

[7] A. Pedrocchi, S Ferrante, et al.: MUNDUS project: MUltimodal Neuroprosthesis for daily Upper limb Support, Journal of NeuroEngineering and Rehabilitation, 2013.

[8] M. Valtin, K. Kociemba, C. Behling, B. Kuberski, S. Becker, T. Schauer; RehaMovePro: A versatile mobile stimulation system for transcutaneous FES applications. European Journal of Translational Myology, 26(3), 2016. DOI: 10.4081/ejtm.2016.6076

[9] S Ferrante, Ambrosini E, et al. The RETRAINER control system for supporting arm functions. 12th Vienna International Workshop on FES. September 08-09, 2016

Author's Address

Markus Puchinger
Vienna University of Technology
markus.puchinger@tuwien.ac.at
www.ikl.tuwien.ac.at

The RETRAINER control system for supporting arm functions

Ferrante S[1], Ambrosini E[1], Ferrigno G[1], Schauer T[2], Wiesener C[2], Bulgheroni M[3], d'Amico E[3], Zajc J[4], Russold M[4], Pedrocchi A[1]

[1]NearLab, Department of Information, Electronics and Bioengineering, Politecnico di Milano, Italy
[2]Control System Group, Technische Universität Berlin, Germany
[3]Ab.Acus, Milan, Italy
[4]Ottobock Health Products GmbH, Vienna, Österreich

Abstract: *RETRAINER proposes a rehabilitative method for the recovery of arm functions after stroke, which combines several principle of motor relearning, such as task-oriented exercises, repetitions, maximization of the patient's involvement, and Neuro Muscular Electrical Stimulation (NMES). The system consists of a light-weight passive exoskeleton for weight relief, a current-controlled stimulator with two EMG recordings channels, an embedded control system for real-time control of the stimulator and the exoskeleton sensors, a windows-based tablet which provides the high level control and a graphical user interface for the therapist during donning and calibration and for the patient during training, and daily life objects equipped with RFID tags which guide the patient throughout the execution of the exercises. An EMG-triggered stimulation controller is integrated in the embedded control system in order to allow the patient to initiate the task. Furthermore, the volitional involvement of the subject is monitored throughout the execution of the task and a visual feedback is provided at the end in order to motivate the patient to be actively involved in the training. A proof-of-concept of the RETRAINER arm system on healthy subjects is provided, while its efficacy on post-acute stroke patients will be evaluated by means of a multicenter randomized controlled trial that will start in Autumn 2016 in the premises of the two clinical partners of the RETRAINER project.*

Keywords: *Hybrid robotic rehabilitation system, stroke survivors, upper limb exoskeleton, neuromuscolar electrical stimulation, myocontrol neuroprosthesis.*

Introduction

Upper limb hemiparesis is widely reported in the literature as one of the primary impairments following stroke. A reduced arm mobility impacts the patient independence in activities of daily life, and his/her capability to perform their normal social and occupational activities, thus resulting often in depression. Therefore, the recovery of arm movements is one of the most important goals of stroke rehabilitation.

There is common agreement in literature that the re-learning of lost functions is encouraged by the functional practice of task oriented exercises aimed at re-acquiring a practical skill, rather than simple repetition of a movement [1]. Other key elements which facilitate the motor relearning process after stroke are the maximization of the patient's involvement during the execution of the exercise and the use of Neuro Muscular Electrical Stimulation (NMES) in combination with the residual volitional effort [2].

RETRAINER supports arm functions combining several technologies to take benefits from the strength of each of them, overcoming the limited performance of each single approach. Indeed, on one side it uses a passive arm exoskeleton for weight relief to increase the possible range of motion and to reduce the effort needed to accomplish daily life tasks; on the other side, it exploits the combination of NMES and volitional contractions to provide an increased afferent feedback able to facilitate cortical plasticity and therefore motor recovery. The aim of the present study is to describe the control modality of the RETRAINER arm system giving some preliminary examples of its potential use.

Material and Methods

Architecture

The RETRAINER arm system includes an exoskeleton characterized by 3 degrees of freedom (DoFs): shoulder elevation, shoulder rotation in the transversal plane and elbow flexion/extension. Each DoF is equipped with an electromagnetic brake to prevent unnecessary fatigue to maintain specific postures. Two antigravity compensation modules based on springs are integrated at the shoulder and the elbow joint to relief the weight of the arm and the forearm, respectively. For more details on the exoskeleton please refer to [3]. The apparatus comprises also a current-controlled stimulator including two stimulation channels and two channels for EMG recordings (RehaMovePro, Hasomed GmbH) [4]. Both the stimulator and the exoskeleton module are connected to an Embedded Control System (ECS), which runs on a BeagleBoneBlack™. The ECS communicates with a state machine, running on a windows-based tablet, which provides both the high level control of the system and a graphical user interface (GUI) for the therapist and the patient. Interactive objects complete the system setup; they are daily life objects equipped with RFID (Radio Frequency IDentification) tags. Within RETRAINER, they are used to identify the target positions and to guide the execution of a sequence of tasks. A suitable reader is embedded in the exoskeleton, in proximity to the wrist

joint. Figure 1 shows the UML component diagram of the RETRAINER arm system.

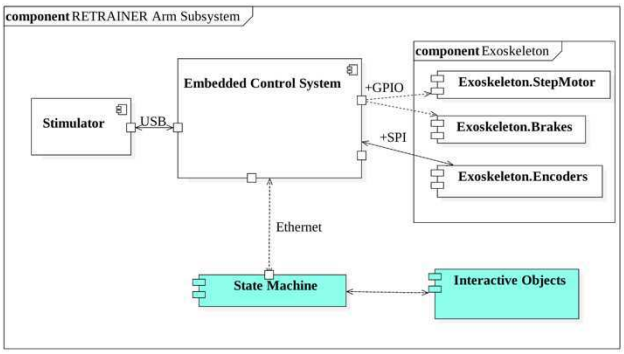

Figure 1: UML component diagram of the RETRAINER arm system architecture. Real-time and non real-time components are shown in white and light blue, respectively.

Figure 2 describes the overall structure of the control system, which is based on two main modules:
1) the State Machine, which is the intelligence of the RETRAINER system, and drives both the setting and the execution of the exercises. It includes a database to store patients' data and to display summaries of the achieved results. The state machine divides the exercise into single movement primitives. The execution of these movement primitives by means of the available actuators is then performed by the ECS.
2) the Embedded Control System controls all the modules requiring real time constraints, such as the stimulator and the exoskeleton sensors. The ECS module is just an executor of the commands sent by the state machine.
The communication between the ECS and the State Machine is developed by means of a raw Ethernet communication UDP protocol.

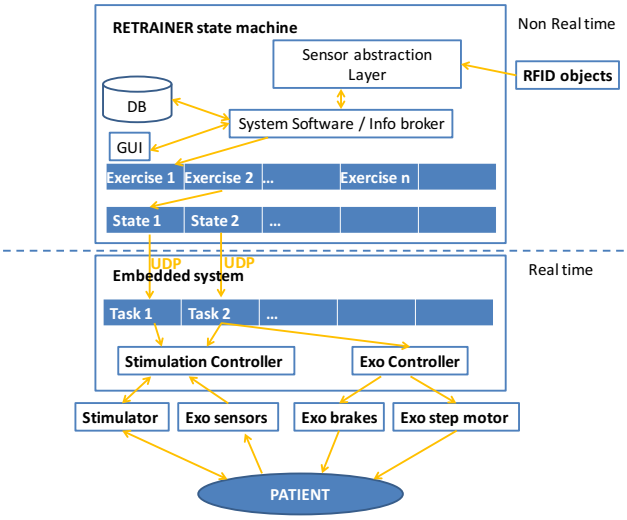

Figure 2 Overall structure of RETRAINER arm system.

Stimulation controller

An EMG-triggered stimulation controller is included in the ECS. Up to two muscles can be stimulated simultaneously and the target muscles are selected by the therapist based on the specific need of each patient. For each muscle, the residual volitional EMG signal is detected and used to trigger the onset of a predetermined stimulation sequence. In case the muscle does not reach the pre-defined threshold, the stimulation is started after a time-out of 5 seconds.
After the execution of each movement primitive, a feedback on the voluntary activity concurrent to NMES is visually displayed to the user with a smiley or not-smiley face in order to promote the active involvement of the subject. To estimate the volitional EMG during NMES a filter previously developed by the Authors is applied [5].
A fast and automatic calibration procedure is required before the beginning of each session. This procedure aims at setting the current amplitude to be used for each stimulated muscles and the thresholds on the volitional EMG. Specifically, three thresholds are set on each muscle: two of them are used to trigger the stimulation, one in case the muscle is the first to be activated and one in case the muscle is activated when the other one is already stimulated; the third threshold is used to define the active involvement of the patient in the task execution.

System setting and usage

Figure 3 shows the workflow of a typical training day with the RETRAINER system, which consists of three main steps: the donning and calibration of the system, and its use during a predefined set of exercises.

Donning & Calibration

The donning phase starts with the placement of the EMG and stimulation electrodes. Once the electrode placement is checked through the GUI, the therapist should adjust the exoskeleton lengths to fit with the patient, let the patient don the exoskeleton and set the gravity compensation level. The following step is the calibration of the current amplitudes and the EMG thresholds. Based on the choice of the exercises for the training session, the required interactive objects are selected and calibrated together with the target positions to be reached. Once the calibration is finished, all the configuration parameters are stored and the training session can start.
On the following training days, the donning and calibration procedure is partly simplified since the therapist can load the parameters of the previous day and eventually adjust them.

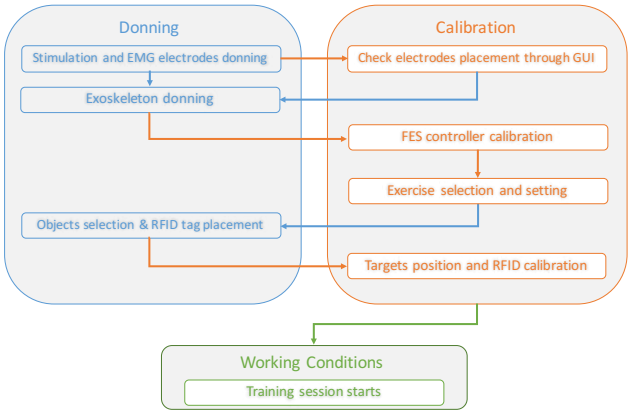

Figure 3: Workflow of the donning, calibration and training phases using RETRAINER system to rehabilitate arm functions.

Working condition

The training consists on the execution of a series of exercises involving the arm during daily life activities. Typical exercises are anterior reaching, moving an objects on a plane and in the space, and moving the hand to the mouth both with and without an object. Each of the exercises is divided into sub-movements which are initiated by the state machine.

Results

Figure 4 reports one screenshot of the GUI during the execution of the anterior reaching exercise. It shows the picture of the subject with the target points to be reached. In the lower part, the angles measured by the exoskeleton at the three DoF, the use of the brakes, the timer of the exercise, and the stimulation parameters are shown. At the end of each sub-movement a feedback to the user related to its volitional involvement will be also shown.

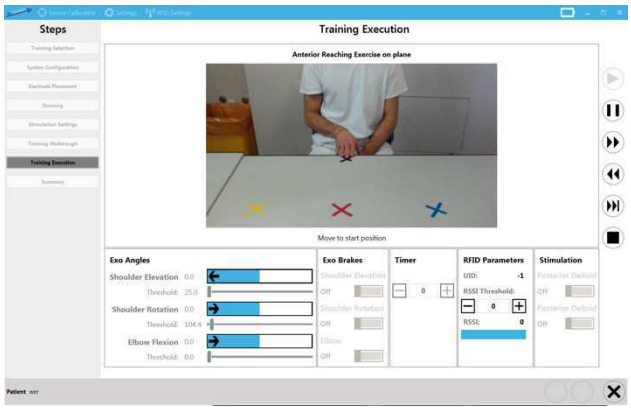

Figure 4: The example of a screenshot of the GUI during the execution of the anterior reaching exercise.

Figure 5 reports the results of a procedure for setting the EMG thresholds, carried out on a healthy subject (male, age of 23 years old). The stimulated muscles were the medial deltoid (in blue) and the triceps muscle (in red). In the upper panel, the stimulation current profiles are shown, while the middle and lower panel depict the volitional EMG estimated for the medial deltoid and the triceps muscle, respectively, as well as the thresholds calculated for each muscle (solid horizontal line). The first threshold corresponds to the double of the mean volitional EMG during a phase in which no stimulation is provided. This threshold is the one used to trigger the stimulation when the muscle is the first to be activated. The second threshold is the double of the mean volitional EMG with the other muscle is constantly stimulated; this is the threshold used to trigger the stimulation when the muscle is the second to be stimulated. Finally, the third threshold is the one used to evaluate the active participation of the subject and is computed as the mean volitional EMG with both muscles stimulated. During the whole calibration phase, the subject is asked to remain relaxed.

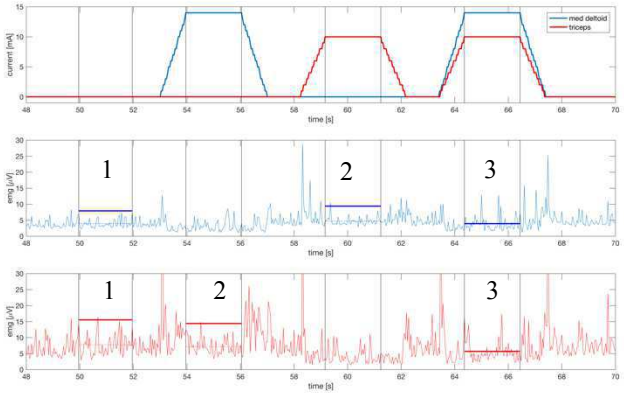

Figure 5: An example of a calibration procedure for setting the thresholds of the volitional EMG, carried out on a healthy subject.

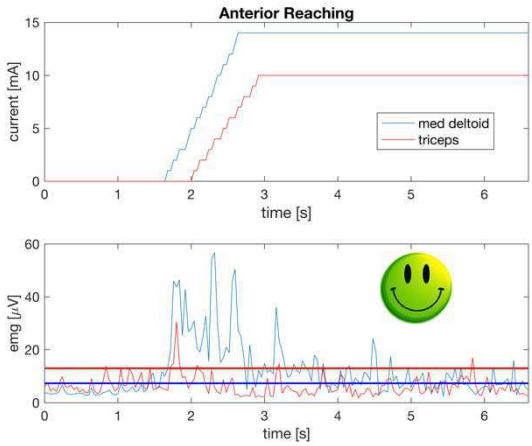

Figure 6: An example of a sub-movement of the anterior reaching exercise. The upper panel shows the stimulation current profiles for the two muscles; the lower panel depicts the volitional EMG as well as the thresholds (horizontal solid line) used for triggering the stimulation.

Figure 6 shows the stimulation current profiles (upper panel) and the volitional EMG (lower panel) obtained for a healthy subject while executing a single sub-movement

of the anterior reaching exercise. Since the activation of the medial deltoid occurred earlier than that of the triceps muscle, the medial deltoid was activated first. Few milliseconds after also the triceps muscle overcame the activation threshold and the stimulation was triggered. The stimulation increased with a ramp of 2 seconds until reaching the maximal value set during the initial calibration. The involvement of the subject in the task execution was judged as active, as indicated by the smiley face.

Discussion

The RETRAINER arm system integrates a novel passive arm exoskeleton for weight relief with an arm neuroprosthesis combining the afferent feedback of NMES with the residual volitional effort of the patient. One of the main requirement of the system was to minimize as much as possible the encumbrance and maximize the portability. To reach this aim, a locking mechanism which allows to mount the exoskeleton of any wheelchair or normal chair has been developed; the stimulator and the EMG amplifier have been integrated in a unique small device and the control system has been implemented partially on a tablet and partially on a BeagleBoneBlack™ to allow real-time calculation without the use of a PC.
The proof-of-concept of the RETRAINER arm system has been tested on healthy subjects, while its efficacy on post- acute stroke patients will be evaluated by means of a multicenter randomized control trial that will start in Autumn 2016 in the premises of the two clinical partners of the project (Villa Beretta, in Italy, and Asklepios Königstein, in Germany).

Acknowledgement

This study was funded by the European project RETRAINER (Horizon 2020, Research and Innovation Program, grant agreement No 644721).

References

[1] Krakauer, J.W. Arm function after stroke: from physiology to recovery. *Semin Neurol*, vol. 14, no. 4, pp. 384–395, 2005.
[2] Gandolla, M., Ferrante, S., Molteni, F., et al, "Re-thinking the role of motor cortex: Context-sensitive motor outputs?," *Neuroimage*, vol. 91, pp. 366–374, 2014.
[3] Puchinger, M., Wiesener, C., Schauer, T., et al. The ReTrainer arm exoskeleton - a modular lightweight device that combines adjustable gravity compensation, lockable joints and neuromuscular electrical stimulation. 12th Vienna International Workshop on FES, Sept 2016.
[4] Valtin, M., Kociemba, K., Behling, C., Kuberski, B., Becker, S., Schauer, T. RehaMovePro: A versatile mobile stimulation system for transcutaneous FES applications. *European Journal of Translational Myology*, vol. 26, no. 3, 2016.
[5] Ambrosini, E., Ferrante, S., Schauer, T., et al. A myocontrolled neuroprosthesis integrated with a passive exoskeleton to support upper limb activities. *J Electromyogr Kinesiol,* vol. 24, no. 2, pp. 307-17, 2014.

Author's Address

Simona Ferrante
NearLab, DEIB, Politecnico di Milano
simona.ferrante@polimi.it
http://nearlab.polimi.it

The RETRAINER hand orthosis:

an event-driven modular lightweight device that combines controlled hand-wrist motion and multi-electrode neuromuscular stimulation

Crema A[1], Raschella F[1], Furfaro I[1], Wiesener C[2], Zajc J[3], Becker S[4], Epperlein M[4], Weber M[4], Russold M[3], Schauer T[2], D'Amico E[5] , Bulgheroni M[5], Micera S[1]

[1]Translational Neural Engineering Laboratory, EPFL, Switzerland

[2]Control System Group, Technische Universitaet Berlin, Germany

[3]Ottobock Health Products GmbH, Vienna, Austria

[4]Hasomed GmbH, Magdeburg, Germany

[5]Ab.Acus , Milan, Italy

Abstract: *RETRAINER is an innovation project aimed at bringing to clinical practice a multimodal rehabilitation platform for daily upper limb support developed in MUNDUS [1]. RETRAINER is aimed at providing rehabilitation to patients with reaching and grasping deficiencies in a context of interactivity with objects of daily living. Two core sub-systems are currently in development: sub-system S1 targets the assisted reaching rehabilitation, sub-system S2 targets hand pre-shaping and grasping of the selected objects by means of power grasp. This paper provides a technical description of S2, its usage scenarios, and the technical assessment of the performances of its submodules. S2 deals with the muscle weakness and spasticity by using a combination of rigid and compliant hand-wrist-forearm orthoses, and multi pad electrodes for FES. Caregivers can create stimulation maps by moving Virtual Electrodes on a GUI, and associate each stimulation map (SM) to a specific task of predefined exercises. Stimulation maps are high level visual abstraction, translated to spatial-temporal stimulation patterns by an embedded controller (EC). An RFID antenna detects tagged objects and areas of the workspace, and informs the EC of the detected events. Position sensors, hosted on the dorsal side of the orthosis, and force sensors on the volar aspect of the hand inform the EC about the hand-wrist kinematics and the grasp forces, which can modulate the stimulation intensity in accordance to the desired task.*

Keywords: *hand rehabilitation, hand orthosis, neuromuscular electrical stimulation, electrodes array*

Introduction

Stroke is endemic and effective methods for recovery are highly dependent on the cognitive and motor impairment of the patient [1,2]. It's usual practice to consider peak neurological recovery within the 1st and the 3rd month after the stroke. Lower pace recovery usually happens within the 6th month. Contradictory information is reported for chronic patients. Factors that can set apart the efficacy of a treatment include the specificity of the performed task, its intensity, and a significant repetition of such task. Functional tasks such as reaching and grasping common objects, and performing basic motion with them is a way to both assess and improve one's independence in activities of daily living. NeuroMuscular electrical stimulation (NMES) is a way to train functionally the muscles that are insufficiently recruited through volitional pathways. One of its limitations is the lack of overall simplicity in its use for functional grasp rehabilitation with standard commercial products. Effective calibration and control strategies of multi-electrode arrays NMES is needed [3] for translating to higher scale the use of NMES, and hybrid approaches appear as the necessary next steps [4]. Research grade prototypes with similar needs were previously tested [5] in the MUNDUS project. Based on this experience, RETRAINER [6,7] is deploying a re-thought and refined prototype, comprising two modules: the S1 [8] sub-system, focused on the arm, and the S2 sub-system, focused on the forearm and hand. The RETRAINER S2 sub-system is aimed at providing rehabilitation to end-users with grasp deficiencies. The approach is twofold. First, patients unable to control the wrist take advantage of a custom orthosis designed to limit wrist movements. Second, hand opening and objects grasping are assisted by NMES, contextually triggered by an RFID system. The aim of this present study is to describe the components of S2 and the control modality.

Material and Methods

Architecture

The RETRAINER hand system includes two sensorized hand-orthoses, used to provide different constraining

characteristics in different scenarios, and a current-controlled multichannel stimulator [9] connected to custom made electrode arrays. Both the stimulator and the orthosis are connected to an Embedded Control System (ECS), hosted on a pocket-size computer (BeagleBone Black, Beagleboard.org Foundation) which provides real-time control of the connected modules. A high level GUI [10], hosted on a tablet (Surface Pro 3, Microsoft Corp.), communicates with the ECS, manages state-machine for the control of the exercises, tasks, patients' data, and data tracking in general. The GUI is also connected to an RFID module providing contextual information about the proximity to reference points in space and tagged objects. Figure 1 shows the UML component diagram of the RETRAINER hand system.

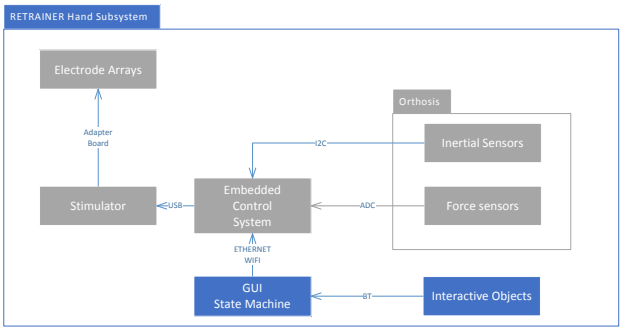

Figure 1: UML component diagram of the RETRAINER hand system architecture. Real-time components are shown in grey, non real-time components are shown in blue

The overall control system of S2 is visible in Figure 2 and, similarly to S1, decouples the operations between high level motor primitives, which are handled by the GUI in relation to the necessary training of the patient, and the low level control, handled by the ECS.

Components

Hand Orthosis

Two hand orthoses are designed to reflect the needs of the various exercises. A set of exercises requires a controlled hand opening, with the wrist motility under the control of the patient, or for exercising wrist mobility also with NMES. The other set of exercises requires the forearm to stay in neutral positions and to assist grasp of cylindrical objects of diameters ranging from 30 mm to 70mm.

The first orthosis holds two inertial sensors (InvenSense, MPU9250, San Jose, California), used to monitor the motion of the hand with respect to the wrist. The second orthosis prevents the hand-wrist movements and holds the thumb in opposition. A gummy ring is used to easily fix the thumb on its support, and to host a force sensor (Tekscan Inc., Flexiforce A201, A401) used to detect object grasp. Flexible clasps, also containing force sensors, are placed on medium and ring finger constrain the movements of the first and second phalanges. Rigid PLA orthoses are available in 5 sizes for left and right side. Adaptation of the orthoses to the individual needs can be performed by heating the part and selectively bending upon need. Flexible TPE clasps and rings are available in 11 sizes. The orthoses are shown in Figure 3.

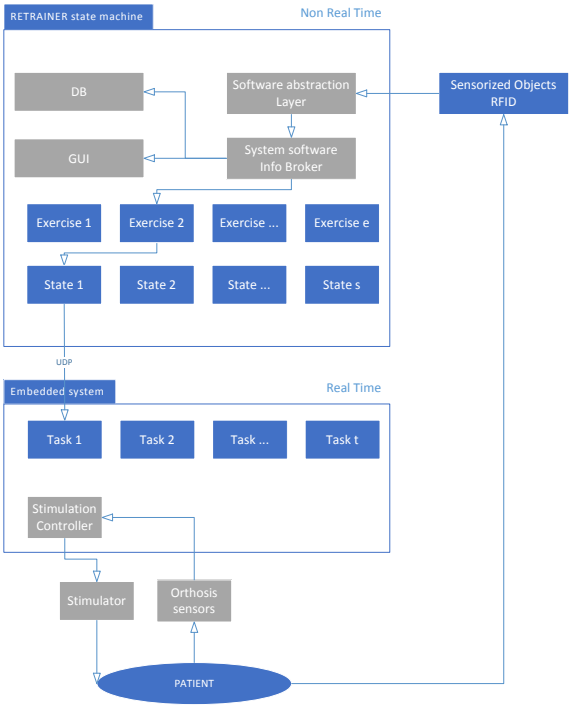

Figure 2: Overall structure of the RETRAINER arm system

Electrode arrays

Custom made electrode arrays (EAs) have been interfaced with the stimulator. EAs contain conductive tracks screen printed on a PET substrate, and selectively isolated with dielectric. Each electrode arrays (EAs) contains 16 independent active pads arranged in four rows and columns. Two ground electrodes are symmetrically positioned on the sides. Active sites measure 10x12mm^2, whereas grounds measure 20x40 mm^2. The EAs can be then cut to improve the local bendability for skin fitting. The interface between electrode arrays and skin is commercial hydrogel (AG735, Axelgaard inc.), which guarantees proper electrical impedance, mechanical adherence to the skin and provides stability of the contact.

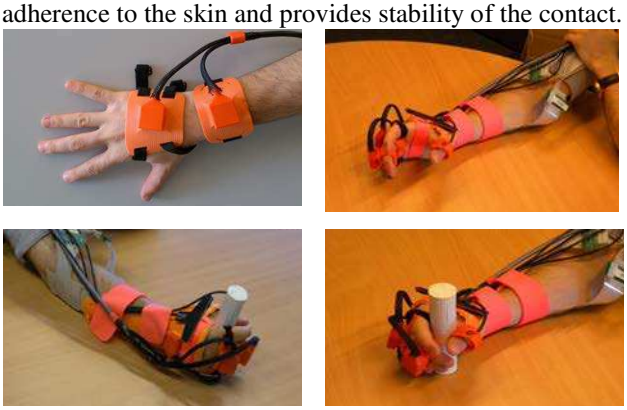

Figure 3: Orthoses, design and wearability. Top left: Wrist motion control orthosis.

Details of the electrode arrays are shown in Figure 4.

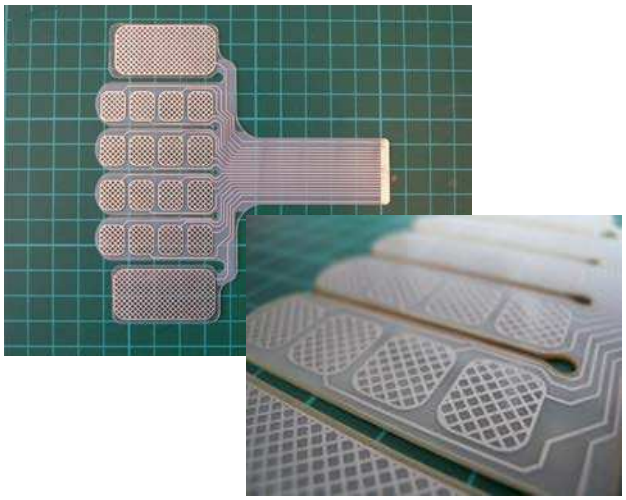

Figure 4: Custom electrode arrays. Top: layout. Bottom: details of the screen printing finishing. The electrodes can be trimmed in accordance to the desired use and mounting.

GUI

The GUI runs on a 12" windows-tablet with touch capabilities. It allows to guide the operator through different phase, such as sensors calibration, orthosis donning, NMES parameters setting and exercises execution stimulation. Two EAs are positioned on the forearm on the extrinsic extensors, and one on proximal extrinsic flexors, thus the most significant muscles that can be transdermally elicited can be targeted. The GUI represents each EA as a grid on which Virtual Electrodes (VEs) can be moved as shown in Figure 5. A VE is a 2D cursor representing the location of the stimulation pattern. As example, if a VE is centred in one square of the grid, the stimulation will be provided exclusively at the corresponding pad on the EA. Conversely, if the VE lies on four adjacent squares, the corresponding electrode pads will be elicited over time in accordance to the percentage of overlap.

Up to five VEs are available on the GUI for defining location and intensity of stimulation current. With this approach the clinical operator is provided with an interactive and intuitive means to create patient-specific stimulation maps for each state.

RFID and Objects

The mechanical structure of the fixed-wrist orthosis hosts the antenna of the RFID module[11]. Objects and locations in the workspace are defined by one or more RFID tags with unique identifiers. For each identifier the returned RSSI is used as a calibrated proximity detector, used for triggering actions or for acknowledging the completion of a task.

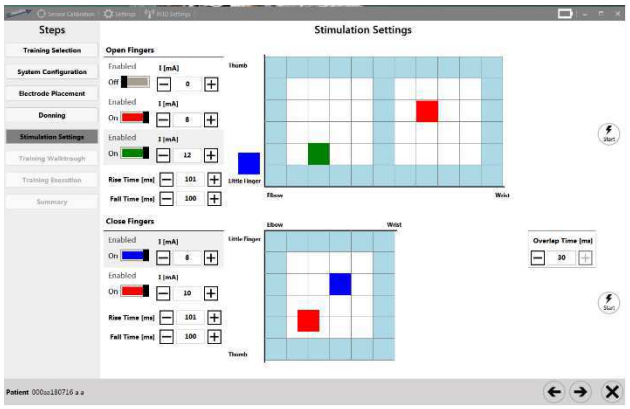

Figure 5: screenshot of the GUI stimulation parameters settings. 3 VEs can be displaced within the extensors stimulation map, 2 VEs within the flexors one.

Stimulation controller

GUI triggered stimulation is included in the ECS. One stimulation map is active a time, with the exception of transients from one stimulation map to another. In cases in which there is a state transition from e.g. "open hand" to "grasp", a selectable overlap of the stimulation profiles can be used to induce co-contraction of agonists and antagonists, and to smooth the motion transition. Excluding transition phases, up to two VEs for extrinsic flexors or up to three VEs for extrinsic extensors are actively stimulating. Before the execution of each movement, the GUI presents the expected motion to the patients. If the volitional motion is not sufficient to achieve the desired task, stimulation as-needed is provided in accordance to the instrumental information. The desired motion is defined as threshold angles for hand opening tasks, and minimum necessary force for grasp tasks. Custom tuned PID controllers control the different phases of hand opening and grasping by adapting the stimulation pulsewidth.

System setting and usage

The use of S2 for intensive training requires a two steps preparation. Differently from S1, which is shared by several patients, S2 is personalized for each patient. During the first use (Day Zero) the clinician can select the parts best matching the patient's size, and can termo-shape the rigid orthoses for best fit. Thermo-shaping can be performed e.g. with hot water, or with a standard heat-gun. Electrode arrays can be also be tested and adapted to specific needs. When the system is physically configured for the very patient, for everyday training (Day One) the system needs to be worn anc calibrated for the desired tasks. Figure 6 reports a schematic workflow of the involved activities.

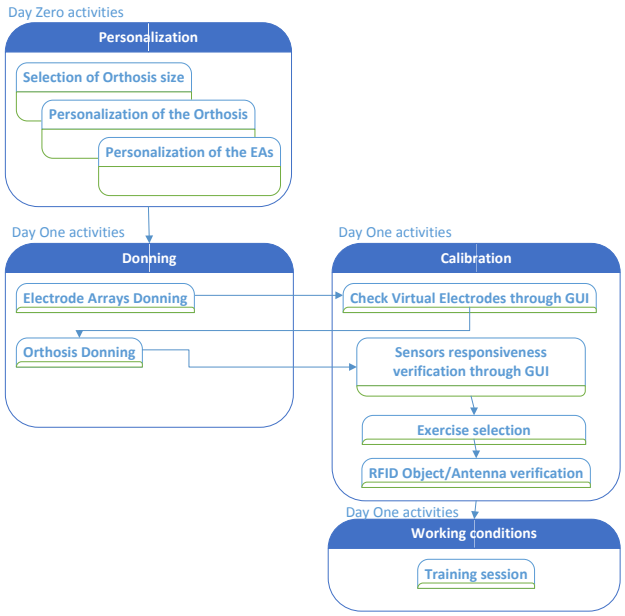

Figure 6: Workflow of the configuration, donning, calibration, and use in working conditions

Results and Discussion

The RETRAINER hand system is a system aimed to provide rehabilitation to end-users with grasp deficiencies. The system consists on a novel set of orthoses aimed at supporting grasp with unobstructed palmar contact. The system is currently aimed for power grasp exercises, and can provide NMES assistance through newly developed electrode arrays. The configuration of the stimulation is performed directly by the clinician or, in general, by the caregiver by positioning through a touch-based GUI virtual electrodes. The direct supervised mapping of virtual electrodes is aimed at finding a conscious optimal trade-off between efficacy of stimulation and nociceptive perception. Each stimulation map defines stimulation location, and standard stimulation intensity. A low level algorithm translates this information in randomized spatial and temporal patterns of stimulation, and modulates the standard stimulation intensity in accordance to the measurable goals of hand opening and grasp intensity. If the patient is able to volitionally obtain the desired goals, no stimulation is provided. Volitional motion that is only partially achieved is supported by stimulation as-needed. Programmed task can rely on time based stimulation execution, event based detection of kinematic thresholds for motion. The exercises benefit from environmental RFID triggering, which allows to define a custom workspace for the patients, and thus personalize the treatment in accordance to specific deficits and clinical goals by simply moving tagged objects and functional landmarks.

Acknowledgement

This study was funded by the European Project RETRAINER (Horizon 2020, Research and Innovation Program, grant agreement No 644721)

References

[1] WHO, *"Global status report on noncommunicable diseases 2014"*, World Health, p. 176, 2014.

[2] R. Teasell et al, "*Evidence Based Review of Stroke Rehabilitation*" 2015 Hearth & Stroke Foundation, Canadian Partnership for Stroke Recovery, ebrsr.com.

[3] A. Koutsou, J. Moreno, A. J. Del Ama, E. Roncon et J.Pons , "Advances in selective activation of muscles for non-invasive motor neuroprostheses".JNER 2016 13:56 DOI 10.1186/s12984-016-0165-2

[4] D. B. Popovic, "Advances in functional electrical stimulation (FES)", Journal of Electromyography and Kinesiology 24 (2014) 795–802

[5] Pedrocchi et al., *"MUNDUS project: MUltimodal Neuroprosthesis for daily Upper limb Support" JNER 2013 10:66 DOI: 10.1186/1743-0003-10-66*

[6] *RETRAINER Project, http://www.retrainer.eu/*

[7] M. Bulgheroni et al., *"Reaching and Grasping training based on robotic hybrid assistance for neurological patients"*. 12th Vienna International Workshop on FES, Sept 2016.

[8] S. Ferrante et al., *"The RETRAINER control system for supporting arm functions"*. 12th Vienna International Workshop on FES, Sept 2016.

[9] M. Valtin, K. Kociemba, C. Behling, B. Kuberski, S. Becker, T. Schauer; "*RehaMovePro: A versatile mobile stimulation system for transcutaneous FES applications."* European Journal of Translational Myology, 26(3), 2016. DOI: 10.4081/ejtm.2016.6076J. Zajc et al., *"Unified Control Interface for multiple Devices used for Upper Limb Rehabilitation after Stroke"*. 12th Vienna International Workshop on FES, Sept 2016.

[10] J. Zajc et al., *"Unified Control Interface for multiple Devices used for Upper Limb Rehabilitation after Stroke"*. 12th Vienna International Workshop on FES, Sept 2016.

[11] M. Bulgheroni, E. D'Amico, and L. Sartori, *"RFID Technology for Objects Recognition and their Position Estimation"*, in J.L. Pons et al. Converging Clin. Eng. Res. on NR, BIOSYSROB 1, vol. 1, pp 1165-1169, 2013.

Author's Address

Andrea Crema
Translationa Neural Engineering Laboratory, EPFL, Switzerland
andrea.crema@epfl.ch
tne.epfl.ch

Unified Control Interface for multiple Devices used for Upper Limb Rehabilitation after Stroke

Zajc J[1], Wiesener C[2], Crema A[3], Ferrante S[4], Bonizzi Ch[5], Bulgheroni M[5], Schauer T[2], Russold M[1]

[1]Otto Bock Healthcare Products GmbH, Vienna, Austria
[2]Control Systems Group, Technische Universität Berlin, Germany
[3]Translational Neural Engineering Laboratory, EPFL, Switzerland
[4]Bioengineering Department, Politecnico di Milano, Italy
[5]Ab.Acus srl, Milano, Italy

Abstract: *RETRAINER is a stroke rehabilitation system comprised of two devices aimed at training arm and hand movements using Neuromuscular Electrical Stimulation (NMES). At the heart of the S1 system is a passive exoskeleton supporting the patient with a weight relief system, and S2 provides a sensorized hand-orthosis to support grasping and flexion/extension of the wrist. The versatile applicability in a huge variety of training exercises, the different stimulation methods for each device, the interactive objects used for a more efficient training and a multitude of different sensors to track the rehabilitation progress render the RETRAINER an immensely powerful yet also technically complex rehabilitation system. RETRAINER will be validated in a multicentre randomized controlled trial using multiple different activities of daily life. Safety and stability of the control system, as well as an optimized usability was therefore a primary focus of the development. This paper describes the realisation of the RETRAINER control interface and the software architecture implemented to guarantee safety, reliability and usability of RETRAINER.*

Keywords: *upper limb rehabilitation, hand orthosis, exoskeleton, electrode arrays, interactive objects, GUI, Hybrid robotic rehabilitation system, stroke survivors, randomized control clinical trial, weight compensation, functional electrical stimulation, myocontrol neuroprosthesis*

Introduction

With non-communicable diseases on the rise [1], stroke has become today's number one cause of disability in the western world [2]. Especially the locomotor disabilities associated with stroke contribute significantly limit meaningful activities and full participation in daily life. Therefore, improving motor outcomes – especially the recovery of voluntary hand and arm function – is not just an important goal during stroke rehabilitation but a major focus of medical research. Nevertheless, still over 60% of patients are left with incomplete motor recovery after rehabilitation and cannot use the affected hand or arm in functional activities [3].

The goal of the RETRAINER project is to develop and validate a novel rehabilitation system. This system is based on the results of the FP7 European project MUNDUS [4]. The project aims at improving the outcome of upper limb rehabilitation following stroke. With strong clinical and scientific evidence, that Neuromuscular Electrical Stimulation (NMES) in rehabilitation can improve arm and hand function [5], RETRAINER exploits NMES to improve upper limp recovery. The system enables rehabilitation of the hand and arm using two rehabilitation devices and several common components.

The S1 device is used to train arm functionality, enhancing the beneficial effect of NMES even further by using the patient's residual muscle functionality to voluntarily trigger NMES stimulation [6][7][8].

The S2 device is used to train hand movements, especially focusing on grasping. S2 provides multi electrode arrays allowing a post-donning calibration due to multiple smaller more selective electrodes.

The RETRAINER system will be validated in a multicentre randomized controlled trial using multiple different activities of daily life. During the trial the two devices will be used to train activities of daily life with a focus on grasping, moving and releasing of objects.

A control interface will guide the user through the training session and supports completion of the specified exercises automatically. Exercise control uses goniometric sensors, Force Sensitive Resistors (FSR), Inertial Measurement Units (IMU) and Radio Frequency IDentification (RFID) technology[9][10].

The NMES in RETRAINER system is provided by the RehaMovePro stimulator provided by HASOMED GmbH – a state of the art multichannel stimulator with EMG triggering and multi-electrode support [11].

Integration of two independent yet compatible rehabilitation devices into one (control) framework, including multiple further components posed a considerable challenge. The complete rehabilitation system is a medical device. Therefore special attention has to be paid to reliability and usability. This paper focuses thus on the implementation of the control interface that supports the system. Moreover, it will explain the software architecture and safety aspects that were considered.

RETRAINER System Overview

This section will give a short overview of the RETRAINER system components and describe these are combined to form the two devices that will be used during the clinical trials.
Fig. 1 depicts an overview of the RETRAINER system components.

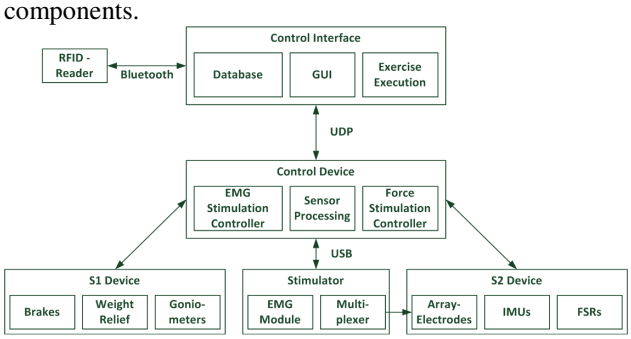

Figure 1: Overview of the RETRAINER system

The system mainly consists of a control interface, a control device and a combination of different components that form either S1 or S2. A brief more detailed description of these is given below:
Control interface: The RETRAINER system is controlled by a graphical user interface (GUI) that will run on every computer using a Windows operation system. The control interface is connected to the control device via Ethernet or WiFi. The control interface features improved usability of the system and allows access to all relevant system settings.
Control device: The plug and play control device acts as hardware interface between the control interface and the components described below. It is connected to the devices' sensors and actuators and communicates with the stimulator via USB.
Stimulator: The stimulator comprises an EMG module, used to measure volitional muscle signals even during stimulation. It also features a De-Multiplexer for use with multi electrode-arrays (S2 device only).
RFID-reader and interactive objects: Objects used in the training exercises are tagged with RFID chips. An RFID-reader, communicating directly with the control interface via Bluetooth provides information about the used object.
Depending on the exercise in mind these components are combined to form either S1 or S2.
S1 device: The S1 device consists of a passive upper limb exoskeleton with a passive, digitally adaptable weight relief, goniometric sensors to measure movement and brakes to block the exoskeleton's joints. Electrical stimulation is used as needed.
S2 device: The S2 device consists of a hand orthosis, harbouring IMU and FSR to measure movement and grasp force. Additionally, S2 comprises two array-electrodes for electrical stimulation.

In training sessions using the S1 device, weight relief, stimulation settings and control parameters are set using the GUI. During the exercise execution, the control device runs the EMG-based stimulation controller to generate stimulation impulses based on the volitional muscle functionality recorded by the EMG module. Goniometric sensor data is polled by the control device and forwarded to the control interface where it is combined with data polled from the RFID-reader. Based on this data, the exercise execution module updates controller parameters, objects visualized in the GUI and sets/resets the brakes as required.
In training sessions using the S2 device, the GUI is used to set stimulation parameters including the position of the virtual electrodes on the multi electrode-array and control parameters are set using the GUI of the control interface. During the exercise execution, the control device runs the stimulation controller based on the measured grasp force to generate appropriate stimulation. IMU sensor data and FSR sensor data is polled by the control device and is forwarded to the control interface where it is combined with data polled from the RFID-reader. Based on this data, the exercise execution module updates controller parameters and objects visualized in the GUI.

Requirements to the Control Interface

The GUI has some basic tasks to fulfil. These include

- Maintenance of patient database
- Control of attached components (via control device)
- Exercise setup and execution for and with patients
- Data logging during exercise execution
- Patient assessment tests
- Usability and patient safety

These basic tasks are embedded into the overall aim to develop a graphical user interface that is optimized for usability during clinical use. The interface also aims to provide an interface to all attached components (including their calibration) without making these steps unnecessary complicated. Moreover, with the RETRAINER system being a medical device, due diligence was put into system safety and reliability. Therefore a risk analysis following follow ISO 14971 was performed, leading to some additional safety considerations:
Uncontrolled user input: It must not be possible to set parameters to illicit values via the GUI.
Control interface crashes/Communication is lost: A loss of communication or a crash of the control interface must not lead to unexpected system behavior.
Synchronization issues: To prevent unexpected system behavior the system state has to be in synchronization with the state depicted in the control interface.
Multi-thread access: To prevent crashes of the control interface, the interface has to be implemented thread save. Special attention has to be given to the communication with the control device and the RFID-reader.

Realization of the control interface

The requirements and safety considerations mentioned above lead to the development of the software architecture depicted in Fig. 2. The solid lines represent the visible GUI components and paths, while the dotted lines represent control interface components working as data containers in the background.

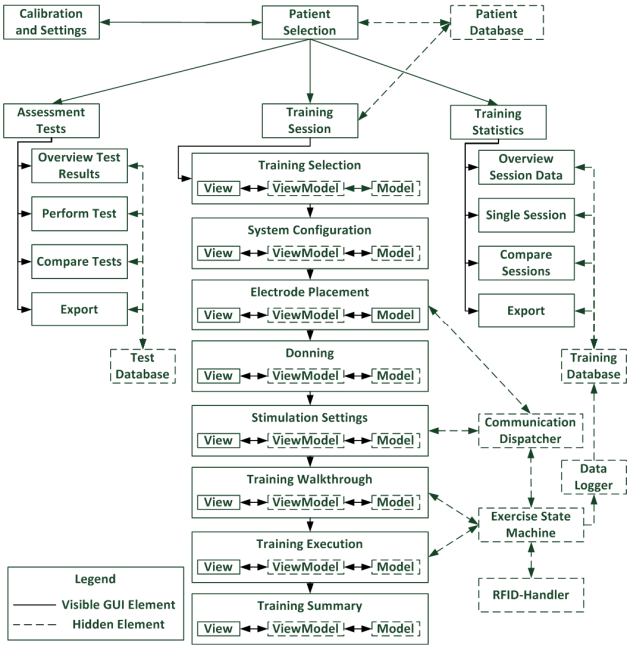

Figure 2: Software Architecture of the RETRAINER system

The entire GUI is implemented using Windows Presentation Foundation (WPF) following the Model-View-ViewModel (MVVM) concept. This concept strictly separates non-critical visual (GUI) components form critical components controlling hardware devices, which therefore contribute to system safety and stability. The viewmodel separates the user input in the view from the algorithm implemented in the data-model, adding an additional safety layer.

The GUI elements used do not allow direct user input and the corresponding parameter value can only be incremented/decremented by a predefined value.

The training session branch is the core of the GUI and enables patient training by means of the S1 and S2 rehabilitation devices. For safety and usability reasons, this entire branch is implemented as a wizard, meaning that one step has to be completed correctly, before the next can be started. This wizard will guide the user through each step of the training session. Textual explanations and images are used to visualize each step to be performed. To further increase usability of the system and because the basic steps are very similar for S1 and S2, the same step sequence is used for both systems. The components visible in the GUI and the underlying algorithms are fundamentally different for the two devices.

In order to keep all components synchronized, a strict master-slave concept was implemented. In this system the control device must not act independently, but only react to commands given by the control interface. Commands are sent by a communication dispatcher, implementing a communication protocol based on the User Datagram Protocol (UDP). The dispatcher is realized using a singleton class, to prohibit the instantiation of multiple instances, which could lead to catastrophic errors. The communication dispatcher comprises a thread save blocking queue, running in a separated thread, assuring that every message is sent and received correctly. Additionally, an idle signal was defined. If the control device doesn't receive an idle signal anymore, it automatically switches into a save state until communication is reestablished.

Similar to the communication dispatcher, the RFID-handler is too realized as a singleton class, enabling direct access from multiple model instances. For a maximal efficiency the direct access to the RFID device is realized using background worker threads. To prohibit conflicts when accessing the reader only one background worker thread associated with the RFID-reader can be active at any time.

All classes and execution of the exercise in question are controlled by an exercise state machine. Each task performed by a patient during a single training session is represented by a specific state in the state machine. Transitions between tasks and thus states can be triggered by sensor data, RFID data (depending on the exercise), manually or by a watchdog timer (to prevent users from being stuck). Transitions have to fulfil certain conditions, so called guards. These guards are predefined and are parameterized during the training walkthrough. Training walkthrough is a process in which the GUI guides the patient and a supporting therapist through each task of a training exercise without stimulation. This also has the added benefit of allowing the patient to learn and understand the system and the exercises.

Discussion

Recent integration tests of the RETRAINER system at multiple research and clinical locations were completed successfully and the feedback concerning the GUI and the control interface was positive. These first trials have also shown that the system can be used efficiently. Communication between components was fast and without problems. Timing between certain components had to be improved in order to improve overall speed of the work-flow. Usability of the GUI was considered as good, with some minor corrections requested by the trial users.

Further improvements are currently being developed and testing will continue in the near future. Start of a full clinical trial is currently planned towards the end of this year.

Conclusions

This paper introduced development of the graphical user interface of the RETRAINER system. Focus of the development was on the inclusion of relevant safety and usability considerations into the GUI. RETRAINER is a

medical device and as such safe communication and safe operation are requested by the standard. Moreover, patient safety is a major concern of the risk analysis. At the same time usability of the system needs to ensure safe operation and the GUI must prevent unsafe transitions or system states by design. On the one hand, this was achieved through the use of suitable software patterns (MVVM, Singleton) as well as the implementation of a strict master-slave hierarchy. On the other hand, the control interface was designed as a finite state machine, with clearly defined transitions and plausibility checks at each transition, further improving safety and usability.

Acknowledgement

This project has received funding from the European Research Council (ERC) under the European Union's Horizon 2020 research and innovation programme (grant agreement No [644721])

References

[1] WHO, *"Global status report on noncommunicable diseases 2014"*, World Health, p. 176, 2014.

[2] S. Mendis, "Stroke disability and rehabilitation of stroke: World Health Organization perspective", International Journal of Stroke, vol. 8, no. 1, pp. 3–4, 2013.

[3] J. Dudel, „Grundlagen der Zellphysiologie", in *Physiologie des Menschen, (R.F. Schmidt, G. Thews* und F. Lang, eds.), ch. 1, pp. 3–19, Berlin, Heidelberg, New York: Springer, 2000

[4] A. Pedrocchi, S. Ferrante, E. Ambrosini, M. Gandolla, C. Casellato, T. Schauer, C. Klauer, J. Pascual, C. Vidaurre, M. Gföhler, W. Reichenfelser, J. Karner, S. Micera, A. Crema, F. Molteni, M. Rossini, G. Palumbo, E. Guanziroli, A. Jedlitschka, M. Hack, M. Bulgheroni, E. D'Amico, P. Schenk, S. Zwicker, A. Duschau-Wicke, J. Miseikis, L. Graber, and G. Ferrigno, *"MUNDUS project: MUltimodal Neuroprosthesis for daily Upper limb Support."*Journal of neuroengineering and rehabilitation, vol. 10, p. 66, 2013

[5] O. A. Howlett, N. A. Lannin, L. Ada, and C. Mckinstry, *"Functional electrical stimulation improves activity after stroke: A systematic review with meta-analysis"*, Archives of Physical Medicine and Rehabilitation, vol. 96, no. 5, pp. 934–943, 2015.

[6] G. I. Barsi, D. B. Popovic, I. M. Tarkka, T. Sinkjaer, and M. J. Grey, *"Cortical excitability changes following grasping exercise augmented with electrical stimulation"*, Exp. Brain Res., vol. 191, no. 1, pp. 57–66, 2008.

[7] G. M. Iftime-Nielsen SD, Christensen MS, Vingborg RJ, Sinkjaer T, Roepstorff A, *"Interaction of electrical stimulation and voluntary hand movement in SII and the cerebellum during simulated therapeutic functional electrical stimulation in healthy adults."* Hum Brain Mapp, pp. 33:40–9, 2012.

[8] M. Gandolla, S. Ferrante, F. Molteni, E. Guanziroli, T. Frattini, A. Martegani, G. Ferrigno, K. Friston, A. Pedrocchi, and N. S. Ward, *"Re-thinking the role of motor cortex: Context-sensitive motor outputs?"*, Neuroimage, vol. 91, pp. 366–374, 2014.

[9] M. Bulgheroni, E. D'Amico, and L. Sartori, *"RFID Technology for Objects Recognition and Their Position Estimation,"* I.L. Pons al. Converging Clin. Engi. Res. NR, vol. 1, p. pp. 1 165–1 169, 2013.

[10] C.-C. CHEN, Y.-L. CHEN, and S.-C. CHEN, *"Application of RFID technology--upper extremity rehabilitation training."*, J. Phys. Ther. Sci., vol. 28, no. 2, pp. 519–524, 2016.

[11] M. Valtin, K. Kociemba, C. Behling, B. Kuberski, S. Becker, T. Schauer; *"RehaMovePro: A versatile mobile stimulation system for transcutaneous FES applications."* European Journal of Translational Myology, 26(3), 2016. DOI: 10.4081/ejtm.2016.6076

Author's Address

Johannes Zajc
Ottobock Health Products GmbH
Johannes.Zajc@ottobock.com
www.ottobock.com

Constantin Wiesener
Control Systems Group, Technische Universität Berlin
wiesener@control.tu-berlin.de

Andrea Crema
Translational Neural Engineering Laboratory, EPFL
andrea.crema@epfl.ch
tne.epfl.ch

Simona Ferrante
Bioengineering Department, Politecnico di Milano
simona.ferrante@polimi.it
www.biomed.polimi.it/nearlab/index.html

Chiara Bonizzi
Ab.Acus srl
chiarabonizzi@ab-acus.eu
http://www.ab-acus.eu/

Maria Bulgheroni
Ab.Acus srl
mariabulgheroni@ab-acus.eu
http://www.ab-acus.eu/

Thomas Schauer
Control Systems Group, Technische Universität Berlin,
schauer@control.tu-berlin.de

Michael Russold
Ottobock Healthcare Products GmbH
michael.russold@ottobock.com
www.ottobock.com

Session 1: Basic Research

Blood pressure related neural profiles extracted from pig left vagus nerves using an interfascicular electrode

Sevcencu C[1], Nielsen TN[1], Struijk JJ[2]

[1]Center for Sensory-Motor Interaction (SMI), Aalborg University, Denmark
[2]Medical Informatics, Aalborg University, Denmark

Abstract: *Efforts are currently made to design neural electrodes suitable for neuromodulation therapies for treating autonomic dysfunctions, including resistant hypertension. The present study was performed to investigate if blood pressure (BP) related neural profiles (BPnPs) similar to those previously derived from pig vagus nerves using cuff electrodes can be derived from the same nerves using an interfascicular electrode. In addition, this study aimed to investigate if the BP-related signals used to derive such BPnPs could be selectively recorded with that electrode. The present experiments were performed on eight farm pigs from which the BP was recorded using a catheter placed in the right carotid artery. An electrode comprising four tripolar channels was inserted longitudinally in the left vagus nerve of the animals. Using that electrode, BPnPs resembling the BP waves were derived from at least one electrode channel in six pigs. Furthermore, a topological or amplitude selectivity in regard to recording the related signals was achieved in four of those pigs. Consequently, this study shows that the tested interfascicular electrode can accurately and to some extend selectively record BP-related signals from the pig left vagus nerve.*

Keywords: *interfascicular electrode, blood pressure, selective.*

Introduction

Designing safer and more effective neural electrodes is a condition for the development of a next generation class of therapies for treating impaired autonomic functions by modulating the activity of peripheral nerves mediating such functions [1]. As the peripheral nerves typically comprise neural fibers mediating more than one function, an ideal electrode for such therapies should be able to record from and stimulate the targeted neural fibers exclusively. Although important advances have been achieved in regard to designing neural electrodes for selective recording and stimulation [2-6], efforts are still made for improving such electrodes.

In some of our previous studies, we have developed interfascicular electrodes for selective stimulation of, and recording from rabbit sciatic nerve fascicles [3;4]. In other studies, we used cuff electrodes to record blood pressure (BP) related signals from the left vagus nerve (LVN) of pigs. Deriving the power of those signals resulted in BP-related neural profiles (BPnPs) resembling the BP waves and mirroring BP changes, which suggests that such BPnPs could be used as BP markers in closed-loop LVN stimulation systems for BP control [7]. As the interfascicular electrodes may be a valuable option for interfacing peripheral nerves such as LVN [3;4], the present study aimed to investigate if similar BPnPs could be derived using an interfascicular electrode and if the related signals could be selectively recorded from the pig LVN with that electrode.

Material and Methods

A. Experimental procedures

The present experiments were performed on 8 farm pigs weighing 50±5 kg. The animals were anesthetized with sevoflurane during surgery and by IV infusion of ketamine (20 mg/kg/hour) and xylazine (2 mg/kg/hour) during the recordings. Following the experiments, the pigs were euthanized with an anesthesia overdose. All experimental procedures were approved by the Danish Animal Welfare Committee.

The LVN and the right carotid artery were exposed at a cervical level through lateral neck incisions. The BP was recorded using a catheter inserted in the carotid artery and connected to a pressure transducer (Edwards Lifesciences TM) and the electrocardiogram (ECG) using two surface electrodes to represent lead II.

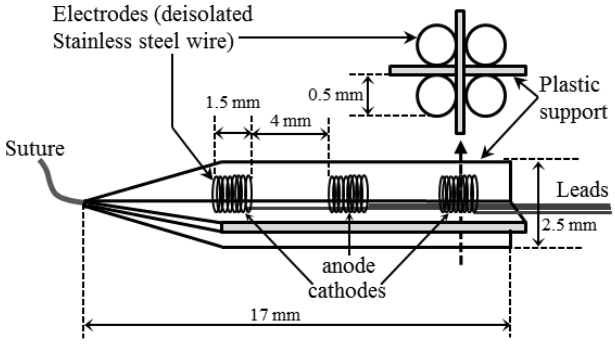

Figure 1: Schematic representation of the interfascicular electrode used in this study. In the right upper corner, a cross-section through the electrode at the indicated location (dashed arrow) shows the positioning of the 4 channels.

A custom-made 4-channel interfascicular electrode (Fig. 1) was inserted in the cervical LVN in a cranial-to-caudal direction and as close as possible to the longitudinal axis of the nerve. This was achieved by pulling the electrode inside the LVN using a suture connected to the tip of the electrode (Fig. 1). The suture was inserted cranially in the

nerve, guided through the nerve and pulled outside the nerve about 3.5 cm caudal from the insertion point using a 25 gauge injection needle. As schematically illustrated in Figure 1, the electrode comprised 4 tripolar channels separated by the cross-oriented wings of a plastic support. Each electrode channel consisted of an anode placed in the middle and 2 cathodes placed 4 mm apart from the anode. All electrode contacts were made by coiling the de-insulated ends of Teflon-coated stainless steel wires (50/114 μm in diameter) and then mounted on the plastic support. All electrode dimensions are shown in Figure 2.
After inserting the electrode, the BP, ECG and the vagus nerve electroneurograms (VENGs), acquired with each channel of the interfascicular electrode, were recorded for 5 minutes in each pig.

B.Data acquisition and analysis
All signals were amplified (ECG = 2.5k-10k, VENG = 100k-1M, and BP = 50k V/V) and filtered (ECG = 1-10 kHz, VENG = 10-10 kHz and BP = DC-10 kHz) using AI402 SmartProbes and a CyberAmp 380 (Axon Instruments, Inc.) and digitized at 16 bits and 50 kHz using a PCI-6251 DAQ (National Instruments). The data were analyzed off-line in MATLAB (The MathWorks, Inc.). The signals were further filtered in
MATLAB (ECG = 0.5-150 Hz, VENG = 300-10 kHz and BP = DC-70 Hz), the ECG and BP were down sampled to 1000 Hz, and the VENGs were squared to obtain the power of the signals.

In order to derive BPnPs, the squared VENG signals were first low-pass filtered at 15 Hz to derive the envelope signals. This VENG power envelope was then high-pass filtered at 1 Hz (second order Butterworth) to remove the respiration-related nerve signal and finally down sampled to 1000 Hz. The R-peaks were then detected from the ECG signal and used to create an ensemble average of the VENG power envelope and BP signal, respectively, relative to the R-peak of a number of heartbeats in order to obtain the BP waves and the BPnP profiles as illustrated in Figure 2. The BPnP amplitude (aBPnP) was calculated as the difference between the minimum and maximum BPnP values.

Results

BPnP profiles resembling the morphology of the BP waves (Fig. 2) were extracted as described from at least one electrode channel in six out of the eight animals included in this study. Such profiles could not be derived from the LVN of the other two animals as the VENGs in those two animals were unstable.
In the six animals with valid recordings, the topological selectivity of the tested electrode ranged from BPnPs derived from one channel exclusively (Fig. 2a) in two pigs, to BPnPs derived from all four channels (Fig. 2b) in one pig. Situations with BPnPs derived from two and three channels occurred in one and two pigs, respectively. In the situations where BPnP profiles were derived from two and three of the electrode channels, the aBPnP

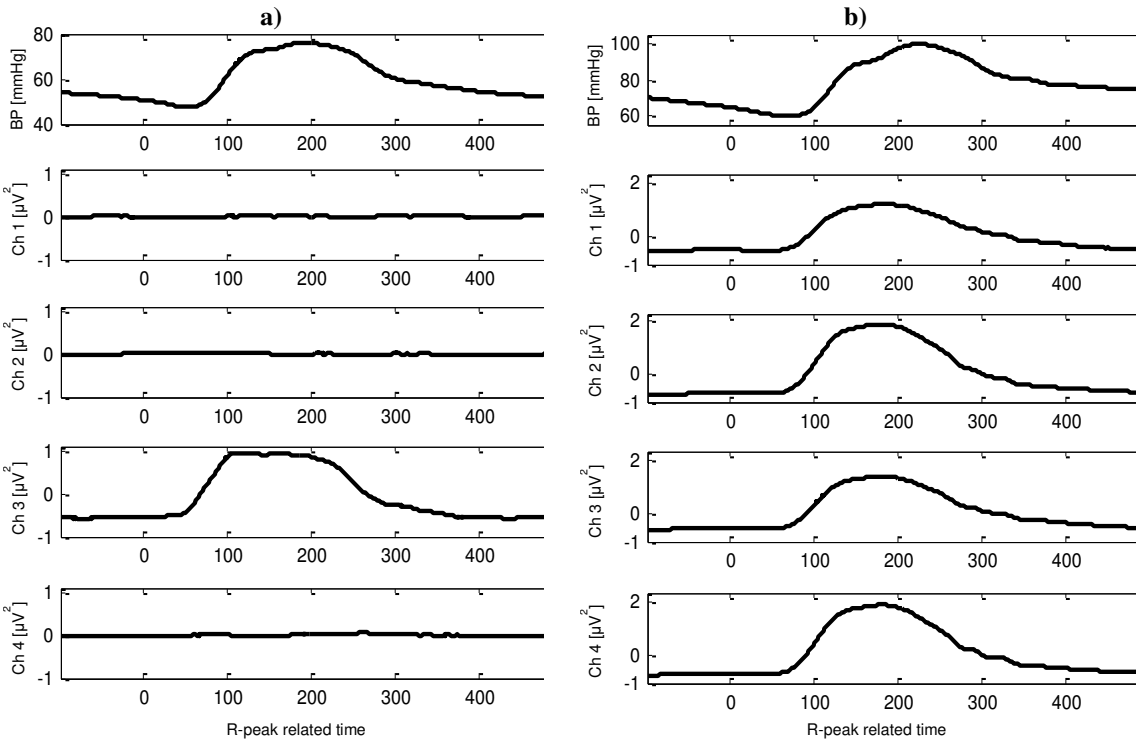

Figure 2: Two examples of BPnP profiles extracted from the LVN recordings collected from two animals. In both examples, the upper traces show the BP waves as recorded from the right carotid artery and the following three traces represent the power of the VENGs recorded with the four electrode channels (Ch 1-4) and averaged as described. In animal A1 (a), a BPnP profile was present in exclusively channel 3. In animal A3 (b), BPnP profiles with similar shapes and amplitudes were extracted from all four channels.

differed between the channels providing an aBPnP selectivity as illustrated in Figure 3.

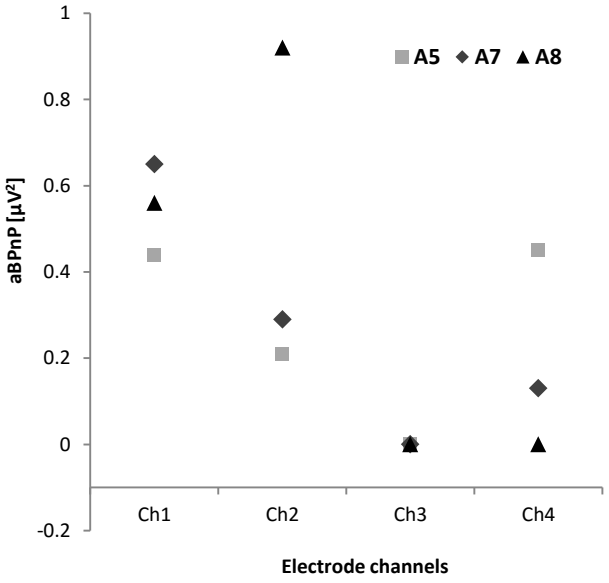

Figure 3: The BPnP amplitude (aBPnP) as measured in the three pigs where BPnP profiles were derived from two (animal A8) and three (animals A5 and A7) of the electrode channels.

Discussion

The present study shows that BPnP profiles resembling the morphology of the BP waves can be extracted from BP-related VENG signals recorded with an interfascicular electrode from the pig LVN. In addition, the present results indicate that such signals can be selectivity recorded using the tested electrode design.

As already mentioned, we previously showed that BPnP profiles resembling the BP waves can be derived from the pig LVN by calculating the power of BP-related VENG signals recorded with cuff electrodes [7]. In the present work, similar BPnP profiles were derived in the same way, but using an interfascicular electrode to record BP-related VENG signals. This indicates that the recording capabilities of this interfascicular electrode are similar to those of the cuff electrodes used in our previous study [7]. As the interfascicular electrodes may be superior to the cuff electrodes in regard to the selective recording and stimulation capabilities [3;4], we consider that the electrode design tested here should be further investigated for possible applications, including closed-loop LVN stimulation for the treatment of resistant hypertension. In this regard, Plachta et al. reported that selective LVN stimulation results in BP decrease [2] and our previous work suggested that the BPnPs can be used to monitor the BP [7].

Concerning the selectivity aspects investigated here, this study shows that either a topological (Fig. 2a), or an amplitude (Fig. 3) selectivity in regard to recording the BP-related signals can be achieved using a four-channels electrode design. However, the aimed BPnP profiles were obtained in only six out of the eight pigs included in this study and in only four of those six animals (i.e. A1, A2, A7 and A8) the recordings can be defined as selective. As those BPnP profiles resulted from the compound signals generated by the baroreceptor fibers running through LVN [8], these mixed results indicate that the electrode channels had a different orientation and/or proximity relative to those fibers in the different pigs.

In this regard, placing the electrode in an ideal position inside the LVN (e.g. with only one channel facing the baroreceptor fibers) is a challenge and this ideal electrode position is difficult to achieve. Consequently, more studies are necessary for establishing more suitable electrode insertion methods and thus for improving the electrode selectivity. In addition, the feasibility of using such electrodes for chronic implants should also be tested in the future.

Conclusions

This study shows that neural profiles resembling the BP waves can be derived from LVN signals recorded with a multiple channel interfascicular electrode. Whereas the tested electrode design seems suitable for selectively recording such signals, further experiments are needed to improve the electrode design, insertion procedures, and to assess the chronic stability of this electrode design.

Acknowledgement

This study was financed by the Innovation Fund Denmark (HTF j.no. 171-2013-6). The authors thank Torben Madsen, Ole Sørensen, and Jens Sørensen, at the Department of Pathology, Aalborg University Hospital, for their assistance with animal care and handling.

References

[1] K. Famm, B. Litt, K. J. Tracey, E. S. Boyden, and M. Slaoui, "Drug discovery: a jump-start for electroceuticals," *Nature*, vol. 496, no. 7444, pp. 159-161, Apr.2013.

[2] D. T. Plachta, M. Gierthmuehlen, O. Cota, N. Espinosa, F. Boeser, T. C. Herrera, T. Stieglitz, and J. Zentner, "Blood pressure control with selective vagal nerve stimulation and minimal side effects," *J. Neural Eng*, vol. 11, no. 3, p. 036011, June2014.

[3] T. N. Nielsen, C. Sevcencu, and J. J. Struijk, "Fascicle-selectivity of an intraneural stimulation electrode in the rabbit sciatic nerve," *IEEE Trans. Biomed. Eng*, vol. 59, no. 1, pp. 192-197, Jan.2012.

[4] T. N. Nielsen, C. Sevcencu, and J. J. Struijk, "Comparison of Mono-, Bi-, and Tripolar Configurations for Stimulation and Recording With an Interfascicular Interface," *IEEE Trans. Neural Syst. Rehabil. Eng*, vol. 22, no. 1, pp. 88-95, Jan.2014.

[5] N. Lago, K. Yoshida, K. P. Koch, and X. Navarro, "Assessment of biocompatibility of chronically implanted polyimide and platinum intrafascicular electrodes," *IEEE Trans. Biomed. Eng*, vol. 54, no. 2, pp. 281-290, Feb.2007.

[6] D. T. Plachta, N. Espinosa, M. Gierthmuehlen, O. Cota, T. C. Herrera, and T. Stieglitz, "Detection of baroreceptor activity in rat vagal nerve recording using a multi-channel cuff-electrode and real-time coherent averaging," *Conf. Proc. IEEE Eng Med. Biol. Soc.*, vol. 2012, pp. 3416-3419, 2012.
[7] C. Sevcencu, T. N. Nielsen, and J.J. Struijk, "A Blood Pressure-Related Profile Extracted from Pig Left Vagus Nerves Using Cuff Electrodes," in *Replace, Repair, Restore, Relieve. Bridging Clinical and Engineering Solutions in Neurorehabilitation,* 7 ed. W. Jensen, O. K. Andersen, and M. Akay, Eds. Springer International Publishing, 2014, pp. 717-723.
[8] J. E. Angell James, "The effects of altering mean pressure, pulse pressure and pulse frequency on the impulse activity in baroreceptor fibres from the aortic arch and right subclavian artery in the rabbit," *J. Physiol*, vol. 214, no. 1, pp. 65-88, Apr.1971.

Author's Address

Name: Cristian Sevcencu
Affiliation: Center for Sensory-Motor Interaction (SMI®) Department of Health Science and Technology, Aalborg University, Denmark.
eMail: sevcr@hst.aau.dk
homepage: www.smi.hst.aau.dk

CAPs in an isolated sciatic nerve of a rat elicited with specific stimulating pulses without and with bupivacaine anaesthesia

Polona Pečlin[1], Janez Rozman[1, 2], Monika C. Žužek[3]

[1]Center for Implantable Technology and Sensors, ITIS d. o. o. Ljubljana, Lepi pot 11, 1000 Ljubljana, [2]Institute of Pathophysiology, Medical Faculty, University of Ljubljana, Vrazov trg 2, 1000 Ljubljana, [3]Institute of Physiology, Pharmacology and Toxicology, Veterinary Faculty, University of Ljubljana, Gerbičeva 60, 1000 Ljubljana, Republic of Slovenia.

Corresponding author: Dr. Polona Pečlin, Center for Implantable Technology and Sensors, ITIS d. o. o. Ljubljana, Lepi pot 11, 1000 Ljubljana, Republic of Slovenia.

Abstract: *The functional performance of a specific current pulse to selectively stimulate Aα-, Aβ- and Aδ-fibers in an isolated rat sciatic nerve (SNR) and when exposed to the bupivacaine anaesthetic was assessed and compared. Nerve conduction velocity (CV) and compound action potential (CAP) measurements were performed on a SNR of four normal growing male adult Wistar Albino rats. The stimulus used was a current, biphasic pulse composed of a quasitrapezoidal cathodic phase and rectangular anodic phase. Results showed that the highest CAP1 was obtained when the parameters of the tested stimulus waveform were set at the following range: i_c=3.8-4 mA, t_c=350-400 μs and t_{exp}=330-440 μs When the bupivacaine was applied onto the SNR, action potential (AP) conduction was gradually reduced until it was blocked. The lowest value of both CAP1 and CAP2 was obtained about eighty minutes after application of local anasethetic. One conclusion was that APs were activated in the Aβ-fibers and Aδ-fibers within the corresponding pathways along with a slight AP inhibition in the Aβ-fibers. It could also be concluded that besides the parameters and waveforms of the specific stimulus, changes in CV can be also affected by bupivacaine anaesthetic and that both slightly differentite between nerve fibres on diameter basis.The obtained results, could serve as an additional tool for developing multi-electrode stimulating systems that potentially enable fiber-type selective stimulation of nerve fibers and to test various anaesthetics when applied directly onto the peripheral nerve containing different types of nerve fibres.*

Keywords*: rat sciatic nerve; nerve fibre diameter; compound action potential; selective nerve stimulation; local anaesthetic.*

Introduction

Non-selective stimulation of a particular nerve often results in undesirable side effects. To alleviate such problems, various models and electrode systems that selectively stimulate certain features have been developed, for example, stimulating intermediate-diameter Aβ-fibers in a nerve, while avoiding the stimulation of Aα-fibers, Aδ-fibers and C-fibers [1-6]. It was shown in early electrophysiological studies that compound action potential (CAP) recorded from a nerve is actually the algebraic sum of the action potentials (APs) of activated nerve fibres for any strength of the stimulating pulse [7]. Nerve conduction velocity (CV) is a reproducible measure of peripheral nerve function and in this relation it is used to diagnose neurological diseases. It is shown in the literature that at the thigh level, the rat sciatic nerve (SNR) is composed of hundreds of myelinated motor axons that innervate different leg muscles [8]. In stimulation of the SNR a larger axon diameter with extensive myelination exhibits a higher CV, while a small axon diameter and no myelination exhibits a low CV. Therefore, the increase in CV should reflect an increase in the relative number of fibers with large diameters. The recording of CAP in the peripheral nerve shows a gradual increase in CAP with an increase in the intensity of the stimulating pulses as nerve fibers with different properties are recruited during the stimulation.

While the effects of ambient temperature, age and size of the nerve are documented, the direct and indirect effects of anaesthetic on nerve CV when applied on the peripheral nerve, are not well reported. Local anaesthetics (LAs) block the generation and the conduction of APs, presumably by increasing the threshold for electrical excitation in the nerve, by slowing the propagation of the nerve impulse, and by reducing the rate of rise of APs.They interrupt neural conduction by inhibiting the passage of sodium through voltage-sensitive ion channels in the neuronal membrane [9]**.** In general, the progression of anesthesia is related to the diameter, myelination, and conduction velocity of affected nerve fibres. Bupivacaine (Hydrochloride) is indicated for the production of local or regional

anesthesia or analgesia for surgery, dental and oral surgery procedures, diagnostic and therapeutic procedures, and for obstetrical procedures [10].
The main aims of our study while using quasitrapezoidal current biphasic stimulating pulses were to i) investigate the functional performance in fiber-type selective nerve stimulation, ii) to separate the CAP peaks corresponding to the categories of nerve fibers (Aα, Aβ, Aδ and C) and iii) to test an influence of the bupivacaine anaesthetic onto the different groups of nerve fibres when applied onto the particular superficial region of an isolated SNR via measurement of CAP during electrical stimulation of the SNR. Precisely, an intention was to separate the AP peaks corresponding to the different groups of nerve fibres namely, Aα-, Aβ- and Aδ-fibres when the SNR was exposed to specific concentration of the aforementioned LA.

Material and Methods

For measurements, we used a measuring chamber, a stimulator, a differential amplifier, a data acquisition system (Digidata® 1440A, Low-noise Data Acquisition System, Molecular Devices, Sunnyvale, CA, USA), data acquisition software (AxoScope 10.3, Molecular Devices, Inc, USA) and desktop PC. The chamber contained seven platinum (99.99% purity) hook-shaped stimulating and recording electrodes at the distance of 4.8 mm. The diameter of the hook was 1 mm. As shown in Fig.1 the first two electrodes were stimulating electrodes, the pair of electrodes (pair1) numbers four and five were CAP1 recording channel and the pair of electrodes numbers six and seven (pair2), were CAP2 recording channel. The stimulating and recording section were separated, using the grounded electrode number three.

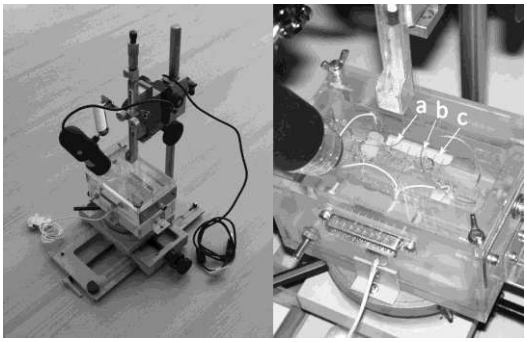

Fig. 1. (left) Stimulating/Recording set-up, (right) Measuring chamber with a ladder of electrodes and SNR: (a) pair of stimulating electrodes, (b) pair of electrodes for recording of CAP1 and (c) pair of electrodes for recording of CAP2.

CVs and CAPs were measured on isolated SNRs obtained from female adult Wistar rats, weighting 200 g to 230 g. Animal handling was consistent with the European Community Directive 2010/63/EU. Offline signal analysis was performed using a Lenovo T420 portable computer (Lenovo, Singapore) and MATLAB R2007a software (The Mathworks Inc., USA). The stimulus used was a current, biphasic, quasitrapezoidal cathodic phase with an intensity i_c, a plateau with a width of t_c, an exponentially decaying phase with a width of t_{exp} and the time constant τ_{exp} and a rectangular anodic phase with a width of t_a and intensity of i_a (shown in Fig. 2).
The experiments consisted of three sub-experiments, referred to as Phases 1-3, where pre-set single stimuli (1 Hz) were used, while the CAPs were recorded simultaneously. In this report however, only phases that elicited the most indicative influence on the recorded CAPs by changing the stimulating cathodic intensity i_c, changing the time of the exponential decay t_{exp}, and by application of the bupivacaine anesthetic are reviewed. Before the beginning of Phases 1-3, the following parameters were fixed: i_c = 3.35 mA, t_c = 155 µs, t_{exp} = 100 µs, τ_{exp} = 45 µs, i_a = 0.45 mA and t_a = 490 µs. In Phase 1 stimulus intensities (i_c) between 0 and 3.35 mA were used. In Phase 2, we used width of the cathodic exponential decay (t_{exp}) between 0 and 500 µs. Finally, in Phase 3, local anaesthetic bupivacaine was applied. The pre-set stimulus waveform and more specific description of the experiment is shown in the publication: [11].

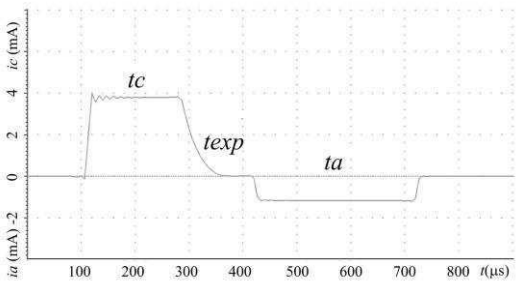

Fig. 2. Current, biphasic pulse composed of a quasitrapezoidal cathodic phase and rectangular anodic phase.

Results

The data on the CAP latencies, CAP amplitudes and other variables in three phases are presented graphically in Fig. 3.

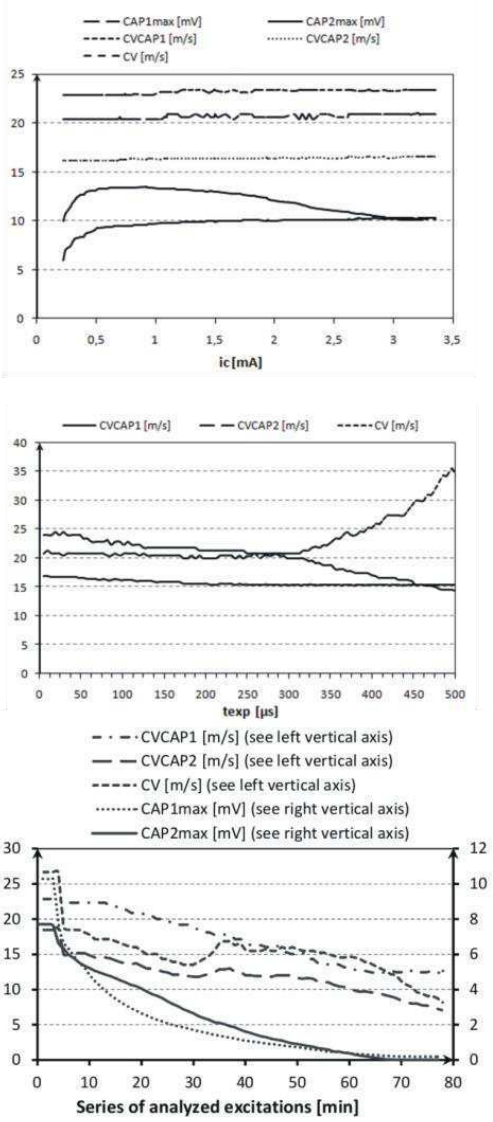

Fig. 3. (a) Relationship between i_c, CAP1max and CAP2max (peak amplitude of the CAP1 and CAP2), CVCAP1 and CVCAP2 (nerve conduction velocity calculated on the basis of CAP1max and CAP2max); and CV in Phase 1, (b) Relationship between t_{exp}, CAP1 and CAP2 conduction velocities and actual conduction velocity CV in Phase 2, (c) Relationship between an ascending time and variables CAP1max, CAP2max, CVCAP1, CVCAP2 and CV in induction phase. 0.25 % Bupivacaine was applied after first 5 minutes.

Discussion

Published studies show that the technique's selectivity for fibers with different CVs, namely Aα-fibers, Aβ-fibers and Aδ-fibers, can only be achieved by adjusting the stimulating cathodic intensity i_c and changing the τ_{exp}. Our data however, showed that the most indicative influence on the recorded CAPs was achieved by adjusting, i_c, and changing the time of the exponential decay, t_{exp} [1-5].

The current work demonstrates for the first time the feasibility of selective stimulation of different types of nerve fibres within the isolated SNR exposed to the bupivacaine anaesthetic using the specific quasitrapezoidal current biphasic stimulating pulses. In the present study, the fascicle geometry and the type of nerve fibre's functional topography were considered while the fibre-type selectivity that could be obtained with various electrode configurations and stimulus waveforms, is proposed. Other published studies showed that the technique's selectivity of fibres having different CVs, namely Aα-fibres, Aβ-fibres andAδ-fibres that is tested in the study, agree with most of the models and electrode systems that selectively stimulate a particular population of nerve fibres within the superficial region of the nerve that have have been developed by the others [12].

Conclusion

One conclusion is that the highest CAP1 value shall be expected when the parameters of the tested stimulus waveform are set within the following range: i_c=3.8-4 mA, t_c=350-400 µs and t_{exp}=330-440 µs. However, this conclusion is valid only for the particular stimulating/recording system used within this study. It can be assumed that predominantly one type of nerve fibers, namely Aβ-fibers, was activated. It can be also concluded that only a t_{exp} values that are slightly shorter and slightly larger than around 271 µs are appropriate for use with the pre-defined stimulus waveform and presented experimental design. It is anticipated that the stimulation parameters related to selective nerve stimulation and recording the CAPs that were established in this study will advance the development of human neural prostheses. It can be also concluded that the findings of our present study show that 0.25% bupivacaine was able to obtain block of different types of nerve fibres in isolated SNR after stimulation with current, biphasic, incompletely charge-balanced asymmetric pulse. Finally, the findings of the present experiment can be used to suggest this methodology as an animal model supporting studies related to human neurological diseases that potentially enable testing performance of various LA via electrophysiological studies related to fibre-type selective stimulation of nerve fibres.

Acknowledgement

This work was financed by research grants P3-0171 and P4-0053 from the Slovenian Research Agency, Ministry of Education, Science and Sport, Ljubljana, Republic of Slovenia.

Part of the results presented are published in the following paper: [11].

References

1. Rozman J, Pečlin P, Kneževič I, Mirkovič T, Geršak B, Podbregar M. Heart function influenced by selective mid-cervical left vagus nerve stimulation in a human case study. Hypertension research 2009; 32(11):1041-1043.
2. Anholt TA, Ayal S, Goldberg JA. Recruitment and blocking properties of the CardioFit stimulation lead. J Neural Eng 2011; 8: 034004.
3. Goodall EV, Kosterman LM, Holsheimer J, Struijk JJ. Modeling study of activation and propagation delays during stimulation of peripheral nerve fibers with a tripolar cuff electrode. IEEE Trans Rehab Eng 1995; 3; 272–282.
4. Ordelman SC, Kornet L, Cornelussen R, Buschman HP, Veltink PH. An indirect component in the evoked compound action potential of the vagal nerve. J Neural Eng 2010; 7: 066001.
5. Deurloo KE, Holsheimer J, Bergveld P. Fascicular selectivity in transverse stimulation with a nerve cuff electrode: a theoretical approach. Neuromodulation 2003; 6: 258–269.
6. Fang ZP, Mortimer JT. A method to effect physiological recruitment order in electrically activated muscle. IEEE Trans Biomed Eng 1991; 38: 175–179.
7. Olsen, W.H., BeMent, S.L., 1981. Compound action potential reconstructions and predicted fiber diameter distributions. In: Conduction Velocity Distributions, Dorfman, L.J., Cummins, K.L., Leifer, L.J., (Eds.), Alan R. Liss, New York, USA, pp. 57-83.
8. Prodanov D, Feirabend HK. Morphometric analysis of the fiber populations of the rat sciatic nerve, its spinal roots, and its major branches. J Comp Neurol 2007; 503: 85–100.
9. Becker DE, Reed KE. Local Anesthetics: Review of Pharmacological Considerations. Anesth Prog 2012; 59(2): 90–102. doi: 10.2344/0003-3006-59.2.90
10. Hu D, Onel E, Singla N, Kramer WG, Hadzic A. Pharmacokinetic profile of liposome bupivacaine injection following a single administration at the surgical site. Clinical drug investigation 2013;33:109-15.
11. Monika C. Žužek, Janez Rozman, Polona Pečlin, Milka Vrecl and Robert Frangež. Analysis of compound action potentials elicited with specific current stimulating pulses in an isolated rat sciatic nerve. Biomed. Eng.-Biomed. Tech. 2016; aop, DOI 10.1515/bmt-2015-0167.
12. Vuckovic A, Tosato M, Struijk JJ. A comparative study of three techniques for diameter selective fiber activation in the vagal nerve: anodal block, depolarizing prepulses and slowly rising pulses. J Neural Eng 2008; 5: 275–286.

Author's Address
Polona Pečlin
MD, PhD
polonapeclin@gmail.com

Neuronal activation characteristics in the electrically stimulated retina during sub- and epiretinal stimulation

Werginz P[1], Rattay F[1]

[1]Institute for Analysis and Scientific Computing, Vienna University of Technology, Austria

Abstract: *Response characteristics of retinal ganglion cells during extracellular electrical stimulation are studied in order to improve the clinical outcome in blind patients using retinal implants. This computational study presents a detailed computer model of a small group of retinal neurons and how these neurons respond to electrical stimulation. Compartmental modeling was combined with a model of the ribbon synapse at the bipolar-ganglion cell connection. Epiretinal stimulation from the inner portion of the retina was shown to produce strongly different spiking outputs in a single ganglion cell when the stimulating electrode is shifted or the pulse polarity is changed. Subretinal stimulation triggers direct and indirect spikes in ganglion cells. Whereas direct ganglion cell activation results in a single or two spikes, indirect (network) activation results in a bursting ganglion cell response. Similar to experimental findings, this bursting response changes from an irregular to a regular temporal pattern when stimulus intensity is systematically increased.*

Keywords: *retinal implant, bipolar cell, ganglion cell, synaptic transmission*

Introduction

Recent improvements in retinal implant technology have led to enhanced visual perceptions in blind patients during clinical trials. Two major approaches are currently utilized to restore vision to blind people suffering from diseases that lead to a degeneration of photoreceptors: i) sub- or suprachoroidal implants placed *under* the retina and ii) epiretinal implants implanted at the innermost portion of the retina. Stimulation from both sides of the retina was proven to be capable eliciting neural signals in the visual cortex.

The quality of artificial vision, however, is still limited and does not provide more than rudimentary features of the visual scenery. The generated neural signal towards the visual cortex is the crucial factor in order to restore vision with higher quality.

This computational study aims to elucidate several neural activation characteristics during electrical stimulation from both sides of the retina. The activation of the two most important retinal cell types, bipolar (BC) and ganglion cells (GC), is modeled.

Material and Methods

The response of BCs and GCs to extracellular electrical stimulation is computed with multi-compartment models. Our modeling discretizes detailed 3-D cell geometries in space, using cylindrical and spherical compartments. Compartment length is below 10 µm; total number of compartments is 500-1500. Dendritic compartments have a constant diameter of 0.5 µm. Axon Hillock and axon initial segment (AIS) have lengths between 30 and 40 µm and diameters are adjusted to experimentally reported data. Current flow between compartments and across the cell membrane leads to a system of ordinary differential equations (Eq. 1 [1]). In this equation V_n denotes the transmembrane voltage, R_n the axial resistance between neighbored compartments, C_n the cell capacitance and $V_{e,n}$ the applied extracellular potential at the nth compartment. Ionic currents ($I_{ion,n}$) are computed with a Hodgkin-Huxley-like model approach at 35 degrees Celsius [2]. Here, V_e, generated by a stimulating electrode, is computed by a simple analytical solution for point sources in homogeneous media (Eq. 2). Thereby, I_{Stim} denotes the stimulus amplitude at the extracellular electrode. Extracellular resistivity ρ_e is set to 1000 Ωcm, r denotes the Euclidean distance of a compartment (center) to the electrode. Extracellular recordings are computed with the same formula; see [3] for details. The used model of the ribbon synapse at BC terminals is presented in [4]. Numerical solutions are computed by a custom-written implicit Euler solver in MATLAB (The Mathworks Inc., Natick, Massachusetts, United States). Time step is set to 0.005 ms in all simulations.

$$\frac{dV_n}{dt} = \left[\begin{array}{l} -I_{Ion,n} + \frac{V_{n-1} - V_n}{R_{n-1}/2 + R_n/2} + \frac{V_{n+1} - V_n}{R_{n+1}/2 + R_n/2} + \\ + \frac{V_{e,n-1} - V_{e,n}}{R_{n-1}/2 + R_n/2} + \frac{V_{e,n+1} - V_{e,n}}{R_{n+1}/2 + R_n/2} \end{array} \right] \frac{1}{C_n} \qquad (1)$$

$$V_e = \frac{I_{Stim} * \rho_e}{4 * \pi * r} \qquad (2)$$

Results

Neural activation of BCs and GCs was monitored either intra- or extracellularly, i.e. either the electrical potential across the membrane at a given compartment or the summed response of all compartments at a virtual recording electrode was computed. Intracellular recordings resulted in typical action potential (AP) shapes with strong depolarization from the resting potential (-65 mV). Extracellular recordings typically have a bi- or triphasic form, depending on the location of the recording electrode and the site of spike initiation.

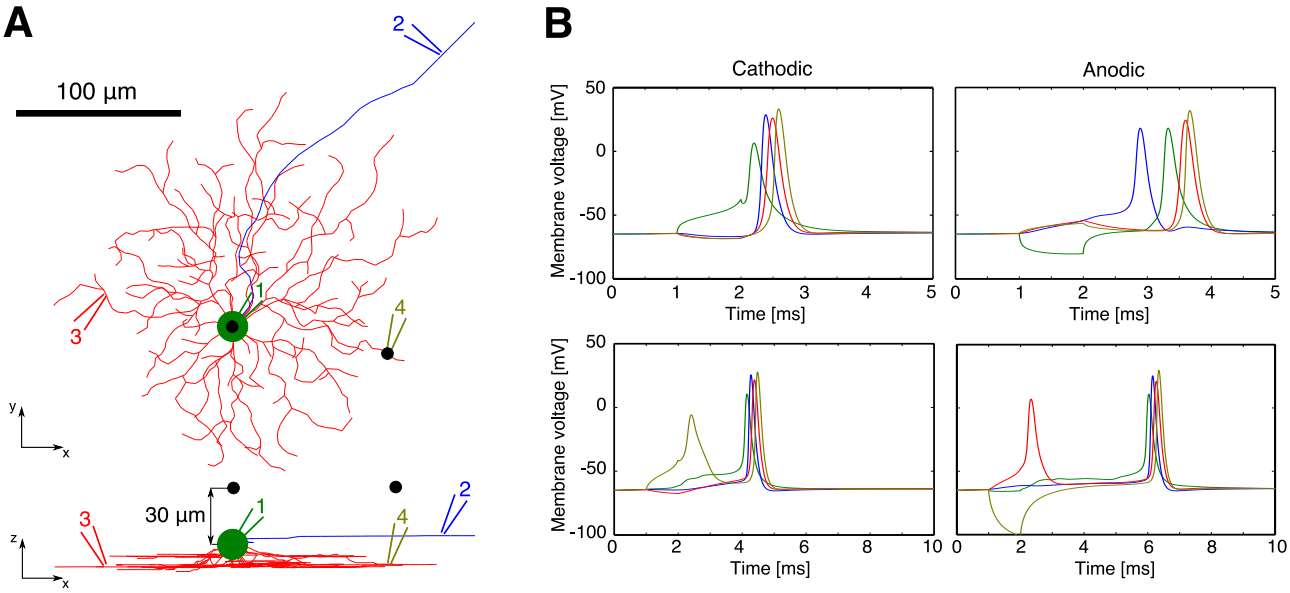

Figure 1: Epiretinal stimulation with anodic and cathodic pulses - (A) The dendritic tree, soma and axonal parts of a mouse GC from [5] are indicated in red, green and blue, respectively. The stimulating electrode (black dots) was either located directly above the soma (0/0/30; 0/0/0 denotes the soma center) or in the distal dendrite (90/-17/30). Z-distance between soma center and electrode was therefore fixed at 30 µm. (B) Intracellular recording at four locations along the neuron when stimulated above the soma (top) and above the distal dendrite (bottom). Simulated membrane voltage was monitored at the soma (green, *1*), the axon (blue, *2*) and two locations within the dendritic tree (red, *3* & brown, *4*).

In a first investigation the response of a single mouse GC during epiretinal stimulation was simulated (Fig. 1). Intracellular recordings were obtained at four different locations along the neuron; at the soma, at the proximal axon (~200 µm from the soma) and at two locations within the dendritic tree (Fig. 1A). The stimulating electrode was located either above the soma or above the distal dendritic tree, z-distance was 30 µm from the soma center in both cases (see Fig. 1A). Stimulation at threshold level (1.2-6.3 µA) resulted in different activation patterns for varying electrode locations and pulse polarities (Fig. 1B). During cathodic stimulation close to the soma an AP is initiated at the AIS and propagates in both directions into the soma and dendrites and towards the distal axon. Anodic stimulation, again, initiates a spike within the axon, however, at more distal locations. Note that if measured experimentally with a patch-clamp recording at the soma both pulses would result in similar recordings. Importantly, however, the relative timing between somatic and axonal spike is different during anodic and cathodic stimulation. Whereas cathodic stimulation leads to somatic spikes prior to axonal APs this order is inverted during anodic pulses.

Shifting the electrode to the distal dendrite leads to a delayed spiking in somatic and axonal portions (Fig. 1B bottom). During cathodic stimulation an AP is initiated in the dendritic part located close to the electrode and further propagates through the dendrite into the soma where it takes some time to charge the large capacitance and reach threshold depolarization. Because of this delay the spike in the soma propagates in both direction towards the axon and the dendrite. This leads to a second spike in the recorded compartment close to the stimulating electrode. A similar activation pattern can be observed during anodic stimulation, however, now locations far from the electrode location are initiating an AP which propagates through the remaining parts of the neuron. Again, the first spiking compartment produces a second spike when the somatic AP returns.

Figure 2 shows a comparison of intra- (top) and extracellular (bottom) recordings during cathodic stimulation from the two electrode locations of Fig. 1.The extracellular potential was measured close to the soma (0/0/15). Overlays show little variance in the recordings.

It was also tested how strong BCs respond during epiretinal stimulation. For the presented 1ms pulses and due to the large distance between the electrode and BCs the membrane voltage was only elevated by a few mV. Such a small depolarization is not able to activate voltage gated calcium channels in BC terminals and consequently the intracellular calcium concentration necessary to start the signaling cascade is not sufficiently elevated. Therefore, BCs were not included during epiretinal stimulation.

Subretinal stimulation was applied anodically only because cathodic pulses are not able to increase $[Ca^{++}]$ in BC terminals. Consequently, the synaptic signaling cascade is not initiated and no excitatory postsynaptic currents (EPSCs) are present at GC dendrites. BC and consequent (indirect) GC response was computed by a simplified simulation. Only a small number of BCs, located in evenly spaced regions along the dendritic tree's main axis were used to compute the average EPSC on a connected GC (Fig. 3A). The intracellular calcium

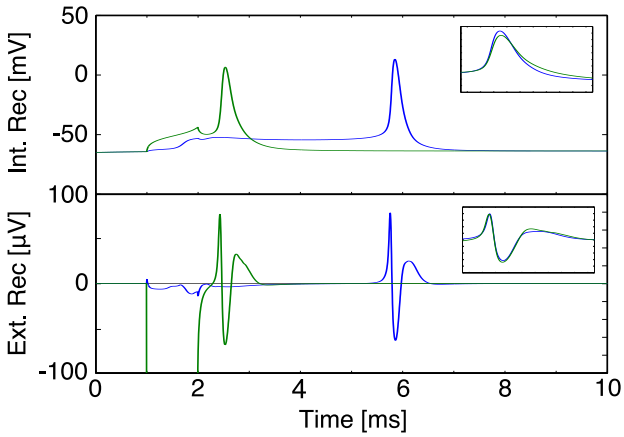

Figure 2: Intra- (top) and extracellular (bottom) recordings at the soma when the electrode is shifted from the soma (green) to the distal dendrite (blue). APs at the soma occur at different points in time. An overlay of both recordings shows that the AP shape is similar in both cases (inset). Extracellular recordings quite close to the soma (0/0/15) don't differ strongly as well.

concentration at one terminal compartment of the BCs was used as input parameter for 100 ribbon synapses randomly distributed on the dendritic tree of the GC (input depending on Euclidean distance from the soma; blue dots in Fig. 3A bottom).

Doubling the stimulus amplitude leads to a totally different spiking pattern (Fig. 3B). Whereas during a 5 µA pulse only one direct spike is generated the stronger pulse elicits a double spike. Also the strength of synaptic activation varies strongly. Higher stimulus amplitudes up to a certain limit generate stronger bursting responses. If BC depolarization is too strong, however, an opposite effect can be observed due to so-called calcium current reversal (not shown, see [4] for more information).

Figure 3C describes spiking characteristics over a wide range of amplitudes for both, modeled (left) and experimental (right, from [6]) results. Only at very low amplitudes a pulse does not elicit a so-called direct spike, i.e. a spike in close temporal relation to the stimulus. After a silence period of approximately 10 ms bursts of synaptic (indirect) spikes start. These spikes are thought to be initiated by the response of BCs to the stimulus and consequent neurotransmitter release.

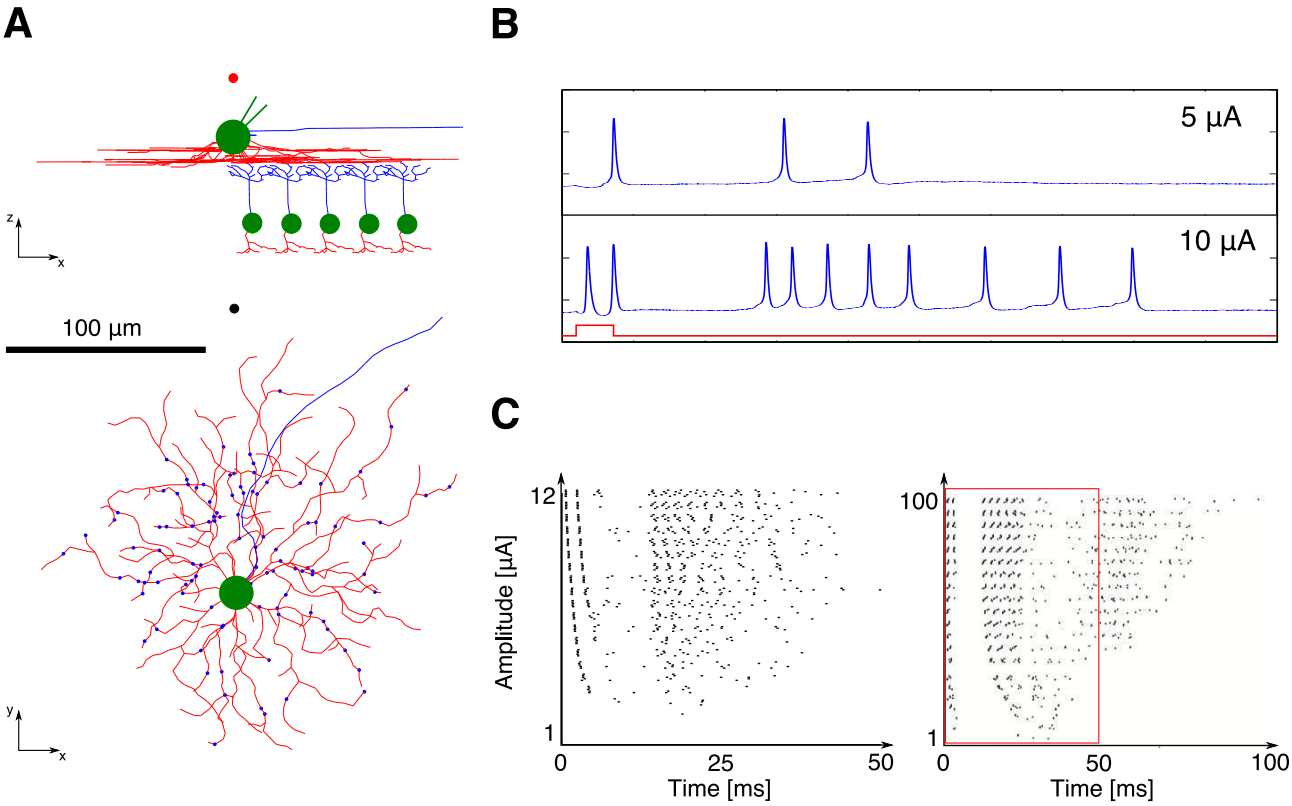

Figure 3: Subretinal stimulation with anodic pulses results in direct and indirect spikes - (A) The responses of 5 BCs define the randomly distributed excitatory inputs (blue dots) at the GC dendritic tree. Stimulating and recording electrode in black and red, respectively. (B) Intracellular recorded membrane potential for stimulus amplitudes of 5 and 10 µA. Stimulus on- and offset is indicated in red at the bottom. (C) Resulting raster plot when the stimulus amplitude is sequentially increased. At each amplitude five repetitions of the same pulse are presented and the spike timing (zero crossing of membrane voltage at the soma) is monitored. Simulated (left) and recorded (right) results show certain similarities. Note that the time scale is different in both plots. Simulated results can be compared to the portion of the right plot within the red rectangle.

The duration from activation of BCs to synaptic input and spiking at GCs depends on the kinetics of $[Ca^{++}]_i$, neurotransmitter release and diffusion through the synaptic cleft, postsynaptic receptor kinetics and biophysical properties of the connected GC. In the presented model, several of these parameters were combined into a single delay time of 10 ms in order to reproduce experimental results. A previous study, however, showed that the first burst of indirect spikes could also occur earlier within a time frame of <5 ms [7].

Long latency spikes occurring after more than 50 ms (see Fig. 3C right) can also be observed in the experiment, however, these spikes are supposed to origin from other parts of the retinal network (e.g. photoreceptors) and therefore can not be simulated with the presented model. The large differences between stimulus amplitudes necessary for the generation of indirect activation in simulations and experiments can have several reasons: i) the relative location between the target fiber(s) and the stimulating electrode, i.e. the distance between BCs and subretinal electrode is not precisely known in experiments; ii) in the presented simulations the microscopic properties of retinal tissues are averaged to a macroscopic resistivity (1000 Ωcm) in order to be able to use a simple analytical solution for the generated potentials.

Several similarities can be found between simulated and experimental results. First, higher amplitudes lead to intense indirect GC firing. Second, if a certain amplitude is exceeded a second direct spike is generated. Third, a regular temporal pattern of the indirect spikes can be observed at high stimulus amplitudes. This effect, however, is more pronounced in experimental results.

Discussion

Our biophysically based model explains several experimentally determined spiking characteristics in GCs during sub- and epiretinal stimulation. A comparison with experimental data was shown to be in general agreement to a previous study. Our model also predicts several plausible spike initiation characteristics which have not been observed in experiments so far, mostly because these characteristics cannot be examined with current standard recording setups (i.e. measuring spiking with a single patch-clamp electrode at the soma). Moreover, our model describes the indirect activation of GC during subretinal stimulation which is thought to be the crucial factor for a higher quality of vision in patients using (sub)retinal implants. Direct and indirect spikes can clearly be discerned and several specific characteristics as found in experiments can be reproduced.

Conclusions

With a deeper understanding of the processes occurring during electrical micro-stimulation as utilized in retinal implants, an improved outcome in clinical trials might be achievable. Single-cell analysis reveals that the site of spike initiation is mainly depending on electrode location and pulse polarity. Especially during epiretinal stimulation, these effects might result in distorted temporal spiking sequences which further are supposed to lead to unwanted sensory inputs. Our model also supports the opinion that the first burst of APs during subretinal stimulation is probably related to activation of BCs. This first burst can be elicited in a controlled way in simulations as well as in experiments. The retinal network also responds with long latency bursts of spikes that cannot be capture with our model. However, it seems that this network activation can elicit complex spiking patterns such as observed under healthy conditions. Thus, subretinal stimulation might be the better approach to generate more physiological spiking patterns with retinal implants.

Acknowledgement

This work was supported by the Austrian Science Fund (FWF), Grant number P 27335-B-23.

References

[1] Rattay, F.: The basic mechanism for the electrical stimulation of the nervous system, *Neuroscience*, vol. 89, pp. 335-346, 1999

[2] Fohlmeister, J.F., Cohen, E.D., Newman, E.A.: Mechanisms and distribution of ion channels in retinal ganglion cells: Using temperature as an independent variable, *J. Neurophysiol.*, vol. 103, pp. 1357-1374, 2010

[3] Rattay, F., Danner, S.M.: Peak I of the human auditory brainstem response results from the somatic regions of type I spiral ganglion cells: evidence from computer modeling, *Hear. Res.*, vol. 315, pp. 67-79, 2014

[4] Werginz P., Rattay F., The impact of calcium current reversal on neurotransmitter release in the electrically stimulated retina, *J. Neural Eng. vol. 13*, 046013, 2016

[5] Kong, J.H., Fish, D.R., Rockhill, R.L., Masland, R.H.: Diversity of ganglion cells in the mouse retina: unsupervised morphological classification and its limits, *J. Comp. Neurol.*, vol. 489, pp. 293-310, 2005

[6] Lee, S.W., Fried, S.I.: Responses to pulsatile subretinal electric stimulation – effects of amplitude and duration, *J. Neurophysiol.*, vol. 109, pp. 1954-1968, 2013

[7] Boinagrov, D., Pangratz-Fuehrer, S., Goetz, G., Palanker, D.: Selectivity of direct and network-mediated stimulation of the retinal ganglion cells with epi-, sub- and intraretinal electrodes, *J. Neural Eng.*, vol. 11, 026008, 2014

Author's Address

Paul Werginz
Institute for Analysis and Scientific Computing
Vienna University of Technology
Operngasse 11/Room DF0106
1040 Vienna
paul.werginz@tuwien.ac.at
http://www.asc.tuwien.ac.at/index.php?id=60

In vivo measurements of tension in the tibialis anterior tendon of the rat using a miniature in-line load-cell – preliminary results

Schmoll M[1,2], Jarvis J C[2], Unger E[1], Haller M[1], Bijak M[1], Lanmueller H[1]

[1]Center for Medical Physics and Biomedical Engineering, Medical University Vienna, Vienna, Austria
[2]School of Sport and Exercise Science, Liverpool John Moores University, Liverpool, United Kingdom

Abstract: *To investigate the behaviour of the neuromuscular system, force-measurement gives a direct measure of muscle fibre activation. While less direct and less invasive methods like EMG provide some indication of muscular activity, force-measurement is capable of giving a quantitative description of the contractile-properties. The present paper introduces a novel force-measurement technique using an in-line load cell to measure tension transmitted by the tendon of the tibialis anterior (TA) muscle in rats. Experiments were conducted on two male Wistar rats (age: 64, 65 days) with a mean body weight of 292 g. The load-cell was used to measure the response to single pulse stimulation of the common peroneal nerve and short bursts of different frequencies, for unloaded concentric (CON) and isometric (ISO) contractions. TA muscles were harvested and weighed directly after completion of the experiments. The results showed a clear increase in peak force for single twitches by 151 % for ISO compared with CON. Mean maximal tetanic force was 839 g, which is in general agreement with other studies. This indicates that the load-cell is able to provide reliable measurements for the force developed by the TA muscle. Because the tendon remains attached to its original insertion, the device allow measurements of TA loading due to plantarflexor co-contraction across the ankle joint. This could give valuable information for designing protocols to provide resistance training for the tibialis anterior muscle.*

.

Keywords: *muscle, strain, force measurement, rat, tibialis anterior*

Introduction

In order to investigate the behaviour of the neuromuscular system, force measurement has proven to be one of the most useful assessment tools. Although the recording of EMG activity is a valuable and easily accessible technique to estimate muscular loading, it still remains challenging to give reliable statements about how the measured signal is actually correlated to the force produced by a particular muscle [1]. As EMG is usually measured using surface or intra-muscular needle electrodes, they may record only part of the activity of a particular muscle. Co-activation of muscles, close to the targeted one, reflect another problem of this technique.
Measuring the muscular force in a direct way therefore gives a more complete picture about the activity of a muscle of interest. The combination with functional electrical stimulation offers further possibilities regarding a controlled study-design.

Besides describing basic contractile properties [2] of a muscle, measured force is also used as an essential parameter to quantify the degree of regeneration after a nerve injury [3]. Other studies have measured force responses elicited by different stimulation parameters in order to achieve selective stimulation [4,5,6] of fast and slow-twitch muscle fibres, which is important when trying to activate the nerve in a more natural way. The investigation of certain training protocols to elicit adaptation of muscle properties is also a well-established field of research [7].

The hind limb muscles of various animals are widely used models to investigate muscular behaviour, as they are generally large in size and their nerves easy to access. Several approaches have been used in the past to assess muscular force in anaesthetised animals. One common technique is to fix the muscle origin appropriately (often by fixation of a bone) and to measure the generated force by exposing the muscle and attaching its tendon of insertion to a load-cell or instrumented lever [2,4,6,7,8,9]. This method has the advantage of being able to measure the force directly for individual muscles and is also applicable to rather small muscles (e.g. rat EDL [7]). A less invasive approach is used by some other studies, which place the intact animal within some specially designed external apparatus [3,5] to determine the contraction strength. A positive aspect of this measurement type is that the muscles remain in situ which allows for measurements across the ankle joint, without distorting the original direction of force transmission. A drawback is the loss of selectivity as all contributing muscles are measured at the same time.

The use of an in-line force transducer offers the advantage that the force transmitted through a particular tendon can be measured while the muscles still keep their physiological position. Buckle transducers, establishing this principle, have previously been used in wallabies [10], pigeons [11] and guinea fowls [12] to measure the tendinous loading of multiple plantar-flexors at the same time.

The present paper introduces a novel miniature in-line load-cell small enough to allow for measurements of force transmitted by the tibialis anterior tendon in rats. The device should be stable enough to withstand peak forces up to 20 N while still being accurate enough to measure the response of a single twitch.

Material and Methods

Surgical procedure

Experiments were conducted under the permission of the Animals (Scientific Procedures) Act, UK on the tibialis anterior (TA) muscle of two male adult Wistar rats (age 64 and 65 days). The animals were anaesthetised using a gaseous mixture of isoflurane and O_2. The percentage of isoflurane was adjusted to maintain deep anaesthesia. Buprenorphine (Temgesic, Indivior, Slough, UK) was administered for analgesia.

Two loop electrodes, formed from PVC-insulated stainless steel wires (Cooner Sales Company, Chatsworth, California, U.S.A.), were placed under the common peroneal nerve (CPN) with the more distal electrode as cathode. The incision was closed after electrode placement to maintain the nerve in its natural environment.

The tibialis anterior muscle was accessed through a longitudinal skin incision on the anterior part of the lower hind limb. Once the TA was clearly visible, the incision was extended further distal being guided by the tibialis tendon. In order to have a longer tendinous part freely accessible, the extensor retinaculum was transected, taking great care not to injure adjacent blood-vessels or tendons. The cleaned tendon was inserted into a custom-built load cell (Center for Medical Physics and Biomedical Engineering, Medical University Vienna, Austria) and gently clamped using two stainless steel screws. Through a small window in the device it is possible to cut the tendon, which is advisable to perform using proper magnification glasses. Once the tendon was cut, the whole force was transmitted through the tendon itself and could thus be continually monitored. A drying-process of at least 20 - 30 min was allowed to strengthen the mechanical properties of the tendon, which turned out to be essential - especially when measuring higher forces. The animals were killed by increasing the anaesthetic dose, followed by cervical dislocation. TA muscles from the left and right side were harvested and weighed immediately.

Experimental set up

(i) Force Measurement

Force that is usually transmitted by the tibialis tendon was quantified using a miniature load cell (see figure 1). The CNC manufactured stainless steel core measured 3 x 3 mm with a length of 7mm and incorporated four strain gauges (1-LY11-0.3/120, Hottinger Baldwin Messtechnik GmbH, Darmstadt, Germany) that were attached using cyanoacrylate glue (EP310S, Hottinger Baldwin Messtechnik GmbH, Darmstadt, Germany) and operated as a temperature compensated half bridge.

Elastic silicone (W2000, NuSil Technology LLC, Carpinteria, CA, USA) was used to cover the actively measuring strain gauges while the passive temperature compensating strain gauges were shielded with instant adhesive (Loctite 4850, Henkel Ltd, Herts, United Kingdom). This was necessary to improve mechanical stability while handling and to allow operation in a humid environment. The tendon was attached to the load-cell by two M2x0.35 fine-pitch threaded screws. A protective element was shaped by flattening and bending a 21G needle around the screws, so that the tendon experienced a lateral clamping force rather than a torsional stress when tightening the screw. This is important because torsional stress tends to cut the fibrous elements of the tendon.

(ii) Data recording

A PowerLab 16/35 (ADInstruments Inc., Colorado Springs, USA) device was used to supply the driving voltage to the load cell and measured the force signal at 10 kS/s. Stimulation voltage was recorded at a sample rate of 100 kS/s along with the force signal. ADInstruments LabChart 7 Pro installed on a standard personal computer (MSI GS60 2PE Ghost Pro, Micro-Star International, Zhonghe District, Taiwan) was used to record, store, pre-process and export the retrieved data.

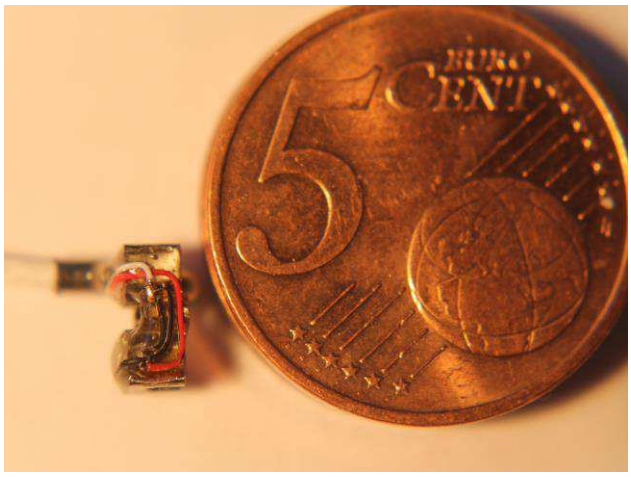

Figure 1: Size of the load-cell compared to a 5 Euro Cent coin, without the clamping screws.

(iii) Stimulation equipment

Passively charge-balanced, pseudo-monophasic, rectangular pulses, were delivered from a MiniVStim test board (equivalent to Type 12B implants, Competence Team for Implanted Devices CTID, Center for Medical Physics and Biomedical Engineering, Medical University Vienna, Austria). All required stimulation patterns were implemented using the MiniVStim-App installed on a standard Android driven tablet computer (Xperia Tablet Z, Sony Corporation, Tokyo, Japan). The tablet computer maintained an active Bluetooth connection to a MiniVStim programming device which served as bridge to communicate with the test board via an additional RF-link.

Stimulation protocol

(i) Single twitch measurements

Single pulses with a phase-width of 258 µs were delivered every 3 s while the stimulation amplitude was increased every other pulse by 0.1 mA, to cover all amplitude levels

from 0.1 to 2.0 mA. The mean force response elicited by two pulses with the same amplitude was used to create a recruitment curve. In a first step, measurements were performed with the foot free to move, allowing for unloaded concentric (CON) contractions of the TA muscle. For isometric (ISO) contractions, the animal´s foot was restrained at a 90 ° position of the ankle joint.

(ii) Force-Frequency Curves
The relation between developed force and stimulation frequency was assessed with short bursts (200 ms, 2 mA) by using frequencies of 10, 20, 40, 60, 80 and 100 Hz. To avoid fatigue and to allow for a complete recovery of the neuronal structures, the time between bursts was set to 30 s. Force was recorded for concentric and isometric contractions.

Data Analysis
LabChart was used to mark the beginning of each twitch and burst. This annotated data was exported for further processing with Matlab R2010a (MathWorks, Natick, Massachusetts, United States). A semi-automatic script was used to analyse the recorded data. After manually selecting the baseline, the peak force was determined for every individual response.
Results were stored and further processed using Microsoft Excel (Microsoft Corporation, Washington, United States).

Results

Animals
Some descriptive parameters that were assessed for each animal can be found in table 1. The investigated rats had an average body weight of 292 g while their stimulated TA was 552 mg. There was no significant difference in the mean weights of left and right TA.

Twitch responses
The average threshold amplitude was 0.35 mA. The isometric case led to noticeable higher peak twitch forces, 251 % of the values achieved with an unloaded concentric contraction.

Force-Frequency Curves
Short supra-maximal bursts of different frequencies (10, 20, 40, 60, 80 and 100 Hz) were applied while the developed force was measured (see figure 2). Isometric contractions showed up to 3 times higher forces than the unloaded concentric case.

Discussion

Our results showed that the load-cell produced consistent results throughout a period of several months while being used in 11 separate experiments. It was possible to measure forces up to almost 9 N while its resolution was high enough to measure single twitches of as little as 0.1 N.

Values for the maximal isometric forces, measured with our device, are in general agreement with earlier published results using fixed transducers. Other research groups, studying the contractile properties of the TA muscle in rats, reported maximal tetanic forces of 8.24 ± 1.34 N [8], 7.75 ± 0.63 N [2] and 8.88 ± 0.63 N [9], which correlates well with our measurements revealing an average of 8.23 N.

Being able to measure the force that is produced while the muscle is still in its original place, offers the great opportunity to gain valuable information about how the muscle is acting in its normal biomechanical environment, rather than looking at it as a single subunit. Force that is transmitted through the tendon via the ankle joint could be potentially used to train the tibialis anterior in various different ways. In order to design a resistance training regime it is important to know about the forces occurring within this system. In future experiments we are going to use the current device to investigate the loading of the tibialis anterior during co-contraction of the plantar-flexors.

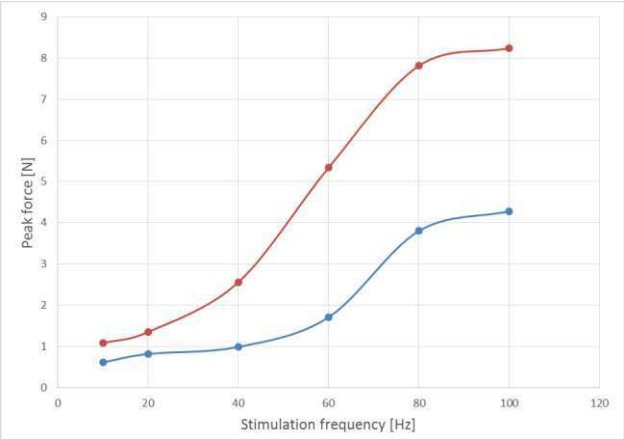

Figure 2: Averaged force-frequency responses of the TA muscle (n=2) obtained by short bursts at different frequencies for unloaded concentric (blue) and isometric (red) conditions

Conclusions

We were able to develop a device to perform in-vivo measurements of the tension transmitted by the tibialis tendon while maintaining the muscle´s position. Because the tendon remains attached to its original insertion, the load-cell potentially allows for measurements of force conducted across the ankle joint, which gives valuable information that could be used in designing training protocols for the tibialis anterior muscle.

Table 1: Overview of weights and corresponding maximal forces of the investigated animals.

Animal	**Age**	**Body weight**	**LTA weight**	**RTA weight**	**F_{max} twitch CON**	**F_{max} twitch ISO**	**F_{max} tetanic CON**	**F_{max} tetanic ISO**
#	days	g	mg	mg	N	N	N	N
1	64	285	533	548	0.87	1.76	4.51	8.62
2	65	300	571	499	0.79	2.41	4.05	7.85

Acknowledgement

This work is the outcome of a collaboration of the Medical University of Vienna together with the Liverpool John Moores University. The project was supported by MED-EL GmbH (Innsbruck, Austria).

References

[1] A. L. Hof, "The relationship between electromyogram and muscle force," *Sportverletzung · Sportschaden*, vol. 11, no. 03, pp. 79–86, Sep. 1997.

[2] R. H. Shin, T. Vathana, G. A. Giessler, P. F. Friedrich, A. T. Bishop, and A. Y. Shin, "Isometric tetanic force measurement method of the tibialis anterior in the rat," *Microsurgery*, vol. 28, no. 6, pp. 452–457, Jan. 2008.

[3] B. P. Spyropoulos, P. M. Santos, and S. L. Williams, "Tension transduction device for functional evaluation of the rat peroneal nerve," *Journal of Neuroscience Methods*, vol. 53, no. 1, pp. 95–100, Jul. 1994.

[4] A. I. van Bolhuis, J. Holsheimer, and H. H. C. M. Savelberg, "A nerve stimulation method to selectively recruit smaller motor-units in rat skeletal muscle," *Journal of Neuroscience Methods*, vol. 107, no. 1–2, pp. 87–92, May 2001.

[5] J. W.M. Grill and J. T. Mortimer, "The effect of stimulus pulse duration on selectivity of neural stimulation," *IEEE Transactions on Biomedical Engineering*, vol. 43, no. 2, pp. 161–166, Feb. 1996.

[6] P. H. Gorman and J. T. Mortimer, "The Effect of Stimulus Parameters on the Recruitment Characteristics of Direct Nerve Stimulation," *IEEE Transactions on Biomedical Engineering*, vol. BME-30, no. 7, pp. 407–414, Jul. 1983.

[7] N. D. Duncan, D. A. Williams, and G. S. Lynch, "Adaptations in rat skeletal muscle following long-term resistance exercise training," *Eur J Appl Physiol*, vol. 77, no. 4, pp. 372–378, Mar. 1998.

[8] R. M. Lovering, M. Hakim, C. T. Moorman, and P. G. De Deyne, "The contribution of contractile pre-activation to loss of function after a single lengthening contraction," *J Biomech*, vol. 38, no. 7, pp. 1501–1507, Jul. 2005.

[9] J. Grasa, M. Sierra, M. J. Muñoz, F. Soteras, R. Osta, B. Calvo, and F. J. Miana-Mena, "On simulating sustained isometric muscle fatigue: a phenomenological model considering different fiber metabolisms," *Biomech Model Mechanobiol*, vol. 13, no. 6, pp. 1373–1385, Apr. 2014.

[10] A. Biewener and R. Baudinette, "In vivo muscle force and elastic energy storage during steady-speed hopping of tammar wallabies (Macropus eugenii)," *Journal of Experimental Biology*, vol. 198, no. 9, pp. 1829–1841, Sep. 1995.

[11] A. A. Biewener, "Muscle Function in vivo: A Comparison of Muscles Used for Elastic Energy Savings versus Muscles Used to Generate Mechanical Power," *American Zoologist*, vol. 38, no. 4, pp. 703–717, 1998.

[12] M. A. Daley and A. A. Biewener, "Muscle force-length dynamics during level versus incline locomotion: a comparison of in vivo performance of two guinea fowl ankle extensors," *J Exp Biol*, vol. 206, no. 17, pp. 2941–2958, Sep. 2003.

Author's Address

Dipl. –Ing. Martin Schmoll
Center for Medical Physics and Biomedical Engineering,
Medical University Vienna,
Waehringer Guertel 18-20,
A-1090 Vienna, Austria
martin.schmoll@meduniwien.ac.at
http://www.zmpbmt.meduniwien.ac.at/forschung/neuroprothetics-fes-rehabilitation-engineering/competence-team-for-implanted-devices/

Session 2: Neuromodulation, Rehabilitation strategies

Transcutaneous spinal cord stimulation to induce standing in individuals with motor complete spinal cord injury

Hofstoetter US[1], Minassian K[1]

[1]Center for Medical Physics and Biomedical Engineering, Medical University of Vienna, Vienna, Austria

Abstract: *Even after severe cervical or thoracic spinal cord injury, remaining sensory-input processing and motor-output generating capabilities of the lumbar spinal cord circuitry caudal to the lesion can be demonstrated. Reactivating the intrinsic motor capacity of this circuitry is a target for neurorehabilitation interventions to improve leg function. Spinal cord stimulation (SCS) via epidural implants was recently shown to induce full body-weight bearing standing in motor complete spinal cord injured (SCI) individuals. Here, we studied whether transcutaneous SCS through skin electrodes would similarly generate motor outputs underlying upright standing in four motor complete SCI subjects. Transcutaneous stimulation was applied to the lumbar spinal cord at frequencies of 10–15 Hz and with intensities above the level generating lower-limb muscle activity. The stimulation, together with weight-bearing related sensory feedback input to the spinal cord, enabled the generation of lower-limb motor activity sufficient for upright standing with only minimal self-assistance for balance. This finding indicates that transcutaneous SCS, which is acting through afferent stimulation, can produce sufficient force in paralyzed legs to support standing.*

Keywords: *neuromodulation, non-invasive, spinal cord injury, spinal cord stimulation, standing*

Introduction

Severe spinal cord injury (SCI) is associated with limited prognosis for the recovery of voluntary motor function, standing and locomotion [1]. Electrical stimulation of the lumbar spinal cord at 20–50 Hz via electrodes implanted in the epidural space was previously shown to generate rhythmic flexion-extension movements in the lower limbs of individuals with clinically complete SCI lying supine [2–5], while stimulation at 5–16 Hz initiated strong bilateral leg extension [6,7]. Recent studies have demonstrated that epidural spinal cord stimulation (SCS) can generate leg extension and upright standing in individuals with motor complete SCI [8,9]. Under ongoing invariant stimulation and by manipulating their body position and centre of gravity, the subjects were able to initiate and maintain full weight-bearing standing with only minimal self-assistance for balance after intensive training [9].

With the development of transcutaneous lumbar SCS, a method became available to activate (a subset of) the same neural structures as with epidural SCS, i.e., large-to-medium diameter afferent fibres within the lumbar and upper sacral posterior roots bilaterally, yet non-invasively from the body surface [10–13]. When applied as a neuromodulation technique with adequate parameter settings, transcutaneous SCS was shown to temporarily alleviate spinal spasticity [14], to facilitate residual voluntary locomotor control in ambulatory, incomplete SCI individuals [15,16], and to considerably enhance the motor output produced by robotic-driven treadmill stepping in paralyzed individuals [17].

Here, we investigated the potential of transcutaneous SCS to induce upright standing in four individuals with clinically motor complete SCI.

Material and Methods

Subjects: Data were derived from four individuals with traumatic, clinically motor complete SCI (Tab. 1) in the chronic stage of recovery (3.3 ± 1.7 years post-injury). The study was approved by the Ethics Committee of the City of Vienna, Austria.

Transcutaneous spinal cord stimulation: Transcutaneous stimulation of the lumbar spinal cord was applied through a pair of interconnected stimulating surface electrodes (Ø 5 cm, Schwa-medico GmbH, Germany) placed paraspinally over the T11 and T12 spinous processes (Fig. 1A). A pair of reference electrodes (8 x 13 cm each) was placed paraumbilically over the abdomen. The targeted neural structures are afferent fibers within the lumbar and upper sacral posterior roots bilaterally. Stimulation of these afferent fibers was verified by the elicitation of posterior root-muscle (PRM) reflexes in the lower-limb muscles by single and double stimulus pulses at varying interstimulus intervals (Fig. 1B) [10,11,14,16,18]. Charge-balanced, symmetric, biphasic rectangular pulses of 1-ms width per phase were delivered by a voltage-controlled stimulator in subjects 1 and 4 and by a current-controlled stimulator (Stimulette r2x+, Dr. Schuhfried Medizintechnik GmbH, Moedling, Austria) in subjects 2 and 3. With reference to the indifferent electrodes, the paraspinal electrode pair was the anode for the first and the cathode for the second pulse phase.

Data acquisition: EMG activity was acquired from quadriceps (Q), hamstrings (Ham), tibialis anterior (TA), and triceps surae (TS) of both legs with pairs of silver-silver chloride surface electrodes (Intec Medizintechnik GmbH, Klagenfurt, Austria), each placed centrally over the muscle bellies [19]. Reference electrodes were placed over

Table 1: Subject characteristics.

Subj.nr.	Sex	Age	Years post-SCI	Level of SCI	AIS
1	M	58	3	T9	A
2	F	18	1	T7	A
3	F	22	3	T5	A
4	M	23	4	C6	B

Subj.nr., subject number; SCI, spinal cord injury; AIS, American Spinal Injury Association Impairment Scale

the fibular heads bilaterally. Abrasive paste (Nuprep, Weaver and Company, Aurora, CO, USA) was used for skin preparation to reduce contact resistance below 5 kΩ. EMG signals were amplified with a gain of 600, filtered to a bandwidth of 10–500 Hz and digitized at 2048 samples per second per channel. Electro-goniometers (Penny & Giles Biometrics, Ltd., Gwent, UK) were used to record hip and knee joint angles. Goniometric data were synchronized to the EMG, filtered to a bandwidth of 0–15 Hz, and sampled at 2048 Hz. In subjects 1 and 4, ground reaction forces exerted between foot and floor in the standing position were recorded for both limbs using two independent force measurement platforms (piezoelectric force sensors, Kistler Instrumente AG, Winterthur, Switzerland) and synchronized to the EMG.

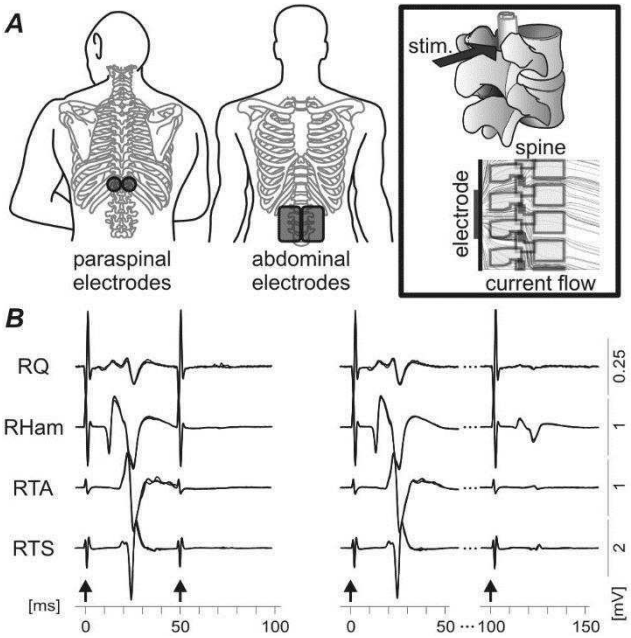

Figure 1: Transcutaneous SCS. *A* Sketch illustrating the placement of the stimulating and reference skin electrodes over the back and the lower abdomen. Drawing on the right depicts stimulation (stim.) through the better conductive elements (ligaments and discs) between the bony structures of the spine, along with a computer simulation of the current flow produced in a mid-sagittal plane. *B* The stimulation of the lumbar and upper sacral spinal cord was verified by the elicitation of PRM reflexes in the L2–S2 innervated quadriceps (Q), hamstrings (Ham), tibialis anterior (TA), and triceps surae (TS) bilaterally and their post-activation depression at varying interstimulus intervals (ISIs). Shown are exemplary responses recorded from the right (R) lower-limb of subject 3 at ISIs of 50 ms (left) and 100 ms (right), respectively. Arrows mark times of stimulus application.

Stimulation and study protocol: Starting from a semi-sitting position supported by an overhead harness (*cf.* Fig. 2A), transcutaneous SCS was applied at a frequency of 15 Hz (subjects 1–3) and 10 Hz (subject 4). The stimulation intensity was slowly increased to a level above the PRM-reflex threshold that induced lower-limb extension. Individually set maximum stimulation intensities were subject 1, 30 V; subject 2, 120 mA; subject 3, 80 mA; and subject 4, 37 V. None of the subjects reported adverse effects induced by the stimulation.

Results

Transcutaneous SCS at 10–15 Hz and with intensities above the threshold for eliciting PRM reflexes in the lower-limb muscles generated motor output in the lower-limb muscles appropriate to induce bilateral leg extension (Fig. 2) in the motor complete SCI individuals, except for subject 2 in whom such output was generated unilaterally only.

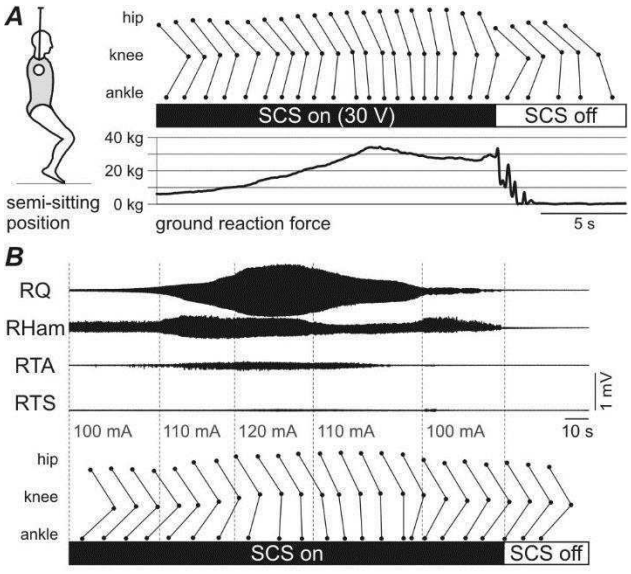

Figure 2: Transcutaneous SCS at 10–15 Hz with an intensity above the PRM-reflex threshold induces upright standing in individuals with clinically motor complete SCI. *A* The stimulation induced leg extension leading to an upright standing position with ground reaction forces of up to 37 kg per leg. The standing position was maintained until the stimulation was turned off (SCS off). Shown are stick-figures of one leg based on hip and knee goniometric data along with corresponding ground reaction forces; subject 1. SCS invariantly applied at 15 Hz and 30 V. *B* EMG activity generated in right (R) quadriceps (Q), hamstrings (Ham), tibialis anterior (TA), and triceps surae (TS) by 15-Hz

transcutaneous SCS with increasing intensity. At an intensity of 120 mA, leg extension was induced and maintained until the intensity was reduced again, as illustrated by the stick-figures; subject 2.

By manipulating the body position, thereby shifting the centre of gravity, and with minimal arm support, the subjects were able to initiate upright standing from a semi-sitting initial position. The standing position was maintained with only minimal self-assistance required for balance control until the stimulation intensity was either reduced to below a critical level or transcutaneous SCS was turned off. With the exception of subject 2, in whom the extended position of the less-responding leg was supported unilaterally by a therapist, no manual assistance was provided to maintain lower-limb extension. Maximum ground reaction forces of up to 450 N per lower limb were generated in subjects 1 and 4 (*cf.* Fig. 2A). Closer inspection of the EMG activities produced by transcutaneous SCS further revealed that they were composed of series of stimulus-triggered PRM reflexes.

Discussion and Conclusion

Transcutaneous SCS, like its epidural counterpart [8,9], induced motor output underlying bilateral leg extension with sufficient force to induce and maintain an upright standing position in three of the four individuals studied with an SCI clinically classified as motor complete, i.e., without the ability to voluntarily induce or maintain standing. Notably, these results were obtained within the first session of transcutaneous SCS applied with the purpose to induce standing. In subject 2, such motor output was obtained in one leg only. Closer clinical examination revealed previously undiagnosed secondary peripheral lesions affecting the less-responding lower limb.

The EMG activity produced by the transcutaneous SCS consisted of series of stimulus-time related PRM reflexes. It can hence be assumed that the stimulation activated large-to-medium diameter afferent fibers within the lumbar and upper sacral posterior roots [10,20] and that the evoked inputs transsynaptically engaged plurisegmentally organized spinal circuits involved in the control of lower-limb activity [14,16], as also suggested in epidural SCS [3,6,7].

The extension movements of the legs induced by transcutaneous SCS were likely further facilitated by the progressive weight-bearing related sensory feedback input to the spinal cord when initiating the standing-up movement, suggesting the active involvement of spinal circuitry and the integration of feedback input [8,9].

The present findings indicate the potential of transcutaneous SCS as a non-invasive training device to induce full-weight bearing, active standing in individuals with severe SCI. Further study in a larger subject population is warranted, also to test potential training effects with repetitive application of transcutaneous SCS to induce standing as well as the effects of individually optimized stimulation parameters [9].

References

[1] Ramer LM, Ramer MS, Bradbury EJ: Restoring function after spinal cord injury: towards clinical translation of experimental strategies, *Lancet. Neurol.*, vol. 13, pp. 1241-1256, 2014

[2] Dimitrijevic MR, Gerasimenko Y, Pinter MM: Evidence for a spinal central pattern generator in humans, *Ann. N. Y. Acad. Sci.*, vol. 860, pp. 360-376, 1998

[3] Minassian K, Jilge B et al: Stepping-like movements in humans with complete spinal cord injury induced by epidural stimulation of the lumbar cord: electromyographic study of compound muscle action potentials, *Spinal Cord*, vol. 42, pp. 401-416, 2004

[4] Danner SM, Hofstoetter US et al: Human spinal locomotor control is based on flexibly organized burst generators, *Brain*, vol. 138, pp. 577-588, 2015

[5] Minassian K, McKay WB, Binder H, Hofstoetter US: Targeting Lumbar Spinal Neural Circuitry by Epidural Stimulation to Restore Motor Function After Spinal Cord Injury, *Neurotherapeutics*, vol. 13, pp. 284-294, 2016

[6] Jilge B, Minassian K et al: Initiating extension of the lower limbs in subjects with complete spinal cord injury by epidural lumbar cord stimulation, *Exp. Brain Res.*, vol. 154, pp. 308-326, 2004

[7] Minassian K, Hofstoetter US: Spinal Cord Stimulation and Augmentative Control Strategies for Leg Movement after Spinal Paralysis in Humans, *CNS Neurosci. Ther.*, vol. 22, pp. 262-270, 2016

[8] Harkema S, Gerasimenko Y et al: Effect of epidural stimulation of the lumbosacral spinal cord on voluntary movement, standing, and assisted stepping after motor complete paraplegia: a case study, *Lancet*, vol. 377, pp. 1938-1947, 2011

[9] Rejc E, Angeli C, Harkema S: Effects of Lumbosacral Spinal Cord Epidural Stimulation for Standing after Chronic Complete Paralysis in Humans, *PLoS One*, vol. 10, p. e0133998, 2015

[10] Minassian K, Persy I, et al: Posterior root-muscle reflexes elicited by transcutaneous stimulation of the human lumbosacral cord, *Muscle Nerve*, vol. 35, pp. 327-336, 2007

[11] Hofstoetter US, Minassian K et al: Modification of reflex responses to lumbar posterior root stimulation by motor tasks in healthy subjects, *Artif. Organs*, vol. 32, pp. 644-648, 2008

[12] Ladenbauer J, Minassian K, Hofstoetter US, Dimitrijevic MR, Rattay F: Stimulation of the human lumbar spinal cord with implanted and surface electrodes: a computer simulation study, *IEEE Trans. Neural Syst. Rehabil. Eng.*, vol. 18, pp. 637-645, 2010

[13] Danner SM, Hofstoetter US et al: Can the human lumbar posterior columns be stimulated by transcutaneous spinal cord stimulation? A

modeling study, *Artif. Organs*, vol. 35, pp. 257-262, 2011

[14] Hofstoetter US, McKay WB et al: Modification of spasticity by transcutaneous spinal cord stimulation in individuals with incomplete spinal cord injury, *J. Spinal Cord Med.*, vol. 37, pp. 202-211, 2014

[15] Hofstoetter US, Hofer C et al: Effects of transcutaneous spinal cord stimulation on voluntary locomotor activity in an incomplete spinal cord injured individual, *Biomed. Tech. (Berl).*, 2013

[16] Hofstoetter U, Krenn M et al: Augmentation of voluntary locomotor activity by transcutaneous spinal cord stimulation in motor-incomplete spinal cord injured individuals: A preliminary study, *Artif. Organs*, vol. 39, pp. E176-186, 2015

[17] Minassian K, Hofstoetter US et al: Spinal Rhythm Generation by Step-Induced Feedback and Transcutaneous Posterior Root Stimulation in Complete Spinal Cord-Injured Individuals, *Neurorehabil. Neural Repair*, vol. 30, pp. 233-243, 2016

[18] Minassian K, Hofstoetter US, Rattay F: "Transcutaneous lumbar posterior root stimulation for motor control studies and modification of motor activity after spinal cord injury", in *Restorative neurology of spinal cord injury (M. Dimitrijevic, B. Kakulas, W. McKay, and G. Vrbova, eds.).* ch. 8, pp. 226–255, New York: Oxford University Press, 2011

[19] Sherwood AM, McKay WB, Dimitrijević MR: Motor control after spinal cord injury: assessment using surface EMG., *Muscle Nerve*, vol. 19, pp. 966-979, 1996

[20] Hofstoetter US, Danner SM, Minassian K: "Paraspinal Magnetic and Transcutaneous Electrical Stimulation," in *Encyclopedia of Computational Neuroscience: Springer Reference (D. Jaeger and R. Jung, eds.)* Berlin-Heidelberg: Springer-Verlag GmbH, 2014

Author's Address

Ursula S. Hofstoetter
Center for Medical Physics and Biomedical Engineering, Medical University of Vienna
Waehringer Guertel 18-20/4L
1090 Vienna, Austria
ursula.hofstoetter@meduniwien.ac.at
http://www.zmpbmt.meduniwien.ac.at/1/

Sensory input with different rates of sustained electrical stimulation can modify motor output of the human lumbosacral spinal cord

Krenn M[1,2], Mayr W[1], Mickel M[3], Keilani M[3], Crevenna R[3], Dimitrijevic MR[4,5]

[1]Center for Medical Physics and Biomedical Engineering, Medical University of Vienna, Vienna, Austria
[2]Institute of Electrodynamics, Microwave and Circuit Engineering, Vienna University of Technology, Vienna, Austria
[3]Department of Physical Medicine and Rehabilitation, Medical University of Vienna, Vienna, Austria
[4]Foundation for Movement Recovery, Oslo, Norway
[5]Baylor College of Medicine, Houston, TX, USA

Abstract: Sensory motor circuits in the spinal cord are constructed with a fine specificity that coordinates motor behavior. Analysis of the dorsoventral connectivity patterns in an animal model showed that the projections of sensory axons to discrete dorsoventral domains of the spinal cord without regard for motor neuron subtype or the presence of motor neurons. By implications, the clustering and dorsoventral settling position of motor neuron pools serve as a determinant of the pattern of sensory input specificity and thus motor coordination. The mechanisms that direct sensory connections with their motor neuron pattern remain unclear. In this study, patterns of spinal sensory-motor output initiated by epidural spinal cord stimulation of lumbar posterior human cord determinant of the patterns of sensory inputs rate and strength.
Six subjects (two females) with chronic, traumatic, motor complete spinal cord injury were studied. The injury level was between Th2 and Th6. The epidural spinal cord stimulation consisted of a cylindrically shaped electrode array and a pulse generator (Pisces-Quad electrode, Model 3487A and Itrel 3, Model 742, Medtronic Inc., Minneapolis MN, USA). Across subjects, the rostrocaudal positions of the electrodes ranged from vertebral levels Th11–L1. The motor output was recorded electromyographically in the major leg muscle. For analysis, the root mean square value (ERMS) of the signal was calculated in a window of 3 s.
The ERMS was facilitated in all muscle groups by 66.3% between a stimulation rate of 2.1 Hz and 10 Hz. Above 10 Hz, the modification of the motor output with increasing stimulation rates showed a progressive suppression. Therefore, the ERMS declined around 19%, 51% and 66% for a stimulation rate of 16, 20 and 30 Hz, respectively. At a sustained stimulation of 100 Hz, the responses were nearly diminished.
We have found crucial evidence of consistently reproducibly patterned response. In contrast, the animal research has different motor behavior, but it predicts some interesting cluster activity which we interpret in our subjects without variability. Moreover, if this pattern response is augmented or suppressed, we can demonstrate the same effect on the result of independent motor unit's activity from background activity. Intriguing differences between results and the insights gathered gives us the opportunity to discuss the significance of the patterned response modifying the motor control in spinal cord injury subjects.

Keywords: *sensory-motor integration, spinal cord stimulation, afferent input, spinal networks*

Author's Address

Matthias Krenn
Vienna University of Technology
Institute of Electrodynamics, Microwave and Circuit Engineering
Gusshausstrasse 27
1040 Vienna, Austria

eMail: matthias.krenn@outlook.com
http://www.emce.tuwien.ac.at/en/biosensorik.htm

Study of the effect's duration of non-invasive trans-spinal stimulation to reduce clonus activity in people with SCI

Vargas Luna JL[1,2,3], Magnúsdóttir G[3], Krenn M[4,5], Guðfinnsdóttir HK[1], Guðmundsdóttir V[3], Mayr W[4], Ludvigsdóttir GK[3], Helgason T[1,3]

[1]Institute for Biomedical and Neural Engineering, Reykjavik University, Iceland
[2]Escuela de Ingenieria y Ciencias, Tecnologico de Monterrey, Mexico
[3]Dept.of Rehabilitation Medicine, Landspitali University Hospital, Iceland
[4]Center for Medical Physics and Biomedical Engineering, Medical Universiy of Vienna, Austria
[5]Institute of Electrodynamics, Microwave and Circuit Engineering, Vienna University of Technology, Austria

Abstract: *Clonus activity is a symptom caused by spasticity and is frequently present in patients with either complete or incomplete spinal cord injury. If present, it interferes with the motor control, causes imbalance and reduces walking speed. In this work we study the changes on the excitability of lumbosacral neural centers—that control the clonus—caused by trans-spinal stimulation immediately after and two hours after its application. The results show that the stimulation significantly modifies the neural excitability of the lumbosacral neural networks, reducing the clonus activity in three out of four subjects even two hours post-stimulation. This suggests that trans-spinal stimulation could potentially be used as a complementary treatment to temporally suppress clonus activity, facilitating the performance of other rehabilitation treatments or leisure activities and, therefore increase the quality of life of SCI people.*

Keywords: *Trans-spinal stimulation, clonus, spinal cord injury*

Introduction

Traumatic spinal cord injury (SCI) is a striking event that can cause muscle paralysis, neuropathic pain and spasticity. Approximately 80% of people with SCI suffer spasticity [1], which can reduce their quality of life by diminishing their ability to perform tasks with the otherwise healthy motor system [2], [3]. One of the major components of spasticity is the clonus, which importantly affects the residual motor control of the people. Currently, clonus is treated as part of the spasticity problem, which treatments induced generalized muscle relaxation, which cause debilitating side effects that limit the patients' mobility.

Alternative treatments have been proposed using trans-spinal stimulation in both, invasive [4] and non-invasive ways [5], [6]. These studies are based on the fact that trans-spinal stimulation is able to selectively depolarize posterior root fibers, which modifies the excitability of the lumbosacral neural centers, triggering a series of neuromodulation processes [4]. Preliminary studies showed that transcutaneous trans-spinal electrical stimulation was able to suppress ankle clonus activity immediately after stimulation on three incomplete SCI [5]. However, although it has been suggested that the effects last for some hours, there are not publications that quantify these effects other than immediately after.

This work presents a pilot study that quantifies the modification on clonus activity with trans-spinal stimulation on complete and incomplete SCI people. The ankle clonus is quantified before, immediately after and two hours after the stimulation.

Material and Methods

The clinical trial was approved as pilot study by the Icelandic Ethical Committee, and conducted according to the principles of Helsinki Declaration. Four subjects (3 males, 1 females) aged between 31 and 60 years old were enrolled. All subjects have SCIs above T10 and are classified as A (2 cases), C (1 case) and D (1 case) in the ASIA Impairment Scale (AIS). In all cases the lesions are chronic (at least 3 years post-injury). The participants were informed of the experimental procedure, benefits and potential risks of the measurements, and they signed an informed consent prior the measurements. Table 1 presents a summary of the enrolled subjects.

The stimulation consisted in unipolar current-controlled electrical stimulation transversally applied at the level of the intervertebral space T11-T12. The current was delivered through self-adhesive hydrogel electrodes. The active electrode consisted of two interconnected small electrodes (5 cm diameter, V.Trodes, Mettler Electronics Corp., USA) placed over the paravertebral skin between the T11 and L1 spinous processes [7]. The reference electrode was composed by a pair of rectangular electrodes (7.5 x 13 cm, ValuTrode, Axelgaard Manufacturing Co., Ltd., USA) placed symmetrically over the umbilicus.

The stimulator device (Stimulette R2X, Schuhfried Medizintechnik GmbH, Vienna, Austria) was configured to deliver charge-balanced rectangular pulses of 1 ms (per phase) pulse width. The stimulation frequency was set to 50 Hz, because previous works has shown that such frequency is able to modify the spasticity [8], [9] and, on the other, to increase the motor control [10]. The polarity was defined to deliver the cathodic phase first over the paravertebral electrodes.

Table 1: Average tibialis anterior and triceps surae EMG activity (in µVrms) during the manual clonus elicitation before (stage 1), immediately after (stage 2) and 2 hours after (stage 3) stimulation.

		TA (µVrms)			TS (µVrms)		
Subject	Side	Stage 1	Stage 2	Stage 3	Stage 1	Stage 2	Stage 3
S1	Left	<1µVrms	<1µVrms	<1µVrms	<1µVrms	<1µVrms	<1µVrms
	Right	7.09±1.23	0.76±0.18	0.29±0.08	5.98±2.97	5.08±2.22	4.66±1.03
S2	Left	2.26±2.20	0.80±0.58	1.67±1.48	<1µVrms	<1µVrms	<1µVrms
	Right	19.66±11.73	1.03±0.70	0.21±0.07	<1µVrms	<1µVrms	<1µVrms
S3	Left	3.08±1.53	0.63±0.22	1.15±0.85	42.06±16.59	10.45±5.33	26.02±20.03
	Right	21.40±17.28	3.14±4.24	1.22±0.49	9.63±4.55	6.74±0.94	1.71±1.52
S4	Left	<1µVrms	<1µVrms	<1µVrms	<1µVrms	<1µVrms	<1µVrms
	Right	<1µVrms	<1µVrms	<1µVrms	0.72±0.14	2.19±0.53	1.39±0.81

In order to reduce the activity suppression due to fatigue, the stimulation intensity was defined as 90% of the smallest motor threshold on the assessed muscles. The stimulation was applied for 30 min with the subject relaxed in a supine position [9].

The effect of the electrical stimulation on the clonus activity was quantified through the activity differences on the lower limb muscles before (stage 1), immediately after (stage2) and 2 hours after the stimulation (stage 3). The clonus was manually elicited through an Achilles tendon stimulation. The maneuver consisted on a rapid dorsiflexion movement that was sustained for ~2.5 seconds; and it was repeated at least three times per stage [11]. The activity was monitored on triceps surae (TS) and tibialis anterior (TA) through electromyography (EMG) of both legs. The EMG signals were recorded with a Wireless EMG system (KINE ehf., Iceland) that apply a band pass filter ranging from 10 to 600 Hz and an acquisition rate of 1600 samples per second.

The muscle activity was quantified through the root mean square voltage (Vrms) of the EMG during the whole maneuver. The muscle activity was considered negligible when, in all the stages, the average values were smaller than 1µVrms. A Welch t-test was conducted over the non-negligible data to compare the muscle activity before and after the stimulation. Because of the high inter-variability in the EMG amplitudes, the statistical test was conducted over Vrms values previously normalized to the average Vrms prior stimulation. The level of significance for the statistical test was $\alpha = 0.05$.

Results

A total of 4 data sets were acquired. Due to the individuality of each SCI, the clonus elicitation maneuver only produce activity on three the volunteers at the first assessment. On subject S4, on the other hand, trans-spinal stimulation triggered TS activity on the right leg. Tab. 1 presents the average Vrms values for each assessment, muscle and leg.

As shown in EMG activity on the right muscles of S3 (Fig. 1), it is observed that the clonus activity—recognized by the sequential burst of triceps surae—is substantially reduce upon stimulating. This trend was similar in S1, while S2 did not present triceps surae activity during the assessment. Although unremarkable, S4 showed a slight increase in triceps surae activity (Tab. 1). Because of the opposite results of S4, no statistical significance was found in triceps surae activity between stages. However, excluding the results for S4, the Welch t-test shows a significant reduction of TS activity immediately after stimulation (0.58±0.33) when compared with stage 1 (1±0.40); $t(17.34) = 2.62$, $p = 0.02$. On stage 3, the muscle activity was slightly smaller (0.52±0.37); $t(18.34) = 2.84$, $p = 0.01$.

In three volunteers—S1, S2 and S3—tibialis anterior also present abnormal activity in at least one leg, while in S4 both triceps surae remained silent. The trans-spinal stimulation significantly reduced such activity to nearly negligible values (0.18±0.18) when compared with stage 1 (1±0.36); $t(19.53) = 5.47$, $p > 0.001$. The suppression slowly start to fade on stage 3 (0.26±0.44), but remain highly significant; $t(30.47) = 4.21$, $p < 0.001$.

In the subjects with the larger reductions of EMG activity (S2 and S3), the reduction of clonus activity—quantified as the number of beets—as detected by the physiotherapist was evident. S2 reduced from 4 or 5 clonus beets at stage 1 to barely one beet post-stimulation,

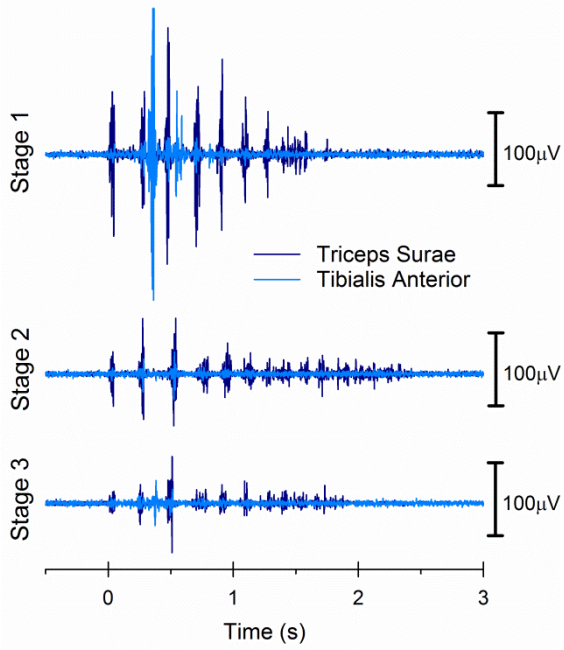

Figure 1: Exemplary EMG signals of the right triceps surae and tibialis anterior of S3 during the Achilles tendon stimulation

while S3 reduced from sustained clonus to none immediately after stimulation and then back to a weaker clonus.

Discussion

The application of low-intensity stimulation at 50 Hz during 30 minutes has, independently of the subject's profile, modify the spinal excitability state. The results show that, if existing, the clonus activity was successfully reduced or suppressed immediately after the stimulation. This is consistent with previous works, where the immediate effects of a similar setup—but using voltage-control stimulation—on three AIS D volunteers were shown [5]. In this report we also quantify the temporality of such effects by assessing the clonus activity two hours after the stimulation offset. The results shown that after two hours, the clonus reduction was still present at various levels.

One volunteer (AIS C), the clonus activity was absent at the beginning of the session. In this special case, the stimulation induced slight clonus activity in one leg, which partially fades 2-hours post stimulation. Although the activity levels after the stimulation were relatively low, it provides evidence that trans-spinal stimulation is consistently able to modify the excitability state of the lumbosacral spinal centres.

The capability of trans-spinal stimulation to effectively modify clonus activity suggests that the action mechanisms aren't exclusively related to increases of neuromodulatory signals from the descending tracts, but also to local processes within the spinal networks. Some of the possible mechanisms are the recovery or increase on Ia reciprocal inhibition, which is normally affected after the SCI [1]. This is supported by the fact that the trans-spinal stimulation targets the posterior roots, which include Ia fibers that are known by have strong synaptic connections to Ia inhibitory interneurons [12].

Conclusion

This preliminary study shows the consistency of trans-spinal stimulation to effectively modify the excitability of lumbosacral neural networks. Therefore, we were able to modify the clonus activity not only in incomplete lesions but also in complete ones. This shows that the technique can be further extrapolate to expand potential treatments for complete SCI people.

The results also show a significant permanence of the induced effect two hours after the stimulation offset. Although the patients reported that the effects were longer than two hours, this period of time is already enough to be applied prior conventional therapies, which may boost their therapeutic effect, or leisure activities, which are often limited for clonus.

Acknowledgment

This work was supported by the Mexican Council of Research and Technology (CONACYT, www.conacyt.mx), and Landspitali Science Fund.

References

[1] S. M. Elbasiouny, D. Moroz, M. M. Bakr, and V. K. Mushahwar, "Management of spasticity after spinal cord injury: current techniques and future directions.," *Neurorehabil. Neural Repair*, vol. 24, no. 1, pp. 23–33, Jan. 2010.

[2] P. Krawetz and P. Nance, "Gait analysis of spinal cord injured subjects: Effects of injury level and spasticity," *Arch. Phys. Med. Rehabil.*, vol. 77, no. 7, pp. 635–638, Jul. 1996.

[3] M. M. Adams and a L. Hicks, "Spasticity after spinal cord injury.," *Spinal Cord*, vol. 43, no. 10, pp. 577–86, Oct. 2005.

[4] M. M. Pinter, F. Gerstenbrand, and M. R. Dimitrijevic, "Epidural electrical stimulation of posterior structures of the human lumbosacral cord: 3. Control Of spasticity.," *Spinal Cord*, vol. 38, no. 9, pp. 524–31, Sep. 2000.

[5] U. S. Hofstoetter, W. B. McKay, K. E. Tansey, W. Mayr, H. Kern, and K. Minassian, "Modification of spasticity by transcutaneous spinal cord stimulation in individuals with incomplete spinal cord injury.," *J. Spinal Cord Med.*, vol. 37, no. 2, pp. 202–11, Mar. 2014.

[6] W. M. Oo, "Efficacy of Addition of Transcutaneous Electrical Nerve Stimulation to Standardized Physical Therapy in Subacute Spinal Spasticity: A Randomized Control Trial.," *Arch. Phys. Med. Rehabil.*, vol. 95, no. 11, pp. 2013–2020, 2014.

[7] F. D. Roy, G. Gibson, and R. B. Stein, "Effect of percutaneous stimulation at different spinal levels on the activation of sensory and motor roots.," *Exp. brain Res.*, vol. 223, no. 2, pp. 281–289, Nov. 2012.

[8] M. R. Dimitrijevic, L. S. Illis, K. Nakajima, P. C. Sharkey, and A. M. Sherwood, "Spinal cord stimulation for the control of spasticity in patients with chronic spinal cord injury: II. Neurophysiologic observations.," *Cent. Nerv. Syst. Trauma*, vol. 3, no. 2, pp. 145–52, Jan. 1986.

[9] U. S. Hofstoetter, W. B. McKay, K. E. Tansey, W. Mayr, H. Kern, and K. Minassian, "Modification of spasticity by transcutaneous spinal cord stimulation in individuals with incomplete spinal cord injury.," *J. Spinal Cord Med.*, vol. 37, no. 2, pp. 202–11, Mar. 2014.

[10] K. Minassian, B. Jilge, F. Rattay, M. M. Pinter, H. Binder, F. Gerstenbrand, and M. R. Dimitrijevic, "Stepping-like movements in humans with complete spinal cord injury induced by epidural stimulation of the lumbar cord: electromyographic study of compound muscle action potentials.," *Spinal Cord*, vol. 42, no. 7, pp. 401–16, Jul. 2004.

[11] W. B. McKay, A. M. Sherwood, and S. F. T. Tang, "A Manual for the Neurophysiological Assessment of Motor Control," in *Restorative Neurology of Spinal Cord Injury*, M. R. Dimitrijevic, B. A. Kakulas, W. B. McKay, and

G. Vrbova, Eds. Oxford University Press, 2012, pp. 261–284.
[12] K. Pearson and J. Gordon, “Spinal Reflexes,” in *Principles of Neural Science*, 4th Editio., E. R. Kandel, J. H. Schwartz, and T. M. Jessell, Eds. McGraw-Hill, 2000, pp. 713–735.

Author’s Address

José Luis Vargas Luna
Institute for Biomedical and Neural Engineering, Reykjavik University / Landspitali University Hospital, Iceland.
Escuela de Ingenieria y Ciencias, Tecnologico de Monterrey, Mexico.
eMail: joseluis.vargasluna@gmail.com

Ca^{2+} model to explain long-term effects of locomotion improvement from paraplegic individuals due to spinal cord stimulation

Anzinger-Weitmann M[1], Rattay F[1]

[1]Institute for Analysis and Sientific Computing, Vienna University of Technology, Austria

Abstract: *Individuals with motor-incomplete spinal cord injury show a restricted possibility for locomotion. Additional occurrence of spasticity restricts the capability of locomotion again. Several studies have shown that epidural spinal cord stimulation is able to reduce spasticity of paraplegic individual. Additional it improves the pattern of locomotion considerable. This improvement of the locomotion pattern is observable for hours even after the stimulation has been removed. To explain this phenomenon a computational Ca^{2+} model has been designed which is able to replicate this long-term effect. An existing population model is combined with a model of glia cells. Both models are communicating over a Ca^{2+} parameter. The Ca^{2+} level of the glia cells controls the post synaptic potential of the neuronal populations. Due to the missing activation of the supra spinal system, the Ca^{2+} level declines in the glial system. Through stimulation of the lumbosacral spinal cord the Ca^{2+} level will rising up again in the glial system. As a result the improvement of the locomotion patterns stays for a fairly long time.*

Keywords: *Ca^{2+} model, spinal cord stimulation, glia cells*

Introduction

Paraplegic individuals with motor-incomplete injury exhibit an altered locomotion pattern. The restricted possibility of movement results mostly in additional spasticity which altered the possibility of locomotion again [2]. Clinical studies have shown that epidural stimulation of the lumbosacral spinal cord can improve the pattern of locomotion distinguished. It will reduce spasticity in the involved lower limbs [1, 3]. Remarkably this improvement of locomotion pattern and reduced spasticity is a long term effect. Even after hours the stimulation has removed, the individuals are showing a more safe motion sequence then before [3, 4].
The reason for this long term effect of lumbosacral spinal cord stimulation is unknown.
In this computational study we propose a model in which Ca^{2+} concentration in the glial system is responsible for the capability of the activation of neuronal pools.
Due to the complexity of the task a model in the Hodgkin & Huxley style is time consuming to compute. Therefore, a population coding model is chosen to reduce the computational effort. Moreover few parameters change the behaviour of the model and the intrinsic properties are more easily to understand.

Material and Methods

We are using a population model to design the neuronal populations from the literature which describes the firing rate of a whole neuronal population [5]. The output of each population is defined over a sigmoidal function to limit the output to a maximum. Each output of a population is normalized to one (corresponds 100 % activation).

The model for the glia cells is derived from the theory of inhomogeneous populations. This model has the property that it does not start to oscillate rather it will move to a stable equilibrium.
One parameter determines the Ca^{2+} level in the glia cells what interconnect the two systems of neurones and glia cells.

$$\frac{dCa_i}{dt} = \sum_{j \in G} \beta_i V_i (Ca\max_i - Ca_i) - \alpha_i Ca_i \qquad (1)$$

$$\tau_i \frac{dV_i}{dt} = -V_i + F(h_i + \sum_{j \in G} \gamma_{ji} V_j, Ca_i) \qquad (2)$$

$$F(x_i, Ca_i) = \frac{1}{1 + e^{-Ca_i (x_i - a)}} \qquad (3)$$

Ca_i ... Ca^{2+} *level in corresponding glia cells*
Ca_{max} ... *maximum* Ca^{2+} *level in glia cells*
β_i ... *slew rate of ascending* Ca^{2+}
α_i ... *slew rate of descending* Ca^{2+}
V_i ... *output of a neuronal population*
h_i ... *external stimulus*
γ_{ji} ... *connection matrix of the neuronal populations*
$F(x_i, Ca_i)$ ... *transfer function of a neuronal population*

The model runs in a MATLAB® toolbox. The toolbox itself is a proprietary development. The solver is running with the Runge-Kutta method with fixed stepping size.

Results

To explain the long-term effect of lumbosacral spinal cord stimulation we propose a two level mechanism to control the output of a neuronal population. The first level is the neuronal net which generates the expected patterns [6]. The second level is the glial system. It controls the postsynaptic potential over the Ca^{2+} level in the glia cells [7, 8]. In the model this performance is described by the transfer function *F(x,Ca)*.
To explain the mechanism we consider one neuronal population with the dedicated glial system (Figure 1). It shall be investigated how the transfer function changes its behaviour corresponding to the stimulus. At the beginning the model is stimulated after a longer phase of rest. Afterwards the model is excited and in the phase of rest.

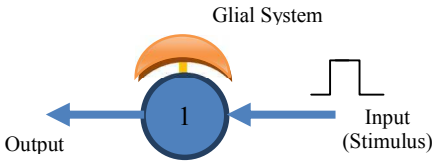

Figure 1: The neuronal population 1 is interconnected with its dedicated glial system (half moon). A stimulus on the input drives the Ca^{2+} level in the glia cells to ascend. The slew rate of the transfer function becomes steeply. Conversely a missing appropriate stimulus will declines the Ca^{2+} level in the glia cells. The slew rate of the transfer function becomes flat.

When the neuronal system gets a stimulus the Ca^{2+} level is rising up in the glial system and the transfer function is climbing up again [9]. Figure 2 shows the coherency of stimulus level (A) and transfer function (C, D) and the corresponding output (B). The stimulus has been varied from 0.5 to 3 in 0.2 steps. The output is growing up over time with each increasing stimulus. Figure 2C shows the progress of the transfer function over time with a stimulus input of 3. For each time point the transfer function has been plotted with the corresponding Ca^{2+} level. At time point 100 the stimulus has been activated for 500 time steps. After a short time at time point 200 the transfer function bounce up very quickly. At time point 600 the stimulus has been removed again but the transfer function is declining its gradient very slowly. In figure 2D the stimulus level is 1.6. The progress of the transfer function shows that the stimulus is not sufficient to activate the system.

How fast the Ca^{2+} level shall sink in the glial system - and therefore how fast the transfer function will descend - depends on the value of α_i in equation (2).

The parameter has been chosen to keep the simulation time as short as possible. The unit of time steps depends on the parameter τ in equation (1).

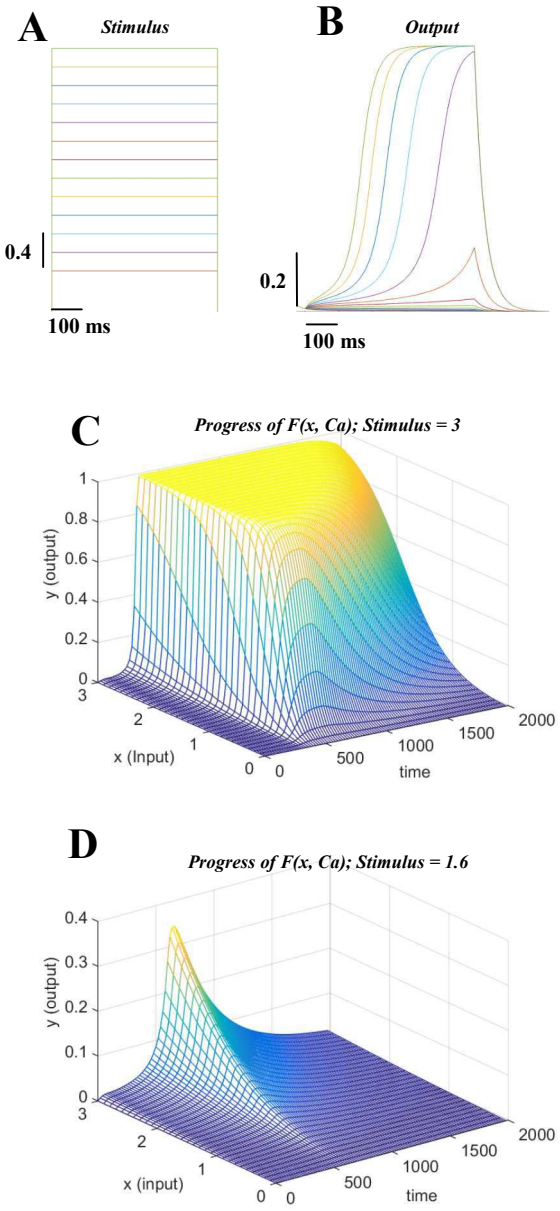

Figure 2: (A) The height of the stimulus to the neuronal population has been varied from 0.5 to 3 for each 500 ms from 100 ms to 600 ms. (B) shows the output level to the dedicated stimulus level. The output level is rising up if the time of stimulus input is long enough respectively the stimulus input is strong enough. By and by the Ca^{2+} level is rising up and the slew rate of the transfer function becomes steeply. (C) shows the progress of the transfer function at the maximum stimulus input level 3 over time. The gradient is at the beginning very slow and is then rising up very quickly until it gets a maximum. After the input has been removed the gradient of the transfer function is climbing down slowly. (D) the stimulus input level is 1.6. The gradient of the transfer function does not become sufficient steeply. Parameter: [α=0.001, β=0.02, τ=30]

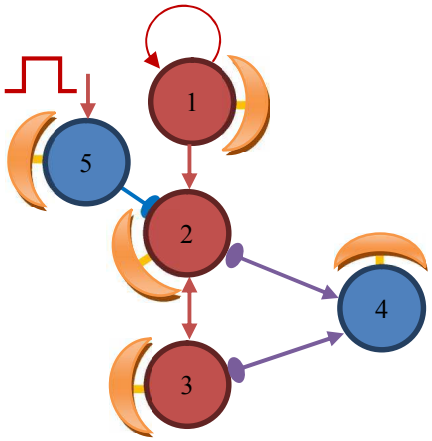

Figure 3: shows a neuronal system which generates an uncertain pattern in the lumbosacral spinal cord. Each circle determines a neuronal population with its dedicated glial system. A blue circle represents an inhibitory population, a red circle represents an excitatory population. Population 2, 3 and 4 forms the pattern generator, population 1 gives a general drive to the system and population 5 steers the pattern (e.g. speed of oscillation)

We extended our model to get a pattern generator formation (Figure 3). Each circle determines a neuronal population and each half moon describes its dedicated glial system. A blue circle determines an inhibitory population a red circle determines an excitatory population.

The populations 2, 3 and 4 are building the pattern generator formation. Population 1 gives a permanent drive. Population 5 shall steer the oscillation of the pattern generator. Doubling this formation and connecting both systems with a contra lateral inhibition unit would result in a so called half center unit to control agonist / antagonist behavior [10].
The lack of activity of the neuronal populations from the supra spinal system (or from afferent input signals) results in reduction of Ca^{2+} level in the inhibiting population 5. The transfer function will become more flat. On the other hand the populations of the pattern generator formation (populations 2, 3 and 4) become overexcited due to the missing inhibition. The permanent drive from population 1 will cause a spastic behavior. Figure 4A shows the Ca^{2+} progress of population 5. The population is activated with an initial value of 0.1 and the Ca^{2+} level is able to rise up quick. Afterwards the Ca^{2+} level is ascending slowly. The output of population 3 is rising up due to the mutual excitation and the permanent drive of population 1 (C). The subsequent stimulus (B) indeed is rising up the Ca^{2+} level in population 5 but the output due to the flat transfer function is too less to steer the pattern generator.

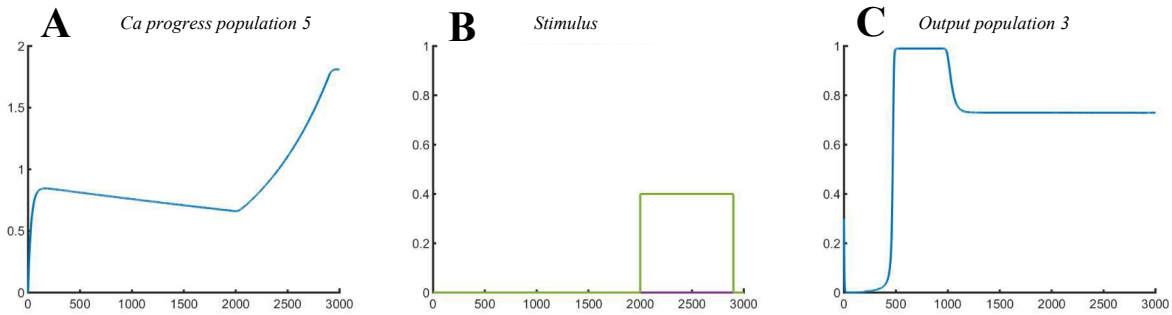

Figure 4: (A) population 5 starts with an initial value of 0.1, the Ca^{2+} progress is descending slowly. The output of population 3 is rising up because of the permanent drive of population 1 (C). A stimulus intensity 0.4 at time unit 2000 (B) leads to an ascending progress of the Ca^{2+} level but it is not sufficient to steer the output.

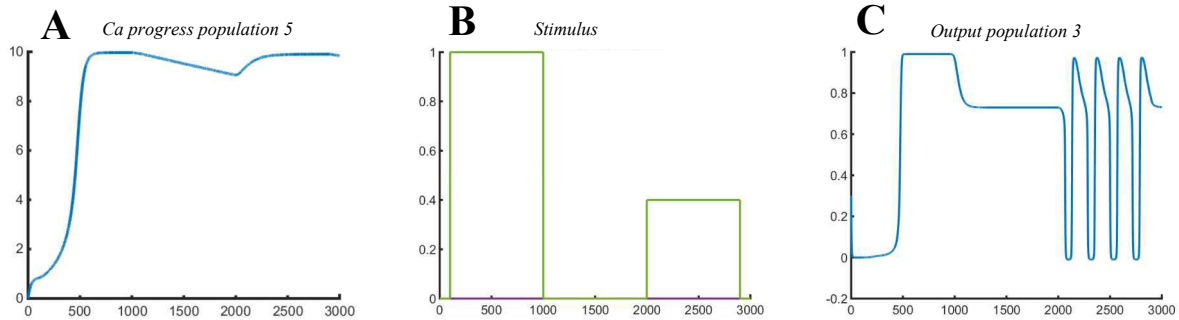

Figure 5: Population 5 gets an external stimulus at time unit 100 for 900 time steps (B), the Ca^{2+} progress is ascending quickly during this time (A). The output of population 3 is rising up again due to the permanent drive of population 1 (C). If the stimulus at time unit 2000 of 0.4 is disposed again (B), the Ca^{2+} level is high enough to bring population 3 into an oscillating status (C).

The Ca^{2+} level is rising up to $Ca_{max} = 10$ if the neuronal system gets a sufficient external stimulus. The transfer function gets its maximum slew rate and the pattern generator can be inhibited sufficient. After population 5 got a stimulus of 1 for 900 time units (Figure 5B) the Ca^{2+} progress (Figure 5A) rising up to a maximum. During the second stimulus (intensity 0.4) from time unit 1000 to 2000 the pattern generator formation can be driven to oscillate. Anyhow during the rest phase when no stimulus is applied to the system for inhibition the output shows again a spastic behaviour.

Discussion

In this simulation study it is shown that a glial system is able to steer the pattern generator units of the lumbosacral spinal cord. Anyhow, it is expected that the pattern generator comes in an oscillating state to generate (in interaction of many) any locomotion behaviour. We have shown that through a previous stimulation the system comes in a more active level. Especially inhibitory interneurons will be lifted up to a higher level of activity.

Additional in the literature it is reported that the glial cells communicate through glial junctions and a stimulus is able to release calcium waves through the system [11]. This phenomenon is not considered in our model to reduce the complexity but it is assumed that such a glial communication could be responsible to generate more complex patterns in the lumbosacral spinal cord [9].

Conclusions

We assume that in individuals with motor-incomplete (but also with motor-complete) injuries the activation of the Ca^{2+} depots in the glial system is missing due to reduced supra spinal cord activity. However, the excitatory neuronal pools are activated mutual and the neuronal system may tend to a spastic behaviour. The inhibitory activation is missing. By electrical stimulation of the lumbosacral spinal cord the neuronal pools will be activated. Consequently the glial system will be activated and the Ca^{2+} levels are rising up and restore the strength of the postsynaptic potential. Glia cells are able to keep the level of Ca^{2+} and the improved locomotion refresh the Ca^{2+} depots additional. This leads to a diminished spasticity and finally in an improved behaviour of locomotion. The observed long term effect after electrical stimulation occurs.

References

[1] Pinter, M.M., Gerstenbrand, F. and Dimitrijevic, M.R., Epidural electrical stimulation of posterior structures of the human lumbosacral cord: 3. Control of spasticity. *Spinal cord*, *38*(9), pp.524-531, 2000.

[2] Adams, M.M. and Hicks, A.L., Spasticity after spinal cord injury. *Spinal cord*, *43*(10), pp.577-586, 2005.

[3] Hofstoetter, U.S., McKay, W.B., Tansey, K.E., Mayr, W., Kern, H. and Minassian, K., Modification of spasticity by transcutaneous spinal cord stimulation in individuals with incomplete spinal cord injury. *The journal of spinal cord medicine*, *37*(2), pp.202-211, 2014.

[4] Minassian, K., Jilge, B., Rattay, F., Pinter, M.M., Binder, H., Gerstenbrand, F. and Dimitrijevic, M.R., Stepping-like movements in humans with complete spinal cord injury induced by epidural stimulation of the lumbar cord: electromyographic study of compound muscle action potentials. *Spinal cord*, *42*(7), pp.401-416, 2004.

[5] Abbott, L., Firing-rate models for neural populations. *Neural networks: From biology to high-energy physics*, pp.179-196, 1991.

[6] Dietz, V., Spinal cord pattern generators for locomotion. *Clinical Neurophysiology*, *114*(8), pp.1379-1389, 2003.

[7] Verkhratsky, A., Calcium ions and integration in neural circuits. *Acta physiologica*, *187*(3), pp.357-369, 2006.

[8] Ge, W.P., Yang, X.J., Zhang, Z., Wang, H.K., Shen, W., Deng, Q.D. and Duan, S., Long-term potentiation of neuron-glia synapses mediated by Ca2+-permeable AMPA receptors. *Science*, *312*(5779), pp.1533-1537, 2006.

[9] Haydon, P.G., GLIA: listening and talking to the synapse. *Nature Reviews Neuroscience*, *2*(3), pp.185-193, 2001.

[10] McCrea, D.A. and Rybak, I.A., Organization of mammalian locomotor rhythm and pattern generation. *Brain research reviews*, *57*(1), pp.134-146, 2008.

[11] Scemes, E. and Giaume, C., Astrocyte calcium waves: what they are and what they do. *Glia*, *54*(7), pp.716-725, 2006.

Author's Address

Manfred Anzinger-Weitmann
Institute for Analysis and Scientific Computing
Vienna University of Technology
Operngasse 11
anzingerm@yahoo.com
http://www.asc.tuwien.ac.at/index.php?id=62

Treatment of chronic neuropathic pain: First clinical experience with Peripheral Nerve Stimulation (PNS)

G. Weigel, W. Girsch

Orthopedic Hospital Speising Vienna, Austria, Hand team, 1. Department

Abstract:

Introduction:
Central nerve stimulation (CNS) already has proved its efficacy for treatment of chronic severe pain. The aim of our clinical study was to prove the effectiveness of Peripheral Nerve Stimulation (PNS) for treatment of chronic neuropathic pain syndrome of the extremities.

Material and Methods:
From 2005 to 2013 31 patients (19 female, 12 male, aging 18-67 years, mean 45a) suffering from Complex Regional Pain Syndrome (CRPS) - mainly CRPS2 (chronic neuropathic pain) - were selected for treatment with PNS. All patients had a history of microsurgical procedures to their peripheral nerves and every possible conservative treatment, but without any significant pain reduction. None of the patients was able to use the extremity functionally. Pain level at the Numeric Rating Scale (NRS) was in mean 9, even at rest, requiring not only psychological treatment but somatical intervention. Stimulation leads were implanted in 28 patients to the upper and 5 patients to the lower extremity in a position along and close to the epineurium of the peripheral nerves. After a testing phase using percutaneous leads the electrodes were connected with an implanted stimulator.

Results:
Relief from pain occurred immediately after onset of stimulation. The positive effect was directly correlated with PNS, and stable over years. PNS was effective to reduce pain from NRS mean 9 to NRS mean 3 and to regain functional use of the extremity in all patients. Several complications as electrode dislocation and technical defects but also infections had to be noted.

Discussion:
PNS reduced pain deriving from peripheral nerves reliable and effective. Regarding our follow up period of 2,5 years PNS produced a stable, nearby pain free interval in all patients. Positioning of
the electrodes direct to the brachial plexus and to the sciatic nerve allowed movement of upper and lower extremity to nearby normal ROM. PNS seems to represent an important technology for treatment of CRPS in carefully selected cases.

Session 3:
FES Excercise

Robotic assisted training in combination with functional electrical stimulation to improve lower limb function after spinal cord injury

Bersch I [1], Koch S[1], Sandner E[2], Brust AK[2], Frotzler A[2]

[1]Therapy Management, Swiss Paraplegic Centre Nottwil, Switzerland
[2] Clinical Trial Unit, Swiss Paraplegic Centre Nottwil, Switzerland

Abstract:
Introduction*: Functional electrical stimulation (FES) is used for neuromodulation after spinal cord injury (SCI) and can be combined with robotics to increase motor function of the lower limbs. The aim of the present study was to investigate the FES-induced and voluntary induced power output of the lower limbs using a stationary robotic system.*
Method: *Data of SCI inpatients who trained lower limb mobilization on a stationary robotic system were retrospectively analyzed. The primary outcome was the improvement in power output from the first through to the last training, during FES-induced as well as voluntary induced flexion and extension.*
Results: *22 SCI patients (AIS A to D, median lesion duration 77 days) each completed a median of 13 training sessions. There was a significant increase in median power-output from 2.14 to 3.38 W for FES-induced extension (p=0.020) and from 1.13 to 3.01 W for voluntary extension (p=0.001). In contrast to FES-induced flexion (p=0.058), voluntary flexion increased significantly from 0.88 to 1.89 W (p=0.001). No significant correlations were found between FES-induced and voluntary movements for flexion (r=0.243, p=0.275) and extension (r=0.382, p=0.079).*
Conclusion: *Robotic assisted lower limb training with FES seems to support the recruitment of further motor units during recovery, which results in increased motor function and power output of the legs.*

Keywords: *Functional electrical stimulation, Robotic, Spinal cord injury, Neuromodulation*

Introduction

Restorative neurology works through the modification of residual nervous system function and is part of the rehabilitation in spinal cord injuries (SCI). Techniques of neuromodulation belong to restorative neurology (1). One of those techniques is functional electrical stimulation (FES), applied with surface electrodes to the treated muscle or muscle group. Depending on the type of lesion, i.e. whether the upper motor neuron or lower motor neuron is damaged, the stimulation occurs via the nerve or directly through the muscle. The approach via nerve needs intact peripheral nerves and neural signal processing of the section of spinal cord which remains after the impairment (2). The following article will focus on patients with an upper motor neuron lesion due to a SCI. FES is often applied in the acute and sub-acute stages after SCI to support the neurological recovery and provide neuromodulation(3,4). Due to neuromodulation, motor function and power output often increase. Robotic assisted training of the lower limbs in combination with FES seems to be a promising method of supporting neurological recovery.
The aim was to investigate the difference between FES-induced and voluntary induced power output of the lower limbs in patients with SCI in the sub-acute phase using a stationary robotic device (MotionMaker™).

Material and Methods

Data of inpatients with acute and sub-acute SCI were included in this retrospective analysis. Data of patients who actively trained limb mobilization during clinical routine for neuromodulation using a stationary robotic system (MotionMaker™) was analyzed. The MotionMaker™ is a stationary robotic device which performs movements of the lower limbs in extension and flexion. A closed loop electrical stimulation system allows application of stimulation in real time based on integrated sensors inside the orthosis, that enable the assessment of position and torque during the movement. Each training session consisted of FES-induced and voluntary repetitive movements of the lower limbs in flexion and extension. First the voluntary movements were performed followed by the FES- induced movements. During the voluntary movements of the legs no electrical stimulations is applied. The integrated power sensors measure the voluntary force of the extensor and flexor muscles of the right and left leg separately. In contrast during the FES-induced extension and flexion of the lower limbs, the following muscles were bilaterally stimulated: M. glutaeus maximus, M. quadriceps (rectus femoris, vastus medialis and lateralis), Mm. ischiocrurales, M. gastrocnemius, M. tibialis anterior. (Figure 1) In the latter case the the FES-evoked force is measured as described before. To perform extension of the legs the M. glutaeus maximus, M. quadriceps (rectus femoris, vastus medialis and lateralis) and M. gastrocnemius were stimulated. To perform flexion, the Mm. ischiocrurales and the M. tibialis received stimulation. Stimulation parameters remained unchanged for each patient. The pulse duration was 300 µsec and the frequency 35 Hz. The amplitude was individually determined for each patient but remained unchanged over the training period.

Primary outcome was the improvement in power output (Watt) of the legs from the first through to the last training session during FES-induced as well as voluntary induced flexion and extension. Secondary outcome was the sum score of active muscle function of seven lower limb muscles before and after the training period. Group differences were analyzed using Wilcoxon-Test and correlation was analyzed using the Spearman's correlation

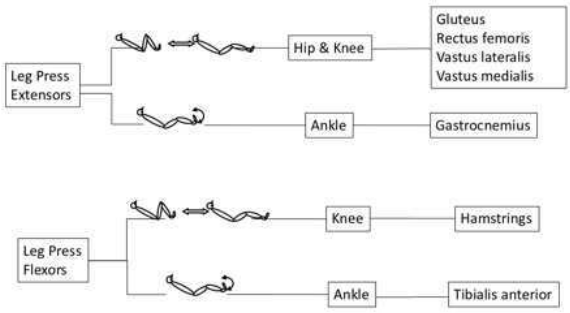

Figure 1: Movements of the lower limbs and stimulated muscles during extension and flexion performed on a stationary robotic system. In the first box the movement is named, followed by the illustration of the movement and the corresponding joint. In the last box the stimulated muscles are listed.

Results

Twenty-two patients with SCI (AIS A to D, median age 59.22 years, median lesion duration 77 days) each completed a median of 13 (range 3 to 19) training sessions. Within the observation period there was a significant increase in median power-output, from 2.14 to 3.38 W for FES-induced extension (p=0.020) and from 1.13 to 3.01 W for voluntary extension (p=0.001). In contrast to FES-induced flexion (p=0.058), voluntary flexion (p=0.001) increased significantly from 0.88 to 1.89 W (Figure 2). No significant correlations were found between the changes in power output from the first to the last training session in FES-induced and voluntary movements for flexion (r=0.243, p=0.275) and extension (r=0.382, p=0.079). However, it must be taken into account that the reproducibility of power output may be reduced due to day to day variation of the electrode placement. The median muscle sum score was 17 points at baseline and 22 points at the last session.

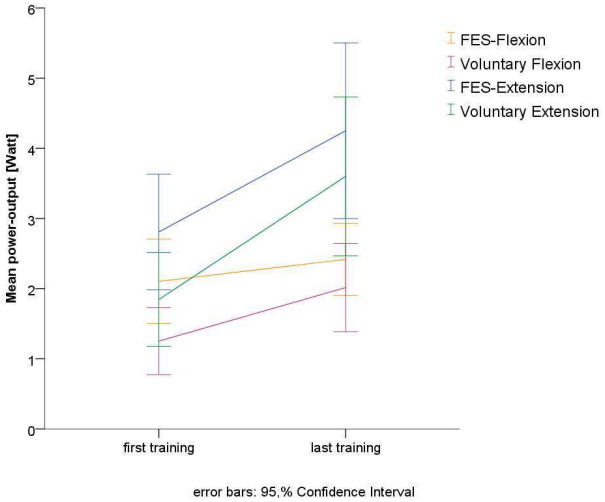

Figure 2: Development of the power-output in Watt presented as Mean and 95% Confidence Interval (CI) using FES-induced and voluntary movements at the first and last training session on the MotionMaker™ (n=22).

Discussion

The results of this retrospective study demonstrates the increase in FES-induced as well as in voluntary power output of the lower limbs in patients with complete and incomplete SCI, The fact that FES can increase torque and power output in persons with motor complete and incomplete SCI has been described in several previous studies (5-8). Our results are therefore consistent with the existing literature. Nevertheless, our results highlight some additional interesting observations. The technical features of the MotionMaker™ allowed us to differentiate between the increase of the FES-induced power-output of the extensor muscle group and the flexor muscle group of the legs. The extensor muscle group increased significantly in contrast to the flexor muscle group. One explanation for this discrepancy could be the difference in the number of stimulated muscles. The stimulation in extension included three muscles, whereas the M. quadriceps has three separate pairs of electrodes for each muscle part (rectus femoris, vatus medialis and lateralis). In contrast, the stimulated flexor muscle group contains only two muscles, the hamstrings and the dorsiflexor of the foot. It should also be taken into account that based on clinical observation, mostly the flexor muscles, namely the hamstrings, show slower and less neurological recovery during primary rehabilitation. Regarding the increase in voluntary power output during the training period in the present study, the extensor muscle group developed more power output (1.88 W) compared to the flexor muscle group (1.01 W). Furthermore, the correlation between FES-induced and voluntary induced movements for flexion and extension were not significantly related. In other words, the patients were probably not able to use and transfer the gain of the FES-induced power output into their voluntary leg movements neither in extension nor in flexion. That leads to another clinical observation that patients training with FES on the MotionMaker™ reported difficulties in coordinating their own voluntary muscle activity with the FES given activity of the stimulated muscles.

Conclusions

Robotic assisted training with FES seems to support the recruitment of further motor units during recovery, which results in increased motor function and power output of the lower limbs. The lack of correlation between FES-induced and voluntary movements mainly for extension may indicate that the patient is not able to transfer the gain in FES induced power output into voluntary movements in the same dimension.

Acknowledgement

Thanks to the Physiotherapists of the Swiss Paraplegic Centre who provide training with the MotionMaker™ in clinical daily practice.

References

1. Holsheimer J. Concepts and Methods in Neuromodulation and Functional Electrical Stimulation: An Introduction. Neuromodulation: Technology at the Neural Interface. Blackwell Publishing Ltd; 2010 Nov 9;1(2):57–61.

2. Illis LS. Central nervous system regeneration does not occur. Spinal Cord. 2011 Nov 22;50(4):259–63.

3. Stampas A, Tansey K. Spinal Cord Injury Medicine and Rehabilitation. Semin Neurol. Thieme Medical Publishers; 2014 Dec 17;34(05):524–33.

4. Sadowsky CL, Hammond ER, Strohl AB, Commean PK, Eby SA, Damiano DL, et al. Lower extremity functional electrical stimulation cycling promotes physical and functional recovery in chronic spinal cord injury. J Spinal Cord Med. 2013 Nov;36(6):623–31.

5. Crameri RM, Cooper P, Sinclair PJ, Bryant G, Weston A. Effect of load during electrical stimulation training in spinal cord injury. Muscle Nerve. 2004 Jan;29(1):104–11.

6. Harvey LA, Fornusek C, Bowden JL, Pontifex N, Glinsky J, Middleton JW, et al. Electrical stimulation plus progressive resistance training for leg strength in spinal cord injury: A randomized controlled trial. Spinal Cord. Nature Publishing Group; 2010 Jan 12;48(7):570–5.

7. Fornusek C, Davis GM, Russold MF. Pilot Study of the Effect of Low-Cadence Functional Electrical Stimulation Cycling After Spinal Cord Injury on Thigh Girth and Strength. YAPMR. Elsevier Ltd; 2013 May 1;94(5):990–3.

8. Hasnan N, Ektas N, Tanhofer AIP, Tanhofer R, Fornusek C, Middleton JW, et al. Exercise Responses during Functional Electrical Stimulation Cycling in Individuals with Spinal Cord Injury. Medicine & Science in Sports & Exercise. 2013 Jun;45(6):1131–8.

Author's Address

Ines Bersch, MSc
Therapy Instructor and Physiotherapist
Swiss Paraplegic Centre Nottwil
Guido A. Zäch Strasse 1
6207 Nottwil
Phone: +41 41 939 42 06
ines.bersch@paraplegie.ch

A clinical trial on arm rehabilitation using task oriented therapy and Myo-electrically controlled FES (MeCFES)

Thorsen R[1], Jonsdottir J[2], Aprile I[3], Galeri S[4], Spannocchi G[5], Beghi E[6], Montesano A[2], Ferrarin M[1]

[1] Biomedical Technology Dept., IRCCS - Don Gnocchi Foundation, Milan, Italy

[2] Larice Lab, IRCCS - Don Gnocchi Foundation, Milan, Italy

[3] Rehabilitation Department, Don Gnocchi Foundation, Rome, Italy

[4] Rehabilitation Department, Don Gnocchi Foundation, Rovato, Italy

[5] Rehabilitation Department 'Palazzolo', Don Gnocchi Foundation, Milan, Italy

[6] IRCCS - Istituto di Ricerche Farmacologiche "Mario Negri", Milan, Italy

Abstract: *We present results from a multicentre clinical trial on the value of adding myoelectrically controlled functional electrical stimulation to task oriented therapy in the rehabilitation of subacute and chronic stroke patients.*

Keywords: *FES, EMG, Rehabilitation, Stroke, Task oriented therapy*

Introduction

In stroke rehabilitation the active participation of the patient is important for the outcome. Task-oriented therapy (ToT) is used for promoting motor relearning of the upper limb [1]. To facilitate activation of impaired movements a combination of EMG and functional electrical stimulation (FES) can be used to overcome the threshold of little motor activity [2]. Spontaneous recovery and the effect of therapy has a large between-subjects variation on the results. Therefore a large sample size is needed to demonstrate superiority of novel interventions. This paper aims to highlight some preliminary results of a multicentre clinical study investigating the increased efficacy of EMG controlled FES (MeCFES).

Material and Methods

Sub-acute and chronic stroke persons with impaired upper extremity were recruited into this prospective randomized clinical trial with a foreseen sample sized of 120 patients. Subjects in the control group were treated 25 times for 45min with standard ToT. The experimental group was treated similarly but also with the use of MeCFES during the ToT. The MeCFES is a multi-channel experimental device using surface electrodes to record myoelectric activity while simultaneously stimulating selected muscles. The therapist may use this to 'boost-up' residual motor activity by letting the muscle control stimulation of itself; typically activating the wrist/finger extensors to facilitate grasping activity. The EMG inputs may be arbitrarily used either as inhibitory or excitatory signal to control FES intensity and, consequently, to modulate paretic muscle contraction. An example is letting shoulder activity minus inadvertent finger flexors contraction control stimulation of hand opening, in a way to train the subject to reach & open while relaxing finger flexors. Primary outcome was the change score of action research arm test (ARAT) from pre-treatment, intermediate, post-treatment, and 1 month follow up (FU).

Results

Eighty-two subjects were enrolled, 68 completed the treatment and 45 were seen at follow-up. Summary statistics of treated subjects are shown in table 1.

Table 1: Summary statistics of the two groups as median [interquartile range]

	Exp. group (A)	**Control (B)**
N. of subjects	32	36
Age [yrs]	68 [56;76]	68 [57;78]
Time since CVA [months]	11 [4;31]	8 [5;14]
ARAT-pre treatment	6 [0;27]	6,5 [0;31]
ARAT-post	21 [2-38]	13 [3-40]

Upper extremity ability was initially low in both groups with a median ARAT score about 6. Both groups improved significantly ($p<0.05$) with the experimental group being superior in recovery with respect to the control group, see figure 1. Within the subjects seen at FU, motor recovery remained stable from post treatment evaluation to FU; median ARAT scores post treatment were 23 & 17 and ARAT FU were 24 & 18, experimental & control respectively.

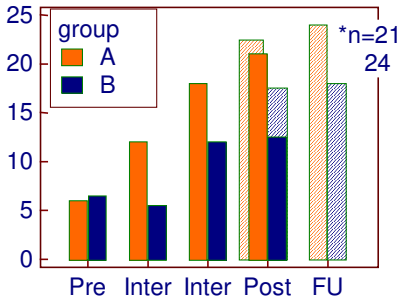

Figure 1: Median ARAT score during the trial (13 subjects missing at FU)

Discussion

Adding MeCFES to physiotherapy may enhance motor recovery. Not having reached the sample size, the results of the study are not conclusive. However, there is a clear and consistent improvement in the experimental group indicating that MeCFES may help the therapist in promoting functional recovery of the paretic upper limb in post-stroke subjects.

Acknowledgement

This project has been founded by a research grant from the Italian region Lombardia 'Regione Lombardia, Ricerca Independente' and the Italian Ministry of Health 'Ricerca Corrente'.

References

[1] Bayona, et al. *Top stroke rehabil* 2005; 12(3): 58-65.

[2] Thorsen R, et al. *J Rehabil Res Dev* 2013; 50(6): 785–94.

Author's Address

Rune Thorsen
Fondazione Don Carlo Gnocchi, Italy
rthorsen@dongnocchi.it
www.thorsen.it

Low power output of FES cycling in subjects with SCI, a biomechanical viewpoint

Szecsi J[1], Fornusek C[2], Straube A[1]

[1]Dpt. of Neurology, University of Munich, Munich, Germany
[2]Exercise, Health and Performance Faculty Research Group, University of Sydney, Sydney, Australia

Abstract: *The goal of Functional Electrical Stimulation (FES) cycling is to provide the health benefits of exercise to persons with paralysis. To achieve the greatest health advantages, patients should produce the highest possible mechanical power. However, compared to normal cycling, the mechanical power output produced during FES cycling is very low. Unfavourable biomechanics is one of the important factors reducing power output. The purpose of this study was to investigate the power generation and the role of antagonistic co-contraction in FES cycling.*
Sixteen subjects with complete SCI pedalled a stationary recumbent tricycle at 60 rpm and a workload of 15 W per leg, while pedal forces and crank angle were recorded. The joint moments, power and work were calculated using inverse dynamics equations. Two characteristic patterns were found; in 12 subjects most work was generated by the knee extensors in the propulsion phase (95% of total work), while in 4 subjects work was shared between by the knee extensors (49%) and flexors (51%), respectively during propulsive and recovery phases. Hip extensors produced only low net work (7-12%). For both patterns, extra concentric work was necessary to overcome considerable eccentric work (-82 & -96%) .The primary power sources were the knee extensors of the quadriceps and the knee flexors of the hamstrings. The antagonistic activity was generally low in subjects with SCI because of the weakness of the hamstrings (compared to quadriceps) and the superficial and insufficient hamstring mass activation with FES.

Keywords: *Generalised muscle moment, Joint power, Electrical stimulation, cycling, Spinal cord injury*

Introduction

The mechanical power output produced during FES cycling is very low (i.e. 8 - 35 W). However, the health benefits bestowed by FES cycling are strongly related to the power output that can be generated. Therefore, it is important to produce the greatest mechanical power possible to enhance the health benefits bestowed. Three factors are thought responsible for the lower power outputs achieved with FES cycling in persons with SCI, poor muscle biomechanics, inefficiency of artificial muscle activation, and muscle changes including early fatigue, due to chronic paralysis and disuse.
The imprecise nature of surface electrical stimulation is a main cause of poor biomechanical cycling performance. Compared to normal voluntary motor control activation, electrical stimulation is much cruder and coarsely recruits groups of mono- and bi-articular muscles (e.g. quadriceps, hamstrings, or gluteal muscle groups). This crude activation strategy of muscle groups does not allow accurate synergistic and antagonistic joint control. Moreover the imprecise activation of muscle may contribute to both positive and negative work across different joints. During FES cycling co-contractions result in a considerable amount of both positive and negative power across the joints, which is assumed to consume considerable metabolic energy, but only their net difference contributes towards PO at the pedal crank. Thus to understand the low power production in individuals with SCI performing FES cycling, the power patterns of the muscles across the joints must be known. The purpose of this study (1) was to define the primary source of power generation during SCI FES propelled cycling by investigating the power patterns at the hip and knee joints. Such information would be useful for optimising muscle stimulation patterns and developing training programs for individual muscles in subjects with SCI [1,2].

Material and Methods

Subjects and equipment: Sixteen subjects with motor complete spastic SCI pedalled a stationary recumbent tricycle using FES at 60 rpm and a workload of 15 W per leg (total 30W). For reference purpose, passive pedalling (driven by the tricycle motor) at 60 rpm was also recorded. Tangential and radial pedal forces and crank angle were recorded by instrumented crank arms and an angular decoder.
Data processing: The joint moment and power were computed based on inverse dynamics, and referred to the crank cycle, composed of a knee extension and flexion phase (TDC =0°). The joint extensor and flexor moments contribute to total mechanical power sequentially, by generating in able-bodied (AB) subjects typically four power components produced by concentric action of the knee extensors, hip extensors, knee flexors and hip flexors, in this order (Fig. 1). However because of the action of bi-joint muscle groups, each concentric extensor/flexor action at a joint may be associated with an eccentric extensor/flexor action from the other joint. Accordingly the first power component (P1) occuring in the early-middle knee-extension phase was defined as the net difference of concentric knee extensor and eccentric hip flexor power (Fig: 2); the second component (P2) in the middle-late hip-extension phase defined as the

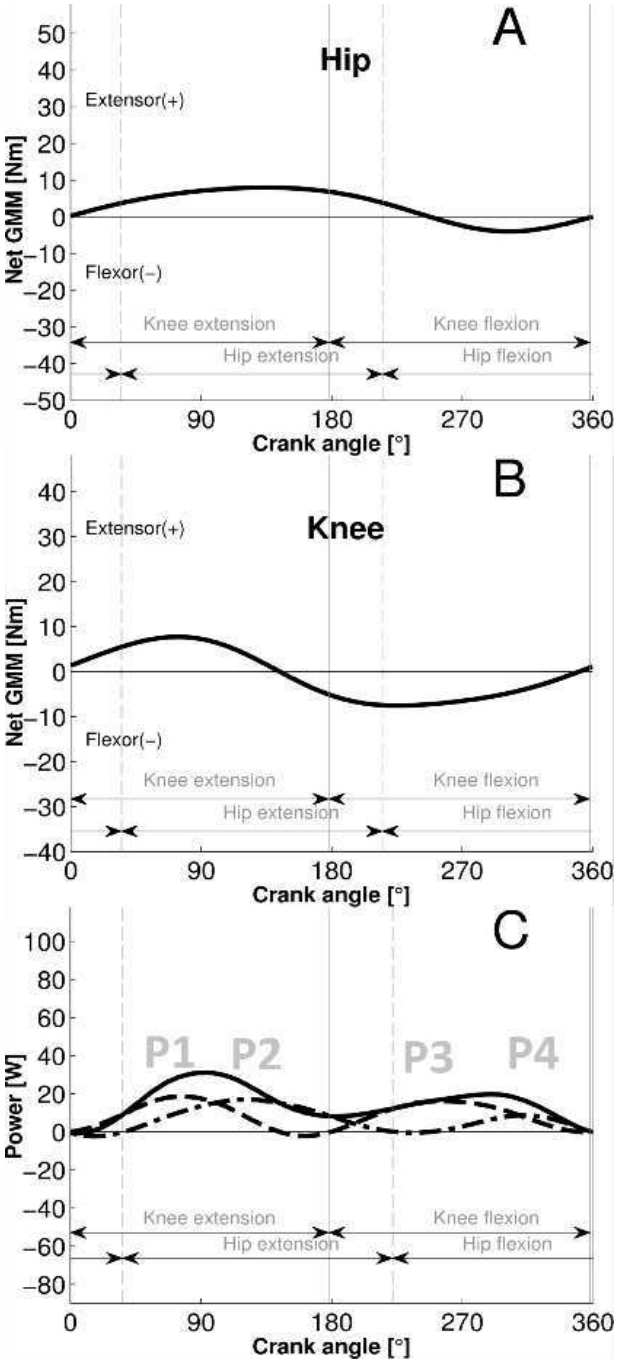

Fig. 1. Joint muscle moments and power in the leg of able-bodied subjects. (C) Knee(dashed), hip (dashed-dotted) and net (continuous) power patterns. Power components P1, P2, P3 and P4.

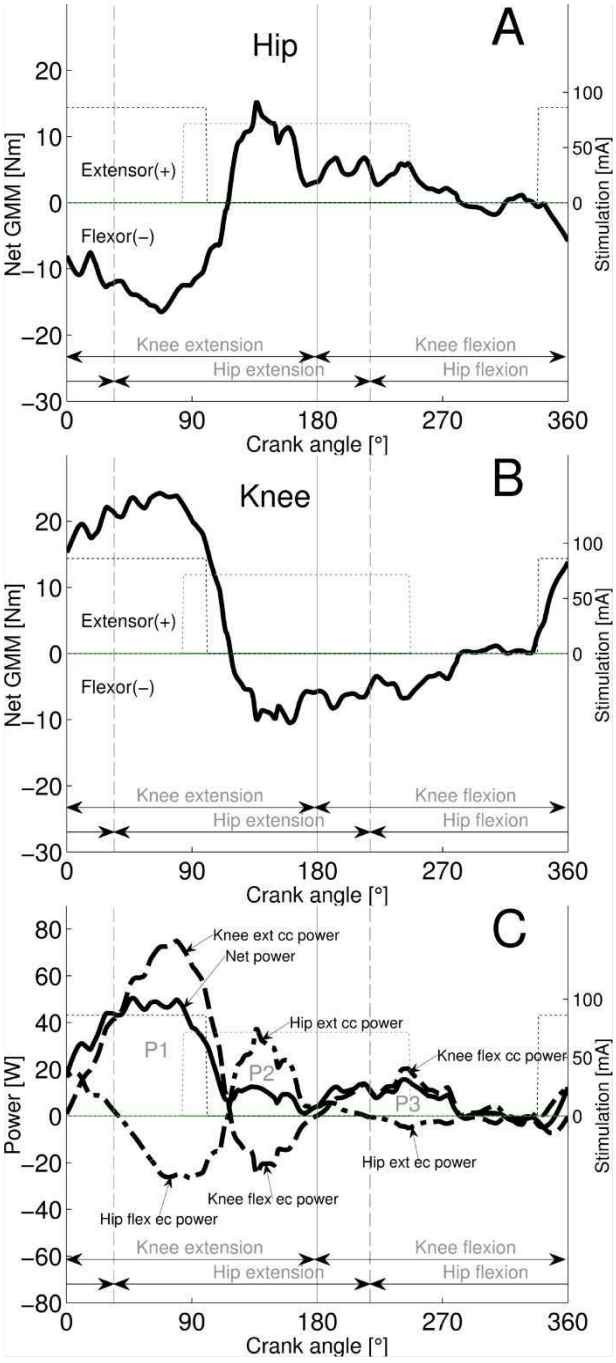

Fig. 2. Joint muscle moments and power in the leg of a subject with SCI. See also Fig. 1.(C)

concentric hip extensor and eccentric knee flexor power; the third component (P3) occuring in the early-middle knee-flexor phase defined as the net of the concentric knee flexor and eccentric hip extensor power. The component (P4) flexor phase was defined as the difference of concentric hip flexor end ecc knee extensor.

Results

Two different power patterns were observed: in 12 subjects with SCI the major part of work (>80%) was extension phase work (P1P2 group, Fig. 3C). In 4 subjects work was produced largely balanced in extension and flexion phase (P1P3 group, Fig. 4C). Thus the power distribution of the P1P2 group strongly contrasts to that in AB subjects. While the power distribution in the P1P3 group is fairly similar to that of AB subjects, the fractional contributions of the power components are different.

In subjects with SCI, the propulsion phase power was dominated by the P1 component, as the contribution of the P2 component was small or absent (Fig. 3C, Fig. 4C),

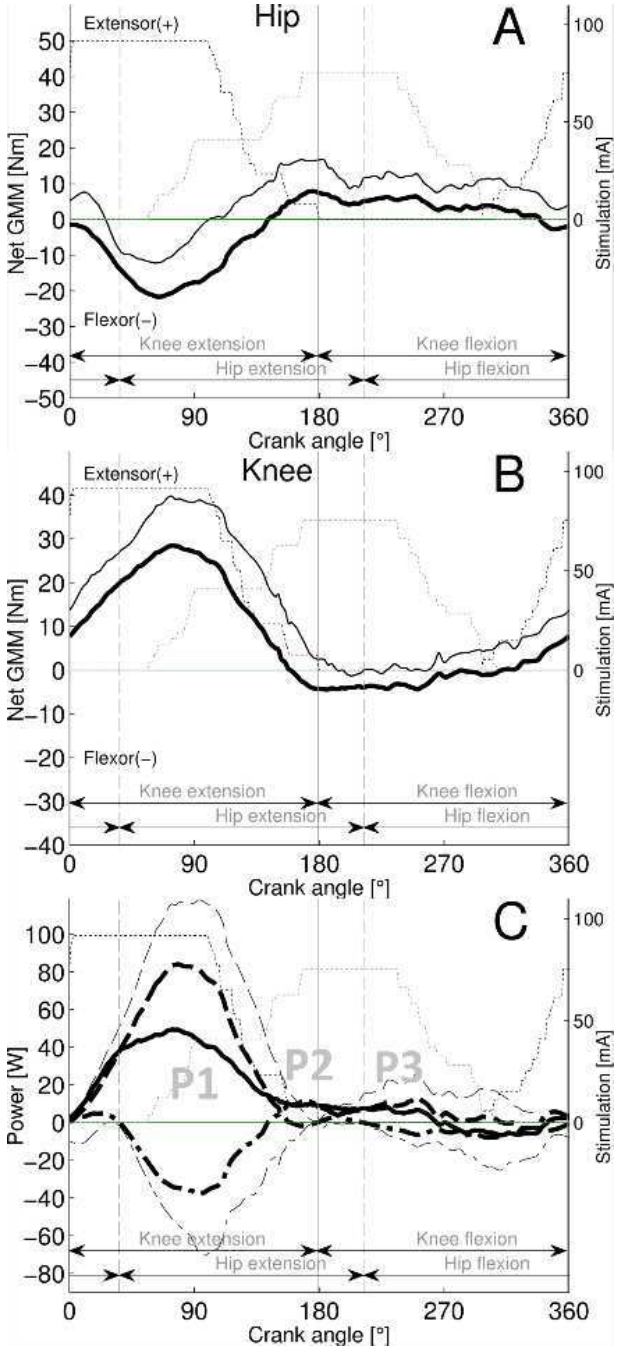

Fig. 3. Joint muscle moments and power for the P1P2 group. For explanations see also Fig. 1(C)

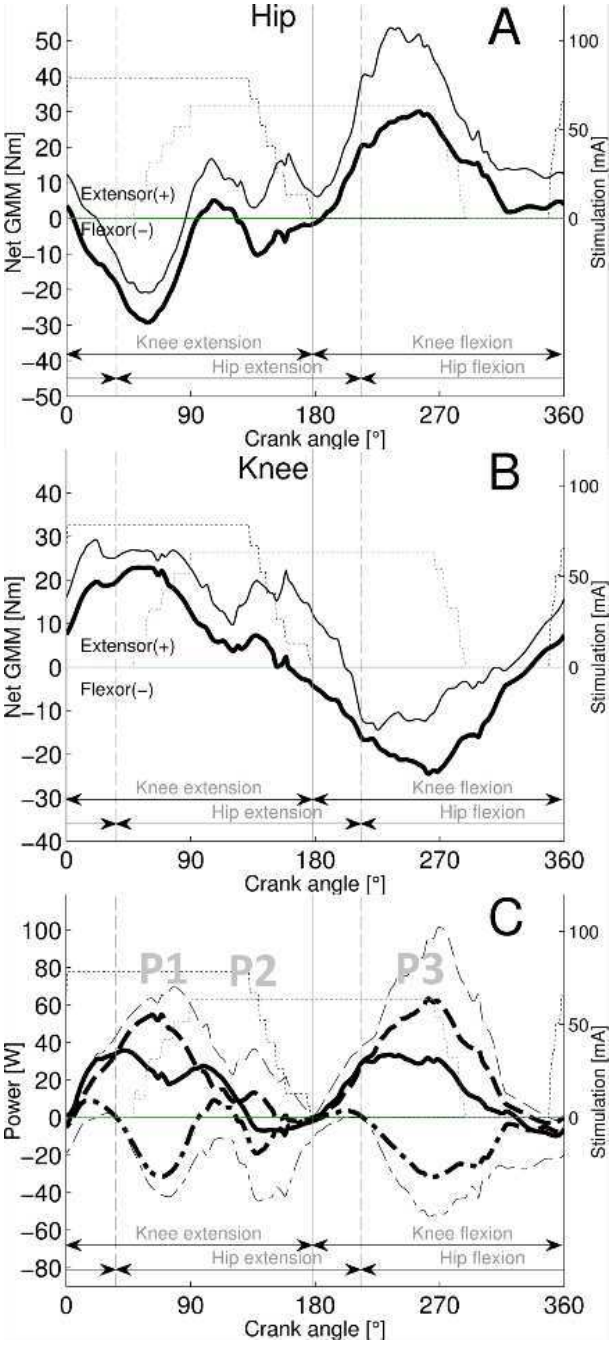

Fig. 4. Joint muscle moments and power for the P1P3 group. For explanations see also Fig. 1(C)

while in AB subjects propulsion phase power was distributed largely equal between P1 and P2 (Fig. 4C). Whether the P2 component is present depends directly on the hamstrings strength, because this is the only muscle that can produce concentric hip extensor power in the propulsion phase (Fig. 2C). Thus, the reduced size of P2 in persons with SCI implies that the contribution of the hamstrings was reduced in the late propulsion phase compared to AB subjects. The high variability of the hamstrings stimulation firing range compared to quadriceps or a delayed increase of the contraction force due to spasticity might be responsible for low hamstrings torque production in this phase.

During the recovery phase, little work was generated by the P1P2 group (small P3) compared to AB subjects due to poor knee flexor torque production from the hamstrings. However strong hamstring contractions were possible for the P1P3 group. The tendency of the hamstrings to develop spasticity in subjects of the P1P3 group, might explain in part the occurrence of the sizeable P3 component in the P1P3 group. AB subjects produce a pronounced P4 component using hip flexors (iliopsoas) during the middle-late recovery phase of volitional recumbent cycling (Fig. 1C). Since m. iliopsoas wasn't

stimulated, only a small P4 power component due to end recovery phase stimulation of the quadriceps was found in the P1P2 and P1P3 groups.
In summary, the net cycling work was generated in subjects with SCI according to two alternative patterns depending on the hamstrings strength. If the hamstrings were weak compared to the quadriceps, the concentric knee extension work of the quadriceps generated most of net work (83%), while if the hamstrings were strong (or spastic) enough, most of net work was produced equally by the concentric knee extensor (42%) and flexor torques (44%) evoked by the quadriceps and the hamstrings, respectively. The primary positive power generating source was the knee joint (during P1 and P3) and the hip mainly absorbed negative power (during P1 and P3). The findings contrast with the balanced power distribution previously found in AB subjects performing volitional cycling using the same setup, workload and cadence (P1 28%; P2 32%, P3 27% and P4 13%;).

Discussion

The FES cycling power patterns generated adhered to one of two characteristic patterns. Power was either generated only from the knee extensors in the propulsion phase (Fig. 3C) or balanced by the knee extensors in the propulsion phase and the knee flexors in the recovery (Fig. 4C). Net power generation was always accompanied by the absorption of considerable amounts of eccentric power.
In the subject shown in Fig. 2C the P1 and P2 components bear considerable amounts of eccentric hip flexor and eccentric knee flexor power, produced by the quadriceps and the (sufficiently strong) hamstrings muscles, respectively. In this case a small degree of co-contraction exists, and thus eccentric power cannot be efficiently cancelled by summation of the P1 and P2 components. However if large co-contraction crank angle ranges of quadriceps and hamstrings exist, corresponding to overlapping stimulation firing ranges, then the summation of the P1 and P2 components results in diminishing or reducing the eccentric power . This happens by cross-cancelling: e.g. the concentric knee extensor power of P1 cancels the eccentric knee flexor power from P2. However, even if sufficiently large overlapping muscle stimulation firing ranges are given, but there is a pronounced imbalance of the component magnitudes (P1 large, P2 small), the eccentric hip flexor power belonging to P1 cannot be cancelled. The overlap (co-contraction) of the quadriceps and hamstrings activation in the middle and late propulsion phase is obvious in AB subjects and known as Lombard's Paradox.
The presented results show that power components P1 and P3 demonstrated considerable negative eccentric power in subjects with SCI (Fig. 3C and Fig. 4C). This strongly contrasts to the situation previously described in AB-subjects, who absorbed only small amounts of eccentric power (Fig. 1C). The occurrence of substantial amounts of eccentric work assigned to P1 work can be explained by the small degree of co-contraction of the quadriceps with the hamstrings muscle that occurs because of the insufficient hamstring contraction during propulsion (small P2). Similarly, because no co-contraction of hamstrings and iliopsoas muscle exists in subjects with SCI, the eccentric power assigned to P3 could not be cancelled by P4.
The work performed by hypothetical joint moment actuators can be used as a measure of the energetic cost of movement. This approach assesses the muscular mechanical energy expenditure (MMEE) as the sum of positive and negative work done by the joint moments. For the P1P3 and the P1P2 group presenting considerable amounts of negative power, the fractional transmission of MMEE to pedal work is 15.06J/ (29.50J+14.44J)=0.34 and 14.93J/(27.23J+12.30J) = 0.38, respectively. This suggest that 2/3 of the MMEE is lost in subjects with SCI because of inefficient co-contraction, while for AB subjects who present only a small or negligible amount of negative power (Fig. 1), the fractional transmission is via much more efficient co-contractions ~1.

Conclusions

The majority of subjects with SCI produced the greatest proportion of FES cycling power from quadriceps knee extension. In a minority of subjects power was generated approximately equally from quadriceps knee extension and hamstring knee flexion. The co-contraction activity of antagonists is generally low in subjects with SCI because of the weakness of the hamstrings (compared to quadriceps) due to the superficial and insufficient muscle mass activation with FES and the missing iliopsoas activation. Low co-contraction however causes considerable amounts of inefficient eccentric power.
Thus clinicians are advised to use overlapping stimulation ranges and to increase hip extensor contribution by developing individual training programs for increase strength and fatigue resistance of the hamstrings and glutei muscles, rather than seeking a selective stimulation of the quadriceps to achieve high knee extensor and low hip flexor moment.

Acknowledgement

This work was supported by the 'Else-Kröner-Fresenius Stiftung' foundation, Bad Homburg, Germany.

References

[1] Szecsi, J. et al., A biomechanical cause of low power production during FES cycling of subjects with SCI, *J. Neuroeng Rehabil,* 11: p123, 2014

[2] Szecsi J., et al., Leg general muscle moment and power patterns in able-bodied subjects during recumbent cycle ergometry with ankle immobilization, Med Eng Phys, 36: 1421-1427, 2014

Author's Address
Johann Szecsi, MD
Department of Neurology
University of Munich
D-81377 Munich, Feodor Lynen Str. 19
e-mail: johann.szecsi@med.uni-muenchen.de

FES driven lower limb cycling by four and eight channel stimulations – a comparison in a case study

Mravcsik M[1], Klauber A[4], Laczko J[1,2,3]

[1]University of Pécs, Pécs, Hungary
[2]MTA Wigner Research Centre for Physics, Budapest, Hungary, [3]Pazmany Peter Catholic University, Budapest,
[4]National Institute for Medical Rehabilitation, Budapest, Hungary

Abstract: *FES driven lower limb cycling has been studied and the results here presented are from the case of a complete spinal cord injured participant. Two stimulation patterns were applied. In the first one, two muscle groups were stimulated, the hamstring and the quadriceps. In the second stimulation pattern, four muscle groups were stimulated on each leg: three parts of the quadriceps separately (vastus lateralis, vastus medialis, rectus femoris) and the hamstrings. We compare the parameters of the two stimulation patterns and present differences in power output and mechanical energy. The cadence of cycling was on average 47-48 rpm (revolutions per minute) in both stimulating conditions. We note that when stimulating four muscles per limbs, lower current amplitude (per muscles) was sufficient to reach a higher power output compared to the stimulations with two muscles per limbs. The participant preferred to cycle longer when only two muscles (per legs) were stimulated. The power output was lower in this case but the total energy (during the training) did not differ significantly in the two examined stimulation conditions.*

Keywords: *stimulation pattern, power output, current amplitude*

Introduction

In Hungary, FES driven cycling training is available at 2 locations - at the National Institute for Medical Rehabilitation (NIMR) and at the University of Physical Education in cooperation with the University of Pecs, the Pázmány Péter Catholic University (PPCU) and the Wigner Research Centre for Physics. During the application of FES assisted training the stimulation device and the stimulation patterns have been continuously developed [1,2,3] and applied to generate cycling movements for Spinal Cord Injured (SCI) individuals. Here we compare the efficiency of two stimulation patterns through the results obtained during the training of one SCI person who participates twice a week in FES driven cycling training in NIMR. The Ethical Committee of the NIMR approved the procedures.

The power output produced during FES cycling by SCI people depends on many factors. Such factors are cycling cadence, crank resistance and the current amplitude, pulse width and frequency of the stimulating current. Here we examine the dependence of power output on the amplitude of the stimulating current. Current amplitude varies among FES cycling protocols. We report on results obtained with stimulation applying low current amplitudes, 20-45mA per muscles, and led to a power output of 7-11W depending on the number of stimulated muscle groups. The aim is to check if the power output is higher when more separate muscle groups are stimulated. In particular we stimulated the quadriceps muscle group as a whole with one pair of electrodes in one stimulation pattern (SP) and in the other SP 3 parts of the quadriceps (vastus medialis, vastus lateralis, rectus femoris) were stimulated separately by three separate pairs of electrodes.

Material and Methods

For the trainings we used a MOTOMED Viva 2 ergometer and an 8 channel stimulator developed at the PPCU in Budapest, Hungary. The hamstring and quadriceps muscle groups of both legs were stimulated through bipolar surface electrodes (PG473W TENS ELEC 45x80mm). The adjustable stimulation parameters were current amplitude, pulse width and pulse frequency. Pulse width (rectangular, monophasic) was set to 300 μs, stimulation frequency was 30 Hz in each training. Current amplitude varied among trainings. The participant sat in a wheelchair in his usual sitting position. At the front of the wheelchair a MotoMed Viva 2 cycle ergometer was placed. The distance between the wheelchair and the ergometer was established keeping in consideration that the wheelchair should not prevent the motion of the pedal and allows appropriate knee extension. The participant's feet were placed on the pedals in pedal boots fixed to the pedal and their shanks were strapped to the boots.
The stimulator was connected to a rotation sensor that recorded the ergometer's crank position (100Hz sampling frequency). The stimulator device allowed the selection of a reference crank position and the direction of cycling and then received the crank angle value during cycling.
The training started with a warm up period while the ergometer's motor rotated the cranks and carried the legs. Then we started stimulating the muscles. The current amplitude for each muscle was increased until the muscles started to generate the cycling and the cranks were rotated at 30rpm, at this time the motor stopped and didn't work during the active cycling period, this is the time interval in which the participant cycled by his own stimulated muscles without the assistance of the motor. The stimulating current was further increased until the cadence reached an approximately constant value

between 45-50 rpm. When this cadence was reached then the current amplitude remained constant during the active cycling period for each muscle. In pattern H2 the same current was applied to all muscles. In pattern H4 the 3 parts of the quadriceps were stimulated with the same current amplitude but the hamstrings' stimulation current was further increased in the 5^{th}-10^{th} training (Table 2). The active cycling period was finished when the cadence fell below 40 rpm or when the participant wanted to stop cycling. He was free to stop cycling at any time when he wanted to finish even when the cadence didn't drop below 40 rpm. The active cycling periods varied among trainings and lasted for about 20-40 minutes (Table 1.) The finishing part of the training is a cool down when the ergometer's motor generated the cycling movement without electrical muscle stimulation and physiological parameters of the participant reverted to the default levels.

The product of angular velocity and crank resistance (torque) gave the cycling power output and it was averaged across time during the active period in each training. The energy output was calculated as the product of average power output and active movement time.
Heart rate and blood pressures were measured with a blood pressure monitor 5 times during the training: before the warm up, after the cool down period and 3 times between these measurements (with intervals of 8-9 minutes) within the active cycling period. Mean arterial pressure (MAP) was calculated from measured systolic and diastolic blood pressure values (SBP and DBP respectively) by the following formula:

$$MAP = (SBP - DBP)/3 + DBP$$

We applied 2 stimulation patterns. We name these patterns as H2 and H4 referring to the number of muscle groups stimulated on one leg. With the H2 pattern we applied 2 pairs of surface electrodes on each leg, one for the quadriceps and one for the hamstring muscle groups. With the H4 pattern three parts of the quadriceps muscles - vastus medialis, vastus lateralis and rectus femoris - were stimulated separately, and the hamstrings. Training set up is presented in Figure 1. and figure 2 for cycling with H2 and H4 stimulation patterns.
Stimulation patterns were based on data obtained during cycling of able-bodied people [1,4]. They performed cycling movements on the stationary ergometer and their muscle activities (EMG) were recorded by surface electrodes, while the crank position and crank angle respect to the top dead position was computed from marker coordinates recorded by a ZEBRIS movement analyzer system. Ranges of crank angles in which a muscle was active, were established for each muscle. First the quadriceps and hamstrings activity was recorded applying pairs of electrodes for each of these muscle groups. The electrodes were placed on the muscular belly with an inter-electrode distance of approximately 50 mm. In a separate measurement the activity of three parts of the quadriceps (Vastus lateralis, vastus medialis and rectus femoris) were measured and the hamstrings. The angular ranges of crank positions, in which a particular muscle was active, were established. A muscle was considered active when its EMG amplitude exceeded the 35% of its mean EMG amplitude. These ranges of muscle activities were used to define H2 and H4 stimulation patterns.

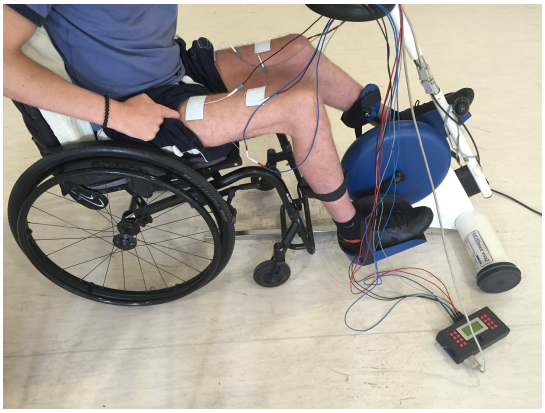

Figure 1: Training setup with the H2 stimulation pattern.

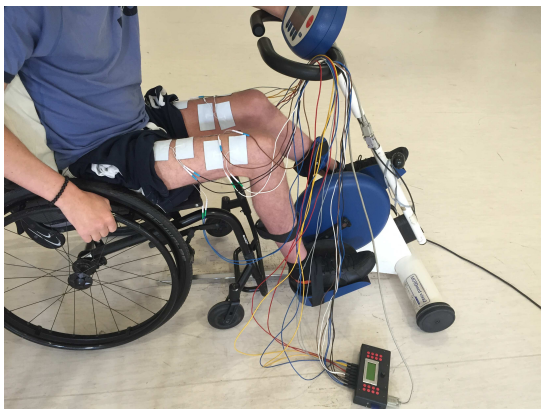

Figure2: Training setup with the H4 stimulation pattern. Three parts of the quadriceps are stimulated.

A 34 years old participant with complete spinal cord injury used both SPs. His level of injury was at Th8 and he started to participate in FES cycling training four years after the injury. Using H2 the participant had 27 training sessions, and then he started to use the H4 pattern. We compare the last 10 sessions performed with H2 and the first 10 performed with H4. Thus the participant had already practiced (17 trainings) and was experienced in FES cycling when we started to include data into this comparison. We compared statistically the power output, the mechanical energy and the cycling time during the FES assisted cycling with H2 and H4 patterns. The differences between values obtained applying the two SPs were assessed with Student's T-test (p=0.05).

Results

Comparison of the total energy during the cycling with two different stimulation patterns didn't show significant difference (p=0.559). However, the power output is significantly higher and the active cycling time is significantly shorter applying H4 comparing to the application of H2 (p=0.001).

Table 1: Comparison of the averaged parameters and standard deviations of the two stimulation conditions

	H2	H4
Cycling time (min)	27.1±3.6	22.3±2.6
Cadence (rpm)	47.4±1.17	48.5±1.3
Current amplitude (mA)	35±7.45	25.9±3.7
Energy (kJ)	12.82±1.82	13.41±2.08
Power output (W)	7.91±0.75	10.08±1.4

The power and energy output, obtained in each training is presented in Figure 3. When H2 stimulation pattern was changed for H4 a significant increase of power output occurred. This change didn't have a significant effect on mechanical energy.

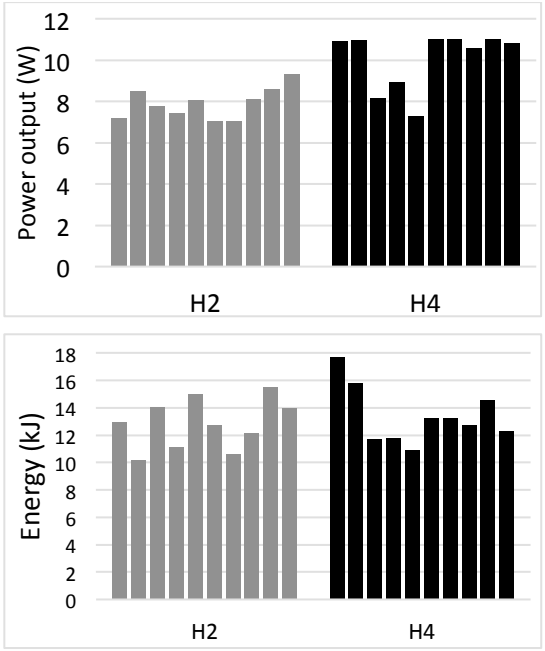

Figure 3. Power output (upper diagram) and mechanical energy (lower diagram) in 10 trainings with H2 (grey bars) and consecutive 10 trainings with H4 (black bars).

In H2 quadriceps and hamstrings muscle groups were stimulated. In H4 three parts of the quadriceps - vastus medialis, vastus lateralis and rectus femoris - were stimulated separately and the hamstrings.

The mean arterial pressure increased during the active cycling period and dropped after the training (Figure 4.). The heart rate remained approximately constant during the training and dropped after the training (Figure 5)

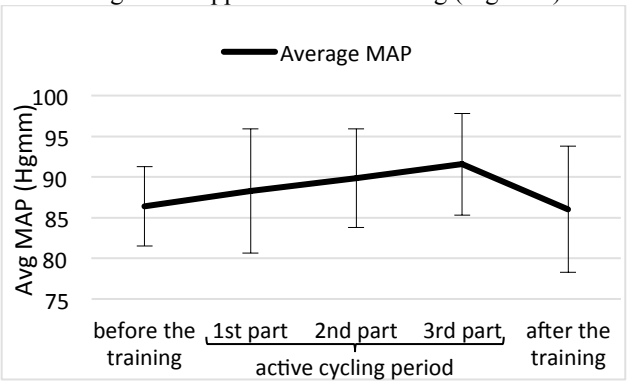

Figure 4: Averaged (across trainings) Mean Arterial Pressures and their standard deviations in five phases of the trainings performed by H2 stimulation pattern: before the warm up period, in the 1st, 2nd and 3rd parts of the active cycling period and after the cool down period.

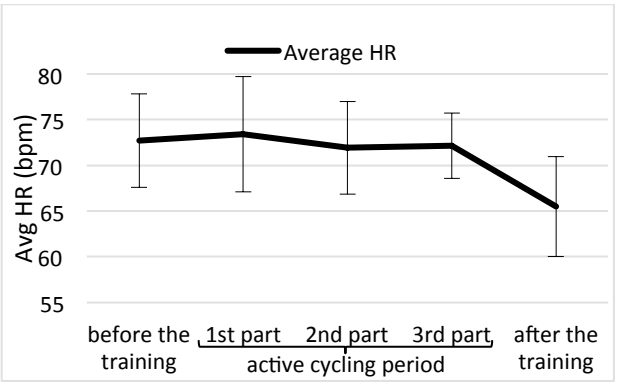

Figure 5: Averaged (across 10 trainings performed by H2 stimulation pattern) heart rates and their standard deviations in five phases of the trainings.

Table 3 shows the relation between cycling time, current amplitude and power output in each individual training.

Table 3. Cycling time, current amplitude (per muscles) and power output in trainings by H2 and H4 stimulation patterns. In the 5th-10th trainings with H4, the hamstrings' stimulation current was higher than that of the 3 parts of the quadriceps.

H2 (training's serial number)	1.	2.	3.	4.	5.	6.	7.	8.	9.	10.	Mean
Cycling time (min)	30	20	30	25	31	30	25	25	30	25	27.1
Current amplitude (mA)	35	45	45	35	45	30	30	30	30	25	35
Power output (W)	7.20	8.48	7.79	7.42	8.05	7.05	7.05	8.11	8.61	9.30	7.91

H4	1.	2.	3.	4.	5.	6.	7.	8.	9.	10	Mean
Cycling time (min)	27	24	24	22	25	20	20	20	22	19	22.3
Current amplitude (mA) (Quad/Ham)	25	20	25	25	30/40	25/35	20/25	25/30	25/30	25/35	24.5/29
Power output (W)	10.94	10.98	8.15	8.92	7.29	11.02	11.02	10.58	11.02	10.80	10.08

Discussion

By stimulating three parts of the quadriceps separately instead of stimulating the quadriceps by one signal, our SCI participant was able to reach a higher power output. This was gained by lower stimulation current amplitude per muscle groups. When instead of 2 muscle groups 4 separate muscle groups were stimulated, the total stimulation current (the sum of the currents applied in all of the channels) was of course higher, although, lower current amplitude per channels may be favourable for the muscles. While the participant reached a higher power output, he preferred to cycle for a shorter time with H4 stimulation pattern, thus the total mechanical energy per session didn't differ comparing the two SPs. The order of the applied SPs in consecutive sessions was not randomized, but because the participant was already a trained person (having 17 sessions before we involved his results in this study) the training may had similar effect on the results gained applying the 2 different SPs. In spite of many studies and application of various SPs [5], effective fatigue control is not well known yet. The cardiovascular effect should also be further investigated. We highlight that we applied relatively low current amplitudes (20-40mA) per muscles. The average current amplitude applied in FES driven cycling of SCI individuals used to be at least around 50-70 mA per muscles and it varies in a wide range [6]. In some protocols current amplitude was increased until 120-140 mA to achieve power output around 10W [7] in extreme cases 20W [8]. Szecsi and coworkers stimulated hamstrings and quadriceps muscles with frequency as we did (30 Hz) but with a higher current amplitude (70-90 mA) and wider pulse width (500 μs) when they reached a power output around 30W [9]. In these works the quadriceps stimulation was not distributed to stimulation of 3 parts of the quadriceps as it was in our case.

Conclusions

We presented the results of a new stimulation pattern for FES cycling by data obtained during the training sessions of one participant. This case study shows that applying more stimulating channels with lower current amplitudes per channel can result in a higher power output. Particularly, stimulating 3 parts of the quadriceps separately, allowed the SCI participant to increase power output in average by 27%. Further studies can investigate this recommendation and may lead to new stimulation protocols applied in rehabilitation of SCI individuals.

References

[1] Pilissy T, Klauber A, Fazekas G, Laczkó J, Szécsi J.: Improving functional electrical stimulation driven cycling by proper synchronization of the muscles, I*deggyogy Sz.,* vol. 61, no 5-6, pp. 162-7, 2008

[2] Laczko J, Katona P, Waszlavik E, Klauber A: Dependence of cycling performance on training time and stimulation frequency during FES driven cycling., IFESS 2012, 17th Annual Meeting–Intnl. Functional Electrical Stimulation Society, pp. 448-451, 2012

[3] Mravcsik M, Klauber A, Laczko J: Power output of spinal cord injured individuals during functional electrical stimulation driven bicycling lower limb movement, Progress in Motor Control X. Conference, 2015. Budapest, Hungary, Program Book p 126., ISBN: 978-615-5187-07-0

[4] Valy A, Laczko J: Timing errors during lower limb cycling under various conditions. Program Number 241.18, 2015 Neuroscience Meeting Planner. Soc. for Neuroscience, Chicago IL, USA, Online. 2015

[5] Ibitoye MO, Hamzaid NA, Hasnan N, Abdul Wahab AK, Davis GM: Strategies for Rapid Muscle Fatigue Reduction during FES Exercise in Individuals with Spinal Cord Injury: A Systematic Review, *PLoS ONE,* vol. 11(2), 2016

[6] Kuhn D, Leichtfried V, Schobersberger W: Four weeks of functional electrical stimulated cycling after spinal cord injury: a clinical cohort study, *International Journal of Rehabilittation Research*, vol. 37, pp. 243-250, 2014

[7] Theisen D, Fornusek C, Raymond J, Davis GM: External power output changes during prolonged cycling with electrical stimulation, *J Rehabil Med,* vol. 34, pp. 171–175, 2002

[8] Eser PC, Donaldson N, Knecht H, Stussi E.: Influence of different stimulation frequencies on power output and fatigue during FES-cycling in recently injured SCI people. Neural Systems and Rehabilitation, IEEE Transactions Eng., vol. 11(3), pp. 236–240, 2003

[9] Szecsi J, Straube A, Fornusek C:. A biomechanical cause of low power production during FES cycling of subjects with SCI, *Journal of NeuroEngineering and Rehabilitation*, vol. 11:123, 2014

Author's Address
Mariann Mravcsik
Affiliation: University of Pécs, Pécs, Hungary
e-mail: mravcsik.mariann@gmail.com

Andras Klauber
National Institute for Medical Rehabilitation, Budapest, Hungary,
e-mail: AKlauber@rehabint.hu
homepage: www.rehabint.hu

Jozsef Laczko
University of Pécs, Pécs, Hungary;
MTA Wigner Research Centre for Physics, Budapest;
Pázmány Péter Catholic University, Budapest, Hungary;
e-mail: laczko.jozsef@wigner.mta.hu
homepage: rehab.wigner.mta.hu

Review: Functional electrical stimulation (FES) for mobility in human spinal cord injury and in muscle spasm and atrophy rehabilitation in horses

Schils S[1], Hofer C[2], Löfler S[2], Zampieri S[2,3] Kern H[2,4], Carraro U[5]

[1]Equine Rehabilitation LLC, River Falls, WI, USA
[2]Ludwig Boltzmann Institute of Electrical Stimulation and Physical Rehabilitation, Vienna, Austria
[3]Laboratory of Translational Myology of the Interdepartmental Research Center of Myology, Department of Biomedical Science, University of Padova, Italy
[4]Institute of Physical Medicine and Rehabilitation, Wilhelminenspital, Vienna, Austria
[5]IRRCS Fondazione Ospedale San Camillo, Venezia, Italy

Abstract: *Functional Electrical Stimulation (FES) is utilized in both human and equine medicine to improve muscle quality and function. When stimulation parameters of these two published applications are compared, differences are evident. The main use of FES for human spinal cord injury (SCI) patients is to assist in standing, walking and sitting activities, reduce muscle atrophy and/or spasms and to improve blood flow in the paralyzed muscle. One primary limiting factor in the successful progress of the patient is early onset fatigue, as well as asymmetry in movement. The main use of FES for horses is to improve muscle symmetry, reduce muscle spasms and atrophy as well as reeducate muscle memory with progressively stronger muscle contractions. One primary limiting factor is the slow speed of the muscle contractions, which does not mimic equine performance. The transfer of horse FES parameters to human SCI physical therapy protocols may be of assistance to: 1. Improve spinal and limb symmetry while also assisting in reducing the frequency of muscle atrophy and spasms; 2. Elicit progressively stronger muscular contractions to induce functional movements of associated joints to improve endurance. The transfer of human FES parameters to horse injury rehabilitation and performance enhancement may be of assistance to: 1. Quicken the reaction time of muscle contractions; 2. Improve the speed of muscle contractions over time.*

Keywords: *Horse, equine, SCI, stimulation parameters, protocols*

Introduction

The multiple uses of functional electrical stimulation (FES) technology have been discussed in the literature for decades. This paper will compare the parameters of two applications of FES; 1. In human medicine for: Spinal cord injury (SCI) patients during standing, walking and sitting; The reduction in muscle atrophy and spasticity and; The improvement in blood flow. 2. In equine injury rehabilitation and performance enhancement for: The improvement in muscle symmetry and muscle endurance; The reduction in muscle spasm and atrophy and; The reeducation of muscle memory. A comparison of the research and clinical results of the two FES systems shows that each system has been effective for their specific applications. The purpose of this paper is to discuss similarities and differences between the systems and to propose that a combined use, at different times during the FES protocols, may improve clinical outcomes.

FES human and horse system comparisons

The basic differences between the human and horse FES systems are as follows:

Human FES parameters

Overall stimulation parameters

Stimulation frequency: 25-30Hz quadriceps and gluteus; 50Hz peroneal nerve
Stimulation pulse width: 600µs (300µs + 300µs)
Pulse shape: Constant voltage biphasic symmetric rectangular pulses, with no pause between positive and negative phases

Electrode design: self-adhesive disposable electrodes
Standing/Sitting - 2 channels, 4 electrodes, each leg
Stepping/Walking - 2 channels, 4 electrodes, each leg; plus 1 channel, 2 electrodes over the peroneal nerve

Standing and sitting training

For standing, 2 stimulation channels (4 electrodes) on each leg are positioned on both the quadriceps and gluteus muscles. The ramp up to the preset stimulation intensity is about 0.8-1 second (depending on the patient). The ramp for sitting is longer in duration than for standing, to achieve a slower and "softer" sitting down motion. Stimulation of the quadriceps and gluteus muscles for standing and sitting produces only a direct muscular response, and is not used to produce a reflex flexion of the knee and hip.

Stepping and walking training with parallel bar assistance
For eliciting electrically activated stepping, initially the stimulation of the quadriceps and gluteus muscles of the non-supporting leg is switched off. The period of time the signal is off is based on the timing of the individual's swing phase, which is typically 0.8-1.5 seconds.
The peroneal nerve is then stimulated to obtain dorsiflexion of the foot and which also produces a reflex flexion in the knee and hip that initiates the swing phase. To obtain the swing phase of the stride, a third independent stimulation channel on each leg produces a short stimulation burst of 1.5-2 seconds in duration, without ramping, and the stimulation frequency for this channel is 50Hz. This specific stimulation combination produces a quick activation of the peroneus and anterior tibialis muscles and induces a reflex flexion in the hip and knee.
At the end of the swing phase, stimulation of the quadriceps and gluteus muscles are activated again to obtain the tension needed for stabilization of the leg for standing.

Research on the use of FES in humans
With the research on FES in humans for complete spinal cord injury, Dr. Helmut Kern and his group has shown positive effects over the past decades to:

- Prevent/revert muscle atrophy/degeneration (Kern, 2014)
- Reduce spasticity (Doucet et al, 2012; Hofstoetter et al, 2014)
- Generate standing and stepping-movements to improve walking speed, distance and improvement of cardiovascular fitness and metabolism (Kern et al, 2014; Graupe et al, 2008; Stöhr et al, 1985; Holle et al, 1984)
- Encourage lower extremity blood flow (Kern 2014).

In addition, there are no lower- or upper-time limits to begin a training program based on FES so the training can begin at anytime after the lesion has occurred and still be effective. (Kern et al, 2008; Graupe et al, 2008). FES has also been used successfully in the long-term therapeutic treatment of foot drop after stroke. (Dunning et al, 2015)

Horse FES parameters
Overall stimulation parameters
Stimulation frequency: 60 Hz
Stimulation pulse width: 500µs + pause (250µs + 250µs)
Pulse shape: Constant voltage biphasic pulses with two symmetric half waves (charge compensated) and pause in between pulses.
Electrode design: 3 channels, 6 electrodes, asterisk pattern of stimulation

Reduction in muscle spasm and atrophy
To reduce muscle spasm and atrophy in horses, the voltage is gradually increased over the 3 stimulation channels until a strong muscular contraction is produced, resulting in spinal or joint movement. Typically, this functional movement is obtained with an intensity of 6-8 volts. The production of functional movement can occur during the first treatment, or it may take several treatments, depending on the severity of the muscle spasm or atrophy. The electrodes are placed evenly on each side of the spine and the major goal is to obtain symmetrical functional movement with smooth and consistent contractions of the targeted muscles and associated joint(s) while the horse is standing.

Reeducation of muscle memory
Treatment time is 35 minutes which produces 525 cycles, to achieve the repetition of movement needed to help reeducate muscle memory. Treatment times are spaced close together in the initial stages with treatments typically being given every day or every other day for 2-3 weeks. At times when the response to the FES treatment is minimal, more than one treatment is given to the same area on the same day.

Research on the use of FES in horses
Specific research on the use of FES for horse rehabilitation has been performed over the past several years. Studies have shown that FES training for horses is a safe treatment that provides clinical improvements in equine epaxial muscle spasms (Ravara, 2015a; Ravara 2015b; Schils, 2015; Schils and Turner, 2014; Schils, 2013). FES training has also been shown to produce a positive effect on mitochondrial density and distribution in equine epaxial muscle, which in turn may help create healthier muscle tissue, that is better able to function during exercise (Schils et al, 2015). Preliminary data showing an improvement in the symmetry of the multifidus muscles of horses after 8 weeks of FES is an encouraging step to show empirically that changes in symmetry are also possible with FES training. The use of FES for horses has been able to produce quick and fairly dramatic changes in muscle tissue. Figure 1 shows the change in muscle atrophy over a period of 9 days with the application of 5 FES treatments to the infraspinatus and supraspinatus muscles, and 2 treatments symmetrically applied across the spine to the thorax region.

Discussion

A comparison of the two FES protocols for human and horse therapy illustrates some distinct differences, most markedly the pause between the positive and negative waves. The reasons for these differences is due to the variation of the outcomes of the two FES therapies. In humans, the purpose is to activate paralyzed muscle for sitting, standing and walking activities. In horses, the purpose of the FES stimulation is for injury rehabilitation and performance enhancement.

The human FES parameters for SCI uses short "bursts" of signal on and off to elicit the appropriate combination of support and swing phases of the limb producing dynamic movement. In addition, the peroneal nerve is stimulated individually to obtain dorsiflexion. In the literature, which discusses the parameters of human FES systems,

frequency, pulse width and duty cycle vary a lot but commonly 20-50Hz, 300-600µs and cycles of 1:2-1:3 are used respectively (Doucet 2012). FES parameters should be tailored to the individual client's needs to reproduce normal activation patterns, optimize force output and reduce fatigue. In humans, home-based therapy in the individual's private environment is increasing rapidly and therefore it is hard to accurately evaluate and record outcomes when compared to a stationary/laboratory setting as practiced in the majority of horse therapy. In addition, the activities of daily living, and personal limitations and effort, cannot be influenced as easily with humans when compared to horses.

In the horse, the stimulus is always used for non paralyzed muscle and this is a distinct difference between the horse and human protocols. One of the short-term effects of horse muscle stimulation may be due to the consequences of reflex activity of the non paralyzed muscle, which is the result of sensory stimulation. To obtain the desired outcomes in horses, functional joint movement is obtained while the horse is stationary. In most cases, the signal crosses the spinal column and is symmetrically applied, however treatments to specific unilateral muscle groups is also performed.

Typically, during the first several FES treatments to the horse, the joint rotations obtained are not biomechanically correct. This incorrect movement pattern of the joint, which is most frequently observed as a lateral twist, illustrates the outcome of asymmetrical muscle development, As FES treatments progress over time, the joint rotation becomes more and more mechanically correct. Clinical observation after several treatments reveals an improved movement pattern in the horse resulting in better balance and performance.

The treatment area over the epaxial muscles of the horse is about 60 cm in length, and the specific area of the topline which is stimulated is changed periodically to target different muscle reactions. Observation of the movement patterns obtained with a variety of placements of the electrodes, trial and error, and observation of results over the past 20 years has refined the treatment protocols. Changes in the movement patterns of the muscles can happen quickly, and this could be due to several factors. One is that the horses are ambulatory so they move around most of the day keeping the muscles active. Horses lay down for only short periods of time so the muscles are constantly stimulated to a certain degree to support the mass of the horse. Second, a series of physical exercises are used to supplement the changes in movement patterns obtained by FES training, and in horses where the rider follows these exercises in combination with FES training, the improvements in the horse have an increased possibility of being quick and long lasting.

An improvement, which may be useful for human FES training outcomes, would be to increase muscle endurance and improve muscle symmetry in SCI patients through the use of horse FES training. In addition, the longer time frame of the horse FES treatment protocols could assist in the re-education of muscle memory and improve blood flow over an extended period of time.

One of the improvements that could be made in the horse FES training outcomes is to mimic the short bursts of activity required in equine performance, since the current stimulus pattern is based more on muscle endurance enhancement. This ability to improve the "quickness" of the muscle reaction time could prove to be a valuable addition to the horse FES protocol, especially for performance enhancement. In addition, increasing the speed of the muscle contractions could also improve the overall outcome of the horse FES training protocols by improving the variety of muscle responses, again better mimicking actual performance. The utilization of the human FES parameters would be useful for these purposes.

The use of the horse FES parameters to obtain stronger and stronger symmetrical muscle contractions over time, which more closely resembles functional movement, is an important element to the success of the outcome. If these stronger contractions are used in SCI patients for a longer period of time, care must be taken that the skeletal and soft tissues can withstand these intense contractions. A gradual increase in the strength and length of time of the contractions is essential for a positive outcome to occur. However, if the stimulus is not strong enough to elicit functional movement, then the full benefits of FES training are likely diminished. In addition, the use of the asterisk design of the horse FES parameters may help to vary the stimulation area and could prove a useful addition to the human protocols.

Conclusions

A discussion of the uses of FES in humans for SCI, and for horses rehabilitating from injury or for performance enhancement, has shown distinct differences between the parameters of the two modalities. The stimulation of paralyzed muscle in SCI patients where the sensory reflex is not present is different from the stimulation of non paralyzed muscles in horses where the sensory reflex is present. In addition, the main purpose of human FES is for short "bursts" of muscle activity for sitting, standing and walking. In comparison, the use of horse FES is mainly for improvements in muscle symmetry, the reduction in muscle spasms and atrophy, and for muscle re-education.

Could the FES parameters used for improvement in muscle function in humans and horses be combined to improve outcomes? The use of the horse FES parameters in human SCI physical therapy may be of assistance to: 1. Improve spinal and limb symmetry while also assisting to reduce frequency of muscle spasms and atrophy which occur during early and long-term disuse; 2. Elicit progressively stronger muscular contractions to induce functional movements of associated joints, while sitting, to improve endurance and increase blood flow. The use of the human FES parameters during rehabilitation from injury and for performance enhancement in horses may be

of assistance to: 1. Shorten the reaction time of muscle contractions; 2. Improve the speed of muscle contractions over time.

A review of the similarities and differences between the human and horse FES has shown distinct and varying benefits of each protocol. It is intriguing to hypothesize that the combination of human and horse FES protocols may be useful in improving outcomes of both species. Future research must be performed to explore if the combined usage of the two types of protocols proves to be valuable.

References

Kern H. Functional Electrical Stimulation on Paraplegic Patients. Eur J Transl Myol. 2014 Jul 8; 24(2): 2940.

Doucet BM, Lam A, Griffin L . Neuromuscular electrical stimulation for skeletal muscle function. Yale J Biol Med. 2012 Jun;85(2):201-15.

Hofstoetter US, McKay WB, Tansey KE, Mayr W, Kern H, Minassian K. Modification of spasticity by transcutaneous spinal cord stimulation in individuals with incomplete spinal cord injury. J Spinal Cord Med. 2014 Mar;37(2):202-11.

Graupe D, Cerrel-Bazo H, Kern H, Carraro U. Walking performance, medical outcomes and patient training in FES of innervated muscles for ambulation by thoracic-level complete paraplegics. Neurol Res. 2008 Mar;30(2):123-30.

Stöhr H., M. Frey, J. Holle, H. Kern, W. Mayr, G. Schwanda, H. Thoma. 20 channel implantable nerve stimulator makes paraplegic patients walk again. Proceedings, 14th Meeting of the Neuroelectric Society, International Symposium on Biomechanics of Muscle, Vravrona-Attica, Griechenland, 51, 1985

Holle J., M. Frey, H. Gruber, H. Kern, H. Stöhr, H. Thoma, J. Functional electrostimulation of paraplegics (experimental investigation sand first clinical experience with an implantable stimulation device). Orthopedics, 7, 1145-1155, 1984

Kern H, Hofer C, Mödlin M, Mayr W, Vindigni V, Zampieri S, Boncompagni S, Protasi F, Carraro U. Stable muscle atrophy in long-term paraplegics with complete upper motor neuron lesion from 3- to 20-year SCI. Spinal Cord. 2008 Apr;46(4):293-304.

Dunning K, O'Dell MW, Kluding P, McBride K. Peroneal Stimulation for Foot Drop After Stroke: A Systematic Review. Am J Phys Med Rehabil. 2015 Aug;94(8):649-64.

Ravara B, Gobbo V, Carraro U, Gelbmann L, Pribyl J, Schils S. Functional electrical stimulation as a safe and effective treatment for equine epaxial muscle spasms: Clinical evaluations and histochemical morphometry of mitochondria in muscle biopsies. Eur J Transl Myol - Basic Appl Myol 2015a;25(2):109-120

Ravara B, Gobbo V, Carraro U, Gelbmann L, Pribyl J, Schils S. Mitochondrial density and distribution by histochemical approaches distinguish muscle fiber types and support clinical improvements due to FES as a treatment of equine epaxial muscle spasms. Eur J Transl Myol/Basic Appl Myol 2015b; 25 (3): 145-182 (149) CIR-Myo News: Abstracts of the 2015 Spring Padua Muscle Days, Terme Euganee Padua (Italy), March 12 - 14, 2015.

Schils S, Carraro U, Turner T, Ravara B, Gobbo V, Kern H, Gelbmann L, Pribyl J. Functional Electrical Stimulation for Equine Muscle Hypertonicity: Histological Changes in Mitochondrial Density and Distribution. J Equine Vet Sc 35 2015a;907–916.

Schils SJ. Functional electrical stimulation (FES) use in horses for musculoskeletal and neuromuscular rehabilitation. Eur J Transl Myol/Basic Appl Myol 2015; 25 (3): 145-182 (148-149)CIR-Myo News: Abstracts of

FIGURE 1. Seven FES treatments to the shoulder and thorax of the horse over 9 days

Online assessment of Volitional Muscle activity from Stimulation Electrodes in a Drop Foot Neuroprosthesis

Valtin M[1], Werner C[2], Schauer T[1],

[1]Control Systems Group, Technische Universität Berlin, Berlin, Germany

[2]Department of Neurological Rehabilitation, Charité Universitätsmedizin Berlin, Berlin, Germany

Abstract: *This contribution investigates the feasibility of realtime muscle activity assessment in an adaptive drop foot stimulator for control of stimulation intensity or for biofeedback. A surface electromyography (sEMG) measurement is realized from the two stimulation electrodes also during active stimulation in between the stimulation pulses using a stimulation device with integrated EMG measurement. A non-causal digital high-pass filter with optimally chosen initial conditions is applied to the batch of EMG samples between two stimulation pulses in order to extract the higher frequent part of the volitionally induced EMG activity. After rectification and averaging of the filter output vector we obtain at stimulation frequency a scalar measure of the residual muscle activity within the last stimulation period. The feasibility of such realtime EMG-processing has been demonstrated with one healthy subject by monitoring the superposed volitional support by the subject during electrical stimulation induced dorsiflexions.*

Keywords: *Functional Electrical Stimulation, Drop Foot Stimulation, Electromyography, Gait, Signal Processing*

Introduction

The limited ability to lift the inner (medial) or the outer (lateral) edge, or both, of the foot by voluntary muscle activation is known as drop foot syndrome and is present in about 20% of the ambulatory chronic stroke patients [1]. The electrical stimulation of the peroneal nerve for correction of foot drop during the swing phase of gait is an established rehabilitation method with proven orthotic and therapeutic (carry-over) effects (see e.g. [2]). In a standard transcutaneous drop foot stimulator, a pair of surface electrodes on the skin close to the head of fibula and on the insertion of the m. tibialis anterior to activate the muscles tibias anterior and fibularis longus. Until now, all commercially available devices have been solely based on open-loop architectures, i.e. they only use sensors to time the stimulation [3] – typically a simple heel switch.

Current research direction aims at the following: 1st) to replace the heel switch by an inertial sensors at the foot or shank for a more detailed gait phase detection and better synchronization of the electrical stimulation with the patient initiated gait, 2nd) to adjust the stimulation intensity to the patients need by sensing the foot motion and 3rd) to promote the volition support of the foot movement by the patient. We developed recently an adaptive drop foot stimulator that uses an internal sensor at the foot to detect gait events and phases and to monitor the foot motion [4]. Based on the obtained measurements iterative learning control is applied to realize a desired physiological foot motion during the swing phase within a couple of strides. For a not changing reference motion the resulting stimulation intensity might be used to assess the patient's active involvement as lower intensities indicate a higher patient involvement.

Alternative approaches propose the use of EMG measurements to trigger or to drive the electrical stimulation of the dorsiflexors in order to directly involve the patient [5, 6, 7]. The volitionally induced EMG activity is extracted from the recorded EMG in between the stimulation pulses by either applying a high-pass filtering approach or by subtracting the predicted M-wave (the electrical stimulation induced EMG activity) (see e.g. [8]). The first 20 to 30 ms after each stimulus are usually discarded from the analysis as this period contains the electrode discharging transients and the higher frequent parts of the M-wave.

Most existing systems require separate electrodes for EMG measurement that may restrict the transfer of such systems into clinically usable systems. A direct EMG measurement from the stimulation electrodes would be a clear technological advantage. Compared to the setup with separate stimulation and EMG electrodes there are several challenges: 1st) The voltage potential difference between the stimulation pulses (up to 150 V) and the EMG signal (less than 1 mV) is huge, 2nd) the electrode area of stimulation electrodes is much bigger than the one of EMG electrodes, and 3rd) the capacitive rest charge on the electrodes will cause significant discharging transients in the EMG recordings that are difficult to predict and make EMG measurements impossible without additional discharge of the electrodes. Protection and passive discharging circuits in front of the EMG amplifier are therefore required. The feasibility of an EMG measurement from the stimulation electrodes was demonstrated in [9, 10] by using classical analog EMG amplifiers, analog high-pass filtering and discharge and protection circuits.

In this contribution we present a stimulation system with an integrated 24-Bit analog front-end for EMG measurements. An input circuit with PhotoMos switches protects the analog front-end and allows passive discharging of the stimulation electrodes after each stimulus. For the extraction of the volitional EMG activity we introduce a digital high-pass filter with optimally chosen initial conditions to reduce transients in the filter output caused by the discharging. The system was initially tested to detect volitional foot lift dur-

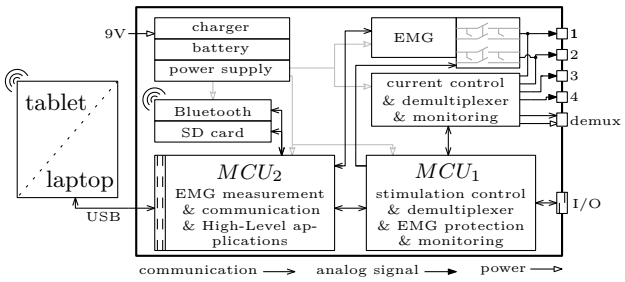

Figure 1: RehaMovePro stimulator block diagram with the main components from [11].

ing active stimulation from stimulation electrodes used in a drop foot stimulator setup.

Materials and Methods

Combined Stimulation and Measurement System

The RehaMovePro stimulation system is used for stimulation and EMG measurement [11]. Fig. 1 depicts an overview of the device. The stimulation module supports four demultiplexed current-controlled stimulation channels and is controlled by MCU1, an ARM Cortex M4 microcontroller (STM32F407, STMicroelectronics). The task of MCU1 is to generate and monitor the stimulation waveform, as well as to control the EMG protection and the demultiplexer. The second microcontroller, MCU2 (STM32F407, STMicroelectronics), is responsible for less safety-critical tasks, like receiving data from the EMG front-end and communication with external devices. Surface electromyography (sEMG) measurements are supported by two of the four stimulation channels through a protected 24 bit EMG front-end (ADS1294, Texas Instruments). The protection circuit enables sEMG recordings even during active stimulation. The inputs of the EMG front-end will be disconnected from the stimulation electrodes during the stimulation pulses by two galvanically isolated PhotoMos switches. A third PhotoMos switch, which is located before the two protection switches, is activated directly after the stimulus, when the protection is still active, to passively discharge the electrodes by shorting the pathways coming from the two electrodes. The start time and the duration of this short-circuit can be adapted in realtime. Any remaining voltage transients from the stimulation pulse is later removed with a non-causal high-pass filter. A SIMULINK interface is available to set all parameters, to control the stimulation intensity and to receive the EMG data with marked stimulation time points[1]. Hence, control and signal processing algorithms can be easily developed in MATLAB/SIMULINK and real-time code can be generated, e.g. by using the Linux Target for SIMULINK Embedded Coder[2].

In this work, only one stimulation channel with an EMG measurement at 4 kHz is used. Electrodes are placed on the skin close to the head of fibula and on the insertion of the m. tibialis anterior. The stimulation frequency is set to 25 Hz. In between two stimulation pulses, 160 EMG samples are collected. $EMG_i(k)$, $k = 1, \ldots, 160$, represents the k-th sample within the i-th stimulation period. The shortening of the stimulation electrodes starts immediately after each stimulus and lasts for 10 ms.

EMG filtering

To determine the volitional EMG activity in each interpulse interval, we first extract the EMG from sample N_1 to N_2 after the last stimulus. This interval contains beside volitional EMG activity the low-frequent tail of the M-wave and the voltage transients from the remaining charge. To remove the two latter both and to extract the higher frequent part of the volitional EMG activity[3] we apply a non-causal high-pass filtering in which the initial filter states are chosen so that filter transients become minimal. A 6^th-order elliptic high-pass filter with a passband edge frequency of 200Hz, 3 dB of ripple in the passband, and 80 dB of attenuation in the stop band is used to filter the EMG data forward and backwards in time. To determine the optimal initial filter states we rewrite the entire filter process in vectorial form. Let the input vector for the filtering process be

$$\boldsymbol{U} = \left[EMG_i\left(N_1\right), EMG_i\left(N_1+1\right), \cdots, EMG_i\left(N_2\right)\right]^T.$$

Filtering forward in time: The 6th order Elliptic high-pass filter is given in form of a state-space model representation ($\boldsymbol{F} \in \mathbb{R}^{6x6}, \boldsymbol{G} \in \mathbb{R}^{6x1}, \boldsymbol{E} \in \mathbb{R}^{1x6}, D \in \mathbb{R}$):

$$\begin{aligned} \boldsymbol{x}(k+1) &= \boldsymbol{F}\boldsymbol{x}(k) + \boldsymbol{G}u(k) \\ y_f(k) &= \boldsymbol{E}\boldsymbol{x}(k) + Du(k), \end{aligned}$$

where $k = N_1, \ldots, N_2$ is the sample index and $u(k)$ are elements of $\boldsymbol{U}$. The vector of the output samples of this forward filtering process is

$$\boldsymbol{Y}_f = \begin{bmatrix} y_f(N_1) & y_f(N_1+1) & \ldots & y_f(N_2) \end{bmatrix}^T$$

Using the Toeplitz matrix

$$\boldsymbol{\mathcal{Q}} = \begin{bmatrix} D & 0 & \cdots & 0 & 0 \\ \boldsymbol{EG} & D & \cdots & 0 & 0 \\ \boldsymbol{EFG} & \boldsymbol{EG} & \cdots & 0 & 0 \\ \vdots & \vdots & \vdots & \vdots & \vdots \\ \boldsymbol{EF}^{N-3}\boldsymbol{G} & \boldsymbol{EF}^{N-4}\boldsymbol{G} & \cdots & D & 0 \\ \boldsymbol{EF}^{N-2}\boldsymbol{G} & \boldsymbol{EF}^{N-3}\boldsymbol{G} & \cdots & \boldsymbol{EG} & D \end{bmatrix}$$

and the observability matrix

$$\boldsymbol{\mathcal{O}} = \left[\boldsymbol{E}, \boldsymbol{EF}, \boldsymbol{EF}^2, \ldots, \boldsymbol{EF}^{N-1}\right]^T$$

we can write the forward filtering problem as

$$\boldsymbol{Y}_f = \boldsymbol{\mathcal{Q}}\boldsymbol{U} + \boldsymbol{\mathcal{O}}\underline{\boldsymbol{x}}$$

where $\underline{\boldsymbol{x}} = \boldsymbol{x}(N_1)$ is the initial state of forward filtering.

[1] Also for pulses with zero intensity the marker is set with the corresponding stimulation frequency.

[2] http://lintarget.sourceforge.net/

[3] The spectral energy of the volitional EMG activity is located between 30 and 300 Hz with a peak around 120 Hz

Non-causal filtering: Let us introduce first the row and and column reversion operators $\mathcal{R}$ and $\mathcal{C}$ with the following properties ($\boldsymbol{A}$, $\boldsymbol{B}$ and $\boldsymbol{C}$ are compatible matrices):

$$\begin{aligned} \boldsymbol{A} &= \boldsymbol{B}\boldsymbol{C} \\ \mathcal{R}(\boldsymbol{A}) &= \mathcal{R}(\boldsymbol{B})\boldsymbol{C} \\ \mathcal{C}(\boldsymbol{A}) &= \boldsymbol{B}\mathcal{C}(\boldsymbol{C}) \\ \boldsymbol{B}\mathcal{R}(\boldsymbol{C}) &= \mathcal{C}(\boldsymbol{B})\boldsymbol{C} \\ \mathcal{C}(\mathcal{R}(\boldsymbol{B}\mathcal{C}(\mathcal{R}(\boldsymbol{C})))) &= \mathcal{C}(\mathcal{R}(\boldsymbol{B}))\boldsymbol{C} \\ \mathcal{C}(\mathcal{R}(\boldsymbol{A})) &= \boldsymbol{A}^T \text{ if } \boldsymbol{A} \text{ Toeplitz} \end{aligned}$$

The forward-backward filtering involves these steps:

1. Filter $\boldsymbol{U}$ through $(\boldsymbol{F}, \boldsymbol{G}, \boldsymbol{E}, D)$ forward in time to obtain the vector $\boldsymbol{Y_f}$,
2. Reverse the result $\boldsymbol{Y_f}$ in time by applying the row reversion operator,
3. Filter the reversed sequence $\mathcal{R}(\boldsymbol{Y_f})$ through $(\boldsymbol{F}, \boldsymbol{G}, \boldsymbol{E}, D)$ again,
4. Time-reverse the last filter output again to obtain the forward-backward filtered sequence $\boldsymbol{Y_{fb}}$

Using the previously introduced matrices $\boldsymbol{\mathcal{Q}}$ and $\boldsymbol{\mathcal{O}}$ we can write this process as follows

$$\begin{aligned} \boldsymbol{Y_f} &= \boldsymbol{\mathcal{Q}}\boldsymbol{U} + \boldsymbol{\mathcal{O}}\underline{\boldsymbol{x}} \\ \boldsymbol{Y_{fb}} &= \mathcal{R}(\boldsymbol{\mathcal{Q}}\mathcal{R}(\boldsymbol{Y_f}) + \boldsymbol{\mathcal{O}}\overline{\boldsymbol{x}}) \\ &= \mathcal{R}(\boldsymbol{\mathcal{Q}}\mathcal{R}(\boldsymbol{\mathcal{Q}}\boldsymbol{U} + \boldsymbol{\mathcal{O}}\underline{\boldsymbol{x}}) + \boldsymbol{\mathcal{O}}\overline{\boldsymbol{x}}) \\ &= \mathcal{R}(\boldsymbol{\mathcal{Q}})\mathcal{R}(\boldsymbol{\mathcal{Q}})\boldsymbol{U} + \mathcal{R}(\boldsymbol{\mathcal{Q}})\mathcal{R}(\boldsymbol{\mathcal{O}})\underline{\boldsymbol{x}} + \mathcal{R}(\boldsymbol{\mathcal{O}})\overline{\boldsymbol{x}} \\ &= \boldsymbol{\mathcal{Q}}^T\boldsymbol{\mathcal{Q}}\boldsymbol{U} + \boldsymbol{\mathcal{Q}}^T\boldsymbol{\mathcal{O}}\underline{\boldsymbol{x}} + \mathcal{R}(\boldsymbol{\mathcal{O}})\overline{\boldsymbol{x}} \end{aligned}$$

with the initial states $\underline{\boldsymbol{x}}$ and $\overline{\boldsymbol{x}} = \boldsymbol{x}(N_2)$ of the forward and the backward filtering, respectively.

Determine the optimal initial states: The initial state vector $\boldsymbol{x}_{\text{initial}} = \left[\underline{\boldsymbol{x}}, \overline{\boldsymbol{x}}\right]^T$ is chosen in such a way that the cost function $J = \boldsymbol{Y}_{fb}^T\boldsymbol{Y}_{fb}$ becomes minimal in order to reduce filter transients. To determine the optimal initial state vector, we set the first derivative of the cost function to zero

$$\frac{\partial \boldsymbol{Y}_{fb}^T\boldsymbol{Y}_{fb}}{\partial \boldsymbol{x}_{\text{initial}}} = 0$$

and solve for $\boldsymbol{x}_{\text{initial}}$. This yields the optimal initial state

$$\begin{aligned} \boldsymbol{x}_{\text{initial}}^{\text{opt}} &= \left[\left(\left[\boldsymbol{\mathcal{Q}}^T\boldsymbol{\mathcal{O}} \quad \mathcal{R}(\boldsymbol{\mathcal{O}})\right]^T\left[\boldsymbol{\mathcal{Q}}^T\boldsymbol{\mathcal{O}} \quad \mathcal{R}(\boldsymbol{\mathcal{O}})\right]\right)^T\right]^\dagger \\ &\quad \cdot \left((-\boldsymbol{\mathcal{Q}}^T\boldsymbol{\mathcal{Q}}\boldsymbol{U})^T\left[\boldsymbol{\mathcal{Q}}^T\boldsymbol{\mathcal{O}} \quad \mathcal{R}(\boldsymbol{\mathcal{O}})\right]\right)^T \end{aligned}$$

where † is the pseudo inverse. The non-causal filter is then

$$\boldsymbol{Y_{fb}} = \boldsymbol{\mathcal{Q}}^T\boldsymbol{\mathcal{Q}}\boldsymbol{U} + \left[\boldsymbol{\mathcal{Q}}^T\boldsymbol{\mathcal{O}} \quad \mathcal{R}(\boldsymbol{\mathcal{O}})\right]\boldsymbol{x}_{\text{initial}}^{\text{opt}}.$$

The volitional muscle activity EMG_i^V of the interpulse interval i is finally obtained by rectification and mean value calculation of the forward and backward filtered EMG:

$$EMG_i^V = \frac{1}{N_2 - N_1 + 1}\sum_{k=N_1}^{N_2}|y_{fb}(k)|.$$

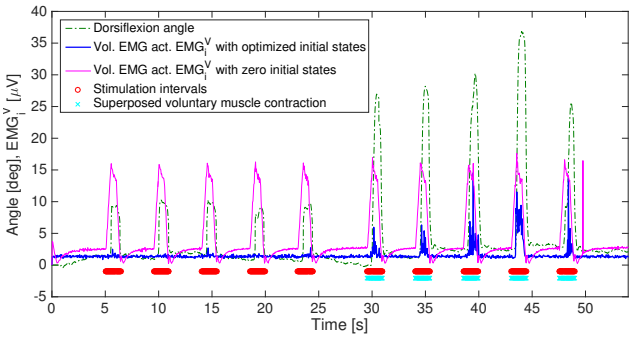

Figure 2: Detected volitional EMG activity and dorsiflexion angle during electrical stimulation. The last five stimulation intervals are superposed by a voluntary muscle contraction. For all remaining time points the subject was relaxed.

Experimental Validation

To evaluate the proposed EMG measurement setup and the filtering approach, first experiments with one healthy subject have been conducted. Informed consent of the subject was obtained and the trials have been approved by the ethics committee of Charité Universitätsmedizin Berlin. The subject sat on a table with the shank free to swing. Stimulation was applied during ten predefined time intervals in order to lift the foot by FES. The subject was asked to relax during the first five intervals and to add volitional effort during the last five time intervals. The dorsiflexion angle with respect to the rest positions was monitored by an inertial sensor attached to the instep of the foot.

Results

Fig. 2 shows the observed volitional EMG activity (with N_1=80 and N_2=160) during the experiment together with the measured dorsiflexion angle. Stimulation intervals are indicated in red. During these intervals, bi-phasic pulses with a pulsewidth of 400μs and a current amplitude of 21 mA were applied at a stimulation frequency of 25 Hz. It is clearly visible that stimulation without volitional muscle activity does not lead to an change of the detected volitional EMG activity (it stays at base line) when the initial filter states are chosen by the proposed optimization. Voluntary muscle contraction during the stimulation intervals can be clearly detected by an increase of EMG_i^V (blue line). Without optimization of the the initial states, also stimulation intervals without voluntary muscle contraction are misinterpreted as periods with volitional muscle activity. The Fig. 3 and 4 show exemplarily interpulse intervals with and without volitional muscle activity during active stimulation, respectively.

Discussion and Conclusions

The feasibility to detect residual volitional muscle activity from the stimulation electrodes during active stimulation was proven. It was demonstrated that a proper selection

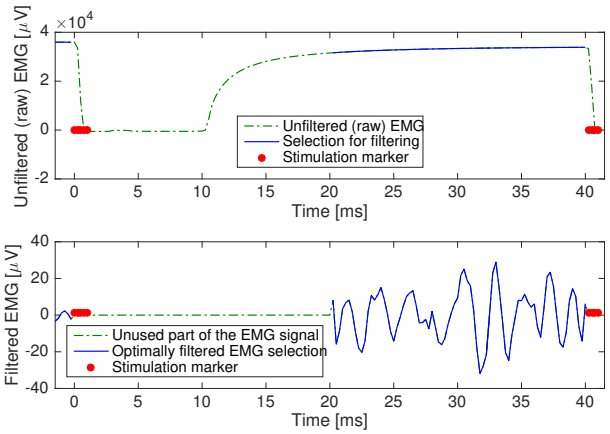

Figure 3: Interpulse interval with volitional muscle activity.

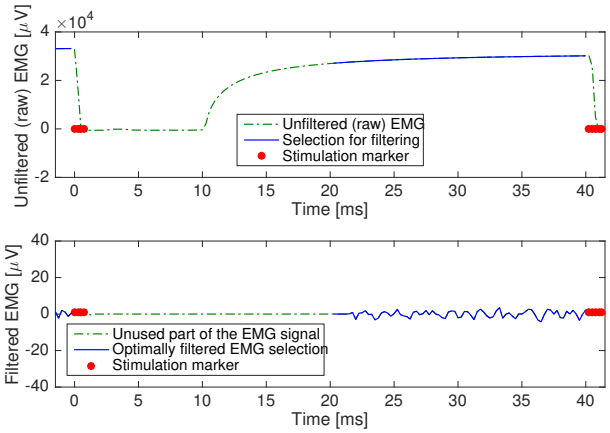

Figure 4: Interpulse interval w/o volitional muscle activity.

of initial filter states is required. The non-causal EMG filter does not introduce any time-shift. This is important for an analysis of the volitional EMG activity vector between to stimulation pulses, e.g. when H- or F-waves are of interest. In future, the system must be evaluated on stroke patients under real walking conditions and the gained information exploited for stimulation intensity control or for biofeedback. Furthermore, an optimization of filter parameters (order, edge frequency and intervals) must take place.

Acknowledgement

This work was supported by the German Federal Ministry of Education and Research (BMBF) within the research project BeMobil (FKZ16SV7069K).

References

[1] D. T. Wade, V. A. Wood, A. Heller, J. Maggs, and R. L. Hewer, "Walking after stroke. Measurement and recovery over the first 3 months," *Scandinavian Journal of Rehabilitation Medicine*, vol. 19, no. 1, pp. 25–30, 1987.

[2] M. Kafri and Y. Laufer, "Therapeutic effects of functional electrical stimulation on gait in individuals post-stroke," *Annals of Biomedical Engineering*, vol. 43, pp. 451–466, Feb. 2015.

[3] P. L. Melo, M. T. Silva, J. M. Martins, and D. J. Newman, "Technical developments of functional electrical stimulation to correct drop foot: sensing, actuation and control strategies," *Clinical Biomechanics*, vol. 30, pp. 101–113, Feb. 2015.

[4] T. Seel, C. Werner, J. Raisch, and T. Schauer, "Iterative learning control of a drop foot neuroprosthesis — Generating physiological foot motion in paretic gait by automatic feedback control," *Control Engineering Practice*, vol. 48, pp. 87–97, Mar. 2016.

[5] R. Thorsen, M. Ferrarin, and P. Veltink, "Enhancement of isometric ankle dorsiflexion by automyoelectrically controlled functional electrical stimulation on subjects with upper motor neuron lesions," *Neuromodulation*, vol. 5, no. 4, pp. 256–263, 2002.

[6] W. L. Chen, S. C. Chen, C. C. Chen, C. H. Chou, Y. Y. Shih, Y. L. Chen, and T. S. Kuo, "Patient-driven loop control for ambulation function restoration in a non-invasive functional electrical stimulation system," *Disability and Rehabilitation*, vol. 32, no. 1, pp. 65–71, 2010.

[7] H. Yeom and Y.-H. Chang, "Autogenic EMG-controlled functional electrical stimulation for ankle dorsiflexion control," *J. of Neurosc. Methods*, vol. 193, no. 1, pp. 118–125, 2010.

[8] E. Ambrosini, S. Ferrante, T. Schauer, C. Klauer, M. Gaffuri, G. Ferrigno, and A. Pedrocchi, "A myocontrolled neuroprosthesis integrated with a passive exoskeleton to support upper limb activities," *Journal of Electromyography and Kinesiology*, vol. 24, pp. 307–317, Apr. 2014.

[9] Y. Muraoka, "Development of an EMG recording device from stimulation electrodes for functional electrical stimulation," *Frontiers of Medical and Biological Engineering: The International Journal of the Japan Society of Medical Electronics and Biological Engineering*, vol. 11, no. 4, pp. 323–333, 2002.

[10] R. Shalaby, T. Schauer, W. Liedecke, and J. Raisch, "Amplifier design for EMG recording from stimulation electrodes during functional electrical stimulation leg cycling ergometry," *Biomed Tech (Berl)*, vol. 56, no. 1, pp. 23–33, 2011.

[11] M. Valtin, K. Kociemba, C. Behling, B. Kuberski, S. Becker, and T. Schauer, "RehaMovePro: A versatile mobile stimulation system for transcutaneous FES applications," in *Proc. of the 20th IFESS Conference*, La Grande-Motte, France, 2016.

Author's Address

Thomas Schauer
Technische Universität Berlin, Control Systems Group
Einsteinufer 17, EN 11,10587 Berlin, Germany
schauer@control.tu-berlin.de
http://www.control.tu-berlin.de

Session 4: Technologies, Engineering, Sensors

The Intracortical Visual Prosthesis (ICVP) System

Troyk P[1], Suh S[1], Bredeson S[1],Cogan S[2], Bak M[3], DeMichele G[4], Hu Z[4]

[1]Illinois Institute of Technology, USA; [2]University of Texas Dallas, USA; [3]Microprobes for Life Science, USA; [4]Sigenics Inc, USA

Abstract: *For the past fifteen years, the Illinois Institute of Technology (IIT) has led a team-based IntraCortical Visual Prosthesis (ICVP) project, consisting of multiple institutions and companies, to develop the ICVP system - for which micro-sized wire electrodes, contained within the Wireless Floating MicroElectrode Array (WFMA), provide electrical stimulation directly to the visual cortex for the purpose of restoring visual perception to individuals with blindness. Based upon the development of electrode materials, electrode array fabrication, implantable wireless hardware design, implantable stimulator fabrication and use, non-human primate psychophysics, normal human psychophysics, surgical feasibility assessment, and psychological assessment/testing methods, the ICVP has reached a state of readiness for a clinical trial.*

Keywords: *Visual prosthesis, intracortical, stimulation, implantable*

Introduction

Our hypothesis is that highly-organized, spatial-temporal, intracortical electrical stimulation of the human visual system can induce visual sensations which can be integrated to provide a usable vision substitute for individuals with blindness. To test this hypothesis, a clinical trial has been defined that will evaluate the use of a multitude of implantable sixteen-channel modular stimulators in forming an artificial neural interface with the occipital lobe of the human brain. From the pioneering work of Brindley and Lewin [1], and later work described in [2,3,4,5,6], it is generally regarded as feasible to induce stable phosphenes via intracortical stimulation. The work of Srivastava [7], and others supports the concept that a multitude of irregularly sized and spaced phosphenes can be used to form an integrated visual perception. Our clinical trial will strive to answer the key question: can individuals with blindness integrate intracortically-induced phosphenes to form useful visual sensory perceptions? This trial addresses neuroscience, health, and quality-of-life issues because, even with currently existing compensatory strategies for vision loss, over two thirds of individuals with blindness are not gainfully employed; individuals with blindness experience higher rates of depression and social isolation, and experience a reduced quality-of-life.

Material and Methods

As reported in [8], and shown in Figure 1, the WFMA is physically comprised of a ceramic substrate platform that maintains the lateral position of eighteen (16 + reference + counter) Parylene-insulated iridium microelectrodes, and provides electrical interconnection between a superstructure that contains an electronic integrated circuit and microcoil, to form a fully-integrated autonomous wireless stimulator module. A group of WFMAs comprise the implanted portion of the ICVP System. The WFMA is operated by a 4.8 MHz inductive link that provides both power and communication to/from

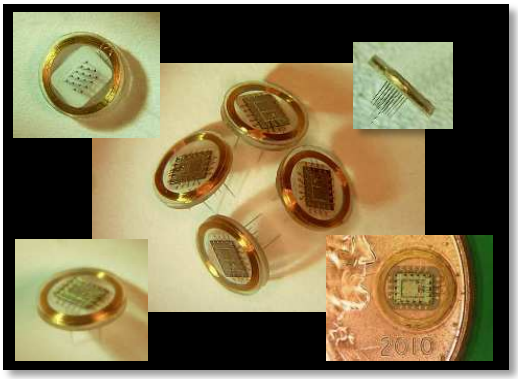

Figure 1 – Microphotographs of the WFMA implantable stimulator. Each WFMA has a unique address. No tethering cables are necessary, reducing the physical stress placed upon the surrounding brain tissue. Size: 5mm diameter x 0.5 mm thick.

the WFMA with about 4cm of separation between the extracorporeal telemetry controller and the WFMA. A summary of the WFMA ASIC performance parameters are shown in Table 1. We plan that up to 40 WFMAs may be implanted on the dorsolateral surface of the human occipital lobe using a high-speed (~1m/sec) insertion method. Although electrodes will be placed in striate and extrastriate cortex, we anticipate obtaining phosphenes as shown in Figure 2. The WFMA devices have been tested in-vivo within rat sciatic nerve [9] and macaque motor cortex [10] as shown in Figure 3a, 3b.

Parameter	*Value*
Wireless Inductive Link	4.8MHz; FSK Modulation; 1.2Mbits/sec
Power Supply	5V regulated; 2.5nF on-chip Capacitance
Electrode Drivers	16 independent cathodic-first; charge balanced;AIROF biasing
Pulse Amplitude	0-64µA in 0.5 µA steps
Pulsewidth	0-450 µs in 30 µs steps
Outward Telemetry	145kHz; PWM; power supply and electrode voltage monitoring
ASIC Fabrication Technology	XFab CX08 die size: 1.8mm x 2.2mm

Table 1 – Operational parameters of the WFMA stimulator.

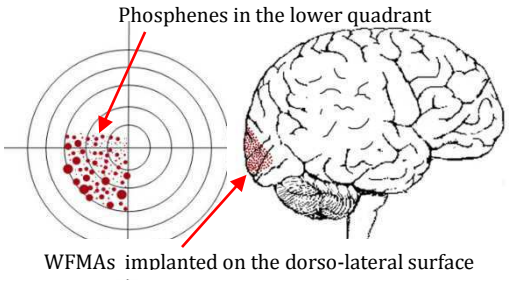

Figure 2. Visual map (left) with various-sized phosphenes and up to 50° eccentricities, for electrodes implanted (right) on the lateral surface area within a radius of 3cm from the occipital pole.

Figure 3a. WFMA devices mounted to silicone cuff used in Rat sciatic nerve implantation. Left: next to nerve, Right: implanted

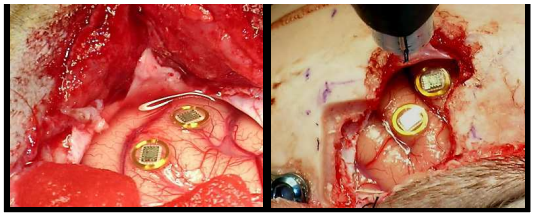

Figure 3b. – WFMAs implanted in two macaques.

Results

The sciatic nerve WFMAs were used to produce distinct movements of the rat digits. Continued operation of the chronically-implanted WFMA was confirmed after 16 months (rats died of natural causes unrelated to the WFMA implantations) with no evidence of electrical malfunction, and stable neural thresholds throughout. Table 2 shows the converging stability of the neural interface formed by the WFMA as evidenced in the measurement of stimulation thresholds vs. time over 142 days. Reverse telemetry allows for the examination of the electrode voltage waveform during constant current stimulation as shown in Figure 4. In the macaques, we measured electrode voltage waveforms from the WFMAs via reverse telemetry at 14 and 43 days (experiment on-going). These data are shown in Table 3.

WFMA Stability of Average µA Thresholds for Peripheral Nerve Implanted WFMAs (32 electrodes)				
Days Implanted			*% Δ per time period*	
Day 1	*Day 72*	*Day 142*	*% Δ D1-D72*	*% Δ D72-D142*
8.4	12.1	13.6	40%	12%

Table 2 – Sciatic nerve stimulation result (142 days).

WFMA Stability for Macaque Cortical Implants Averages for 32 electrodes (2 WFMAs)			
Electrode Parameter	*Days Implanted*		
	in-vitro	Day 16	Day 43
Access Resistance (kΩ)	12.6	61.7	52.4
Polarization (V)	0.92	1.25	0.99

Table 3 – Macaque WFMA telemetry data (43 days)

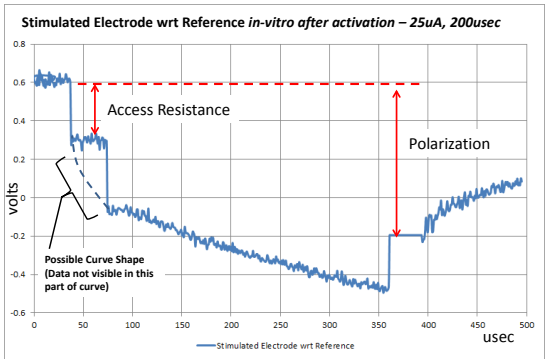

Figure 4. – Representative electrode voltage transient for constant current pulse recorded in vitro.

Discussion

Being able to assess the electrode conditions during stimulation via the reverse telemetry of the voltage waveforms is crucial to being able to evaluate the continued operation of the system in-vivo. The critical parameters of access resistance and polarization can be used to determine the stability of the interface, and observing the expected waveform shape permits the verification that stimulation current is being delivered to the biological tissue.

References

[1] Brindley G. S. & Lewin, W.S., The sensations produced by electrical stimulation of the visual cortex. J. Physiology (Lond), 196, 479-493. 1968.

[2] Bartlett JR, Doty RW, An exploration of the ability of macaques to detect microstimulation of the striate cortex. Acta Neurobiologiae Expermentalis (Warzawa) 40:713-728., 1980

[3] Bak M, Girvin JP, Hambrecht FT, Kufta CV, Loeb GE, Schmidt EM, Visual sensations produced by intracortical microstimulation of the human occipital cortex. Med Bio Eng Comput 28:257-259, 1990.

[4] Schmidt EM, Bak MJ, Hambrecht FT, Kufta CV, O'Rourke DK, Vallabhanath P. Feasibility of a visual prosthesis for the blind based on intracortical microstimulation of the visual cortex. Brain 119:507-22, 1996.

[5] Dobelle WH. Artificial vision for the blind by connecting a television camera to the visual cortex. Asaio J 46: 3-9, 2000.

[6] Troyk, PR; M Bak, J Berg, D Bradley, S Cogan, R Erickson, et al., "A model for intracortical visual prosthesis research," Artificial Organs, vol. 27, pp. 1005-1015, 2003.

[7] Srivastava NR, Troyk PR, Dagnelie G. Detection, eye-hand coordination and virtual mobility performance in simulated vision for a cortical visual prosthesis device. J Neural Eng;6:035008, 2009.

[8] Troyk, PR; DE Detlefsen, GA DeMichele, "A Multifunctional Neural Electrode Stimulation ASIC using NeuroTalk Interface," 28th Conf EMBC pp. 2994-2997, Aug 2006.

[9] S. Bredeson, A. Kanneganti, F. Deku, S. Cogan, M. Romero-Ortega and P. Troyk, "Chronic in-vivo testing of a 16-channel implantable wireless neural stimulator," EMBC, Milan, pp. 1017-1020, 2015.

[10] Troyk, et al, Implantation and Testing of WFMA Stimulators in Macaque, (EMBC), 2016, Orlando, in press

Author's Address

Name: Philip Troyk
Affiliation: Illinois Institute of Technology, Chicago, IL, USA
eMail: troyk@iit.edu
homepage: http://neural.iit.edu/

Miniaturized Implantable Electrical Stimulator for small Animals Preliminary Results

M. Bijak, E. Unger, M. Haller, M. Schmoll, J. Jarvis1, H. Lanmüller

Institute, Medical University of Vienna, Austria

[1]Liverpool John Moores University, UK

Abstract: *According to PubMed roughly 10% of the annually added publications are describing findings from the animal model. Half of these studies are done in mice and rats. It can be assumed that there is a need for implantable electrical stimulators which are flexible, reliable and small enough (~1 cm^3) that even mice can tolerate it and move freely. The MiniVStim 12A is a battery powered implant with an outer diameter of 15 mm and a volume of 1.2 cm^3. It can be preprogrammed according to the experimental protocol and controlled by resetting it with a magnet. It can deliver constant current monophasic pulses up to 2 mA and 1ms pulse width.*

Keywords: *Implantable Electrical Stimulator, Small Animals*

Introduction

In vivo basic research is strongly supported by the animal model. In 2014 roughly 1.2 Mio publications where added to Pubmed [1]. Out of this 580000 publications are related to humans (Search term: 2014[dp] AND "humans"[MeSH Terms]) and 188000 are related to animals (search term: 2014[dp] AND "animals"[MeSH Terms:noexp]). Half of the animal related publications deal with mice and rats, making 9% of all added publications.

Investigations in the field of muscle physiology, muscle conditioning and related require electrical activation of the target tissue [2], [3], resulting in the need of a reliable electrical stimulation system. Moreover, the availability of genetically engineered mice to study specific diseases might lead to an increased interest in reliable and fault proof stimulators, well tolerated by these small animals.

Two major approaches for implantable stimulators for small animals are found [4]. Battery powered implants on the one hand and externally radio frequency (RF) powered implants on the other. More or less the advantages of one system are the disadvantages of the other. Both systems require implantable electronic components which have to be encapsulated in a biocompatible and bio resistive material. Also both systems require electronic circuitry but RF implants can be typically built with fewer components. So battery powered implants require, also related to the chosen battery higher volume. Battery size is crucial. In combination with the stimulation protocol it determines the implants lifetime. A battery powered implant does not require external components; the animal can move freely throughout the entire investigation timespan and must not be separated from the other animals during stimulation time. Vice versa, externally powered implants have "infinite lifetime" since there is no battery which drains but require, when active, a transmission coil close to the implant [5].

This might limit the animal's freedom to move. Alternatively the coil could be integrated in a special cage [6] but this requires separation of the animal from the others while stimulation is active, and only one animal at the time can be stimulated in such a cage. There are also hygienic issues with the coils attached to the cage and with the other required external components like transmitter electronics, power supply and cables.

With these thoughts in mind, a battery powered stimulation implant, as long as it is small enough that even mice can tolerate it (V ~ 1 cm^3) seems to be a good choice in terms of easy handling and reliability.

To fulfill the different requirements of studies the stimulation protocol must be as flexible as possible in terms of programmable stimulation parameters like pulse width, pulse frequency and stimulation intensity. The flexible deliverance of the stimulation dose over the investigation time, like length of activity periods and rest periods or even continuous stimulation are of importance too.

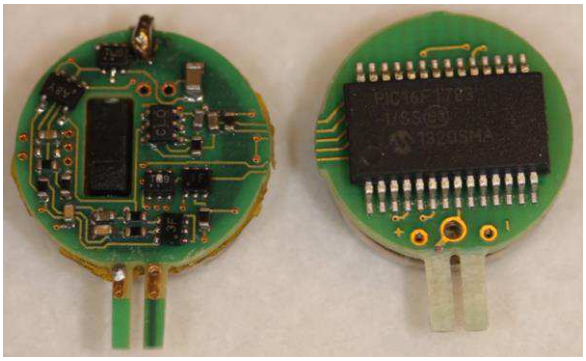

Fig. 1: MiniVStim12A, Microprocessor PIC16F1783 on one side of the circuit board (right), electronic components for power management, output stage and reed switch (left)

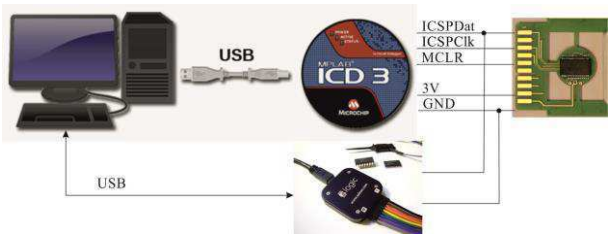

Fig. 2: Setup for calibrating the implantable stimulator Components: PC with Microsoft Visual Studio program for semi-automated testing, Microchip ICD3 flashing device, Salea Logic 8 Logic analyzer

Material and Methods

The MiniVStim12A implantable stimulator (Fig. 1) is built around the Microchip (Chandler, AZ, USA) PIC16F1783 microcontroller. This microcontroller has an integrated 8bit Digital to Analog Converter (DAC), an integrated Operational Amplifier (OPA), an uncalibrated 31 kHz RC Oscillator for low power operation and a calibrated 500 kHz RC Oscillator for higher computational performance. Different sleep modes, quick wake up time, the possibility to switch between the oscillator frequencies programmatically and to turn on and off the peripheral components (DAC, OPA) allow the implementation of energy saving strategies within the firmware.

A transistor output stage takes care of generating monophasic constant current stimulation pulses. A decupling capacitor in series with the electrodes keeps the electrodes DC free.

The duties of an implemented reed switch are twofold. A magnet attached to the implant interrupts power supply and minimizes draining of the battery while the implant is on the shelf. Bringing the magnet for a short time in proximity of the implant resets the microprocessor. This feature is used to advance in a circular manner through pre-programmed stimulation patterns like Sleep → Testing pattern → Study protocol pattern → sleep → … . This kind of implant control is not suitable to advance through a high number of different protocols mainly because there has to be some sort of feedback to confirm the currently active pattern.

The first batch of manufactured implants revealed that from device to device the integrated low power oscillator (31 kHz) scatters in a ±10% range from its nominal value. Since all timing parameters are derived from the oscillator they deviate from their nominal value in the same percentage range. When thinking of the pulse width and stimulation frequency in a physiological manner this deviation might not be very crucial. But when looking at the overall stimulation protocol, for instance 23 h rest and 1 h stimulation the stimulation might occur in a time window of ±2 h away from the expected onset. This might be impractical when animal monitoring during stimulation is desired. Furthermore the stimulation time might shift from day to day.

So we decided to individually calibrate the stimulators during the firmware flashing procedure. (Fig. 2)

The circuit board is connected to the Microchip programming device ICD3 and the Salea (San Francisco, CA, USA) Logic 8 Logic Analyzer. Both manufactures provide a dynamic linked library (dll) that can be accessed from within Microsoft Visual Studio .net development environment. A custom built C# application first flashes a very simple firmware into the microprocessor, just producing a rectangular signal on the ICSPDat pin. The logic analyzer evaluates the frequency of the signal. Out of this the actual RC oscillator frequency can be calculated and further, the related microprocessor register values to achieve the desired stimulation parameters are calculated using a parameter variation and optimization algorithm. The calculated values are inserted in the source code of the firmware; the final individual tailored firmware is compiled and finally flashed via ICD3. All data are linked to the serial number of the implant are stored in a MySQL database.

Results

The fully encapsulated MiniVStim12A (Fig. 3 right) has a diameter of 15 mm, is 7 mm thick and has a volume of 1.2 cm^3. Achievable stimulation parameters are: Monophasic, charge balanced constant current rectangular pulses with amplitudes the range of 0 to 2 mA with 8 bit resolution, pulse width ranging from 32 µs to 820 µs in steps of 32 µs and stimulation frequency range from 0.1-200 Hz.

Lifetime strongly depends on the chosen stimulation paradigm. With a CR1220 (35mAh) battery (Fig. 3 left) the lifetime is 200 days if every hour a 1s lasting stimulation train is delivered and goes down to 10 days if continuous 20 Hz stimulation is applied.

The calibration procedure improved significantly the overall accuracy of the time dependent stimulation parameters. All implants from the initial batch with a ±10% deviation from the 31 kHz nominal oscillator frequency stayed finally in a ±1% range. The only exception is the pulse width. It is directly derived from the oscillator frequency and cannot be optimized for small pulse width.

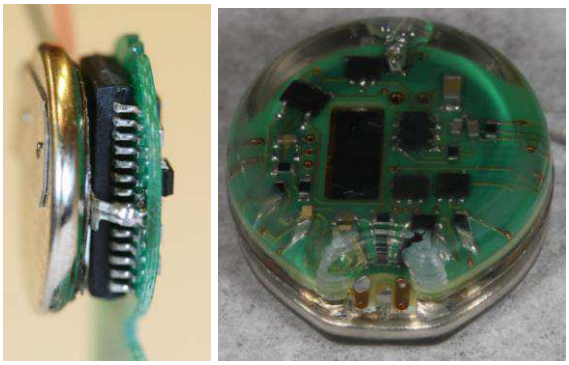

Fig. 3: Circuit board with mounted battery (left)
Encapsulated battery and electronics (right)

Conclusions

A small battery powered implantable stimulator that even mice can tolerate was developed. The stimulator receives during the manufacturing process an individually tailored firmware according to the study protocol. Oscillator calibration during the manufacturing process brings time dependent stimulation parameter accuracy to a ±1% level. Only the pulse width stays linearly related to the oscillator frequency. Basic pattern control by magnet kept the handling simple and was well accepted by the users.

Acknowledgement

This work is partially supported by MEDEL http://www.medel.com/

References

[1] "Home - PubMed - NCBI." [Online]. Available: http://www.ncbi.nlm.nih.gov/pubmed. [Accessed: 07-Mar-2016]

[2] J. C. Jarvis, T. Mokrusch, M. M. Kwende, H. Sutherland, and S. Salmons, "Fast-to-slow transformation in stimulated rat muscle," *Muscle Nerve*, vol. 19, no. 11, pp. 1469–1475, Nov. 1996.

[3] Z. Ashley, H. Sutherland, M. F. Russold, H. Lanmüller, W. Mayr, J. C. Jarvis, and S. Salmons, "Therapeutic stimulation of denervated muscles: the influence of pattern," *Muscle Nerve*, vol. 38, no. 1, pp. 875–886, Jul. 2008.

[4] J. I. Laughner, S. B. Marrus, E. R. Zellmer, C. J. Weinheimer, M. R. MacEwan, S. X. Cui, J. M. Nerbonne, and I. R. Efimov, "A fully implantable pacemaker for the mouse: from battery to wireless power," *PloS One*, vol. 8, no. 10, p. e76291, 2013.

[5] G. E. Loeb, F. J. R. Richmond, and L. L. Baker, "The BION devices: injectable interfaces with peripheral nerves and muscles," *Neurosurg. Focus*, vol. 20, no. 5, p. E2, 2006.

[6] R. E. Millard and R. K. Shepherd, "A fully implantable stimulator for use in small laboratory animals," *J. Neurosci. Methods*, vol. 166, no. 2, pp. 168–177, Nov. 2007.

Author's Address

Manfred Bijak (manfred.bijak@meduniwien.ac.at), Center for Medical Physics and Biomedical Engineering. Medical University of Vienna, Währinger Gürtel 18-20/4L, A-1090 Vienna, Austria

Implantable electrical stimulator optimized for animal studies

Lanmüller H[1], Bijak M[1], Unger E[1], Haller M[1], Schmoll M[1], and Jarvis J[2]

[1] Center of Medical Physics and Biomedical Engineering, Medical University of Vienna, Austria
[2] School of Sport and Exercise Science, Liverpool John Moores University, United Kingdom

Abstract: *Implantable pulse generators (IPG) are used in animal studies to investigate neuromuscular changes related to various trainings conditions in healthy and diseased organisms, at different ages. Compared to mechanical training equipment like treadmill or running wheel, the use of an IPG has the advantage, that intensity and duration of neuromuscular excitation can be precisely determined for days or weeks. The success rate of a study increases, if stress factors that influence the animal are kept as low as possible, failure rate of the technical equipment is minimised and the equipment handling is simplified. Beside technical requirements, these facts have been the main criteria for the development of the "MiniVstim" IPGs.*
MiniVstim's `s are programmed via a bidirectional RF link. Therefore the implanted animal is placed on a programming tablet and the connection to the implant is established. Additionally, the programming tablet connects via Bluetooth to an Android based computer offering a comfortable graphical user interface for setting up the entire stimulation protocol.. Amplitude, burst duration and frequency of single bursts can be freely defined and combined to stimulation blocks. These stimulation blocks complemented with pause blocks are summarized to a trainings session, which are repeated depending on the defined values, maybe once a day, twice a day or every other day. Once programmed, the IPG activates the trainings sessions automatically. The IPG is powered by a single Lithium primary. Weight and volume 1,2cm^3 and 2,3g for devices intended for the use in mice and 5,1cm^3 and 9,6g when used in rats.
The automated activation of the trainings session decreases the stress for the animals. The animals can remain in their cages without any additional intervention. Moreover, this decreases the work load of the care takers. The programmer was designed to operate completely wireless and without mechanical switches; two measures to reduce technical failures. Complex training patterns can be created making by the system flexible and easy adoptable to the study protocol . However, the possibility to choose from a huge range parameters increases the risk of handling failures.. In order to minimize those errors various simplified input masks are implemented. The desired trainings patterns are setup from experts in an unrestricted mask and pre-tested. The end user just downloads these patterns and uses a "light weighted" user interface version during the study. Only relevant parameters to fit the pattern to the individual animal like the stimulation amplitude are accessible. Actual and previous versions of the MiniVstim stimulation system have been successfully used in four research studies up to now, each application helped to further improve the overall system usability.

Keywords: *Implantable pulse generator, animal study,*

Author's Address

Hermann Lanmüller
Center of Medical Physics and Biomedical Engineering
Hermann.Lanmueller@meduniwien.ac.at
http://www.meduniwien.ac.at/zbmtp/

Modular multi-channel real-time biosignal and sensor interface for movement control applications

Christoph Kast[1,3], Weerayot Aramphianlert[1,3], Matthias Krenn[1,2], Christian Hofer[3,4], Oskar C. Aszmann[3], Winfried Mayr[1,3]

[1]Center for Medical Physics and Biomedical Engineering, Medical University of Vienna, Austria
[2]Institute of Electrodynamics, Microwave and Circuit Engineering, Vienna University of Technology, Austria
[3]Christian Doppler Laboratory for Restoration of Extremity Function, Division of Plastic and Reconstructive Surgery, Department of Surgery, Medical University of Vienna, Austria
[4]Otto Bock Healthcare Products GmbH, Vienna, Austria

Abstract: *An active prosthetic arm as well as an FES-controlled paralyzed upper extremity need reliable control inputs for accurate and safe positioning in the three-dimensional space. Here, we present a control concept based on multichannel electromyography (EMG) and inertia sensors for positioning feedback. The modular hardware design is based on an eight-channel interface-module, a motion capture module, a synchronization module and an electrical stimulation module or an actuator control module. Recorded data are analyzed on a connected personal computer that allows to perform complex decisions and control algorithms fast enough for real-time control of stimulator or prosthesis actuators.*

The recording system is capable of combining up to eight acquisition modules, each with eight bipolar inputs, and data transfer using the USB-interface. Important for control applications as well as experimental multi-channel recording, is reliable synchronization of all acquired signals. Therefore, the modules are synchronized by an external separated clock module, which provides the time-base for the microcontrollers and generates repetitive trigger pulses. The developed system ensures a synchronization error smaller than 10 µs within 10 s. The analog front-end is based on the ADS1299 (Texas Instruments Inc., Dallas, TX, USA). In addition to EMG control inputs, the device is capable of acquiring sensor and other bioelectrical signals like electrooculogram (EOG) or electroencephalogram (EEG) the latter e.g. for use in a brain-computer interface.

The advantage of the system is a flexible design which supports real-time control of mechanical and neural prostheses. Additionally, each module is directly connected to a computer, which reduces the front-end complexity and enables simple integration of various module combinations.

Keywords: *prosthesis, neuroprosthesis, control, electromyography, bioelectric signal, FES, ADS1299;*

Introduction

Control of a prosthetic arm as well as of an upper limb neuroprosthesis needs reliable control sources, accurate tracing of the joint positions and sensory feedback is desirable. Here, we present a modular concept, which integrates a control system based on electromyography (EMG), inertia sensors for position feedback and functional electrical stimulation (FES) to provide sensory feedback or control neuromuscular functions, respectively an actuator control interface. In biomedical applications, EMG recordings are widely used [1] and there are different concepts for data acquisition systems for EMG signal detection [2], [3]. However, most of them do not offer the possibility to record as much as 64 channels or lack synchronization.

One main benefit of multiple channels, EMG electrode arrays and multi-channel data acquisition systems is that it can replace the need of invasive needle electrode techniques and calculate single motor unit activities from multiple projections.in certain cases [4]. Another useful application is the use of array based multi-channel EMG recordings to identify optimal electrode positions without multiple repositioning of skin attached electrodes by applying quantitative selection algorithms [5].

A further important application is the use of EMG for control of prostheses and neuroprostheses [6]; in particular there have been significant improvements in the development and control of prosthetic arms [7], [8] in the recent years. However, sensory feedback to the amputee or paralyzed is still used rather rarely. This negatively influences and limits the control performance of prostheses, because proprioceptive and tactile sensory feedback are important integral components of a physiological body image, as basis of movement control, and interaction with objects [9]. E.g. Chai et al. [10] used transcutaneous electrical nerve stimulation as a tactile feedback modality and demonstrated that it is possible to evoke haptic perception to some extend.

Our hardware design is based on four modules: eight-channel recording module, motion capture module, electrical stimulation module and synchronization module. The system is capable of combining up to eight acquisition modules via universal serial bus (USB) data link. In addition to EMG measurements, the device is capable of recording various sensor or bio-electrical signals like electroencephalogram (EEG) or electrooculogram (EOG). A computer generates the control signals based on the recorded biosignals which activate either actuators of a

mechanical prosthesis or stimulator modules. Sensors on the arm and finger tips can provide signals, which again are processed and used for sensory feedback in the form of electrical stimulation to appropriate skin surface areas.

Finally, the system should get comfortably wearable. Therefore, it has to be lightweight, compact, and battery-powered. For real-time signal analysis, the system requires high computing capacity which will be solved by integrating a compact single-board computer.

In this paper we present the exemplary configuration of the system for control of a bionic arm prosthesis prototype.

Implementation of the system

We designed a modular system for data acquisition (DAQ) which integrates recordings of EMG and motion signals. The recorded data should be processed using customized algorithms and support real-time control of an upper extremity prosthesis.

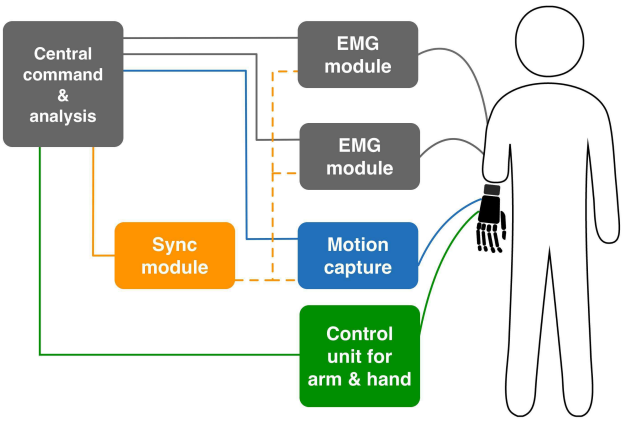

Fig. 1. This system configuration contains recording units for electromyography (EMG) and motion capture. These units are synchronized with a separate module (Sync module). A personal computer (PC) or a Raspberry Pi 3 analyzes the input data and controls the prosthetic arm.

The prosthesis is a custom-built prototype developed at the Center for Medical Physics and Biomedical Engineering, Medical University of Vienna. Therefore, we designed various modules interconnected with the USB-interface that allows simple plug and play solutions. Reliable synchronization of all acquired signals is necessary for control applications as well as for data analysis. The main drawback of comparable commercial devices is the limited access to the raw data. Furthermore, simultaneous recordings of different sensor signals are usually more difficult to handle.
The designed system consists of one or more EMG modules (usbEMG) that are connected to the participant via surface electrodes to acquire the input control signals. The USB port powers the modules and transmits the measured data to a personal computer (PC) or a single-board computer (Raspberry Pi 3, Raspberry Pi Foundation, Caldecote, United Kingdom). The synchronization module (usbCLK) is also directly connected to the computer, to set up the clock rate and trigger outputs. Additionally, the computer provides the power supply for the module.

The module for motion capture is currently in the developing phase. We plan to use 9-axis sensors that combine gyroscope, accelerometer, and magnetometer (MPU-9250, InvenSense Inc., San Jose CA, USA). With multiple sensors mounted on the prosthesis it will be possible to detect its exact position in space. The main purpose will be to generate a feedback signal for highly accurate multi-joint movements of the prosthetic arm.

In addition, we plan to integrate a stimulation module to generate cutaneous input for sensory feedback. FES is not only suitable to reduce phantom pain or stump pain caused by amputation [13], [14]. It is also known that electrical stimulation of afferent nerves using implanted electrodes can generate sensations of touch, joint movement, and position in the missing phantom limbs of amputees [13], [14]. Using different stimulation patterns, it is even possible to convey various sensory feelings [10].
The external neural input should improve the control performance of the prosthesis by providing sensory feedback.

Hardware Design

The usbEMG module (Fig. 2) is based on an ADS1299 analog-to-digital converter (Texas Instruments Inc., Dallas, TX, USA) and is applicable for various electrical biosignals. The ADS1299 is capable of simultaneous sampling of eight channels with an overall sampling rate of 16 000 samples per second (SPS) and a resolution of 24-bits. The amplifier gain is programmable up to 24. The microcontroller (PIC32MX250F128D, Microchip Technology Inc., Chandler AZ, USA) is used for controlling the data stream. The clock frequency is up to 50 MHz, which allows a high recording rate. The integrated 64 KB memory is used to buffer the data which is received from the ADS1299. The microcontroller provides a USB 2.0 compliant full speed interface.

Because of the fact, that the device will be used in medical applications an electrical isolation barrier is mandatory. An ADuM4160 (Analog Devices Inc., Norwood MA, USA), which is suitable for this purpose, is implemented and offers 5 kV isolation.

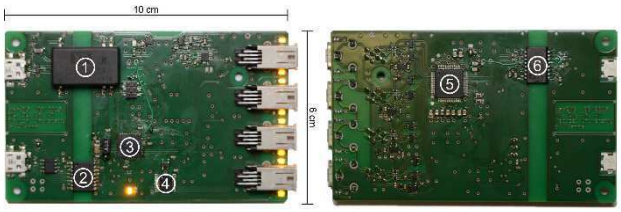

Fig. 2. Eight channel EMG module (usbEMG). 1 – isolated DC/DC converter; 2 – digital isolator for clock and trigger signals; 3 –microcontroller (PIC32MX250F128D); 4 – LED driver; 5 – analog frontend (ADS1299); 6 – USB port isolator.

The usbEMG module can be used as a standalone device with eight bipolar recording channels or integrated in a cascaded system of multiple modules interconnected by an additional USB cable for receiving clock trigger impulses from the synchronization module.

To synchronize data from up to 64 inputs, another USB module (usbCLK) was developed that acts as a clock distributor, which provides the time base for the microcontrollers and delivers trigger signals to reset the timestamp of the data packets. The developed system ensures a synchronization error smaller than 10 µs within 10 s for simultaneous signal recording. A microcontroller generates a reliable clock source that is distributed to up to eight different modules. The low-voltage differential signaling (LVDS) standard was used to distribute the high frequency clock signal to all peripheral modules.

The central element of the system is a computer (PC or Raspberry Pi 3), which is used to process the data and to generate control signals for the actuator control unit of the prosthesis.

The prosthesis control unit is based on a Fubarino™ Mini (Schmalz Haus LLC and Fubar Labs). The board is Arduino API compatible, which uses a PIC32MX microcontroller. It controls the motors and reads the encoder values. Commands are processed and corresponding pulse-width modulated (PWM) signals are sent to servo motor controllers (Maxon motor – ESCON Module 50/5, Maxon motor, Sachseln, Switzerland) that drive the prosthesis.

Firmware

The firmware of the PIC32MX-microcontroller is programmed with MPLABX an IDE (Microchip Technology Inc.) which includes an assembler, software simulator, and a debugger. The MPLAB Harmony Integrated Software Framework (Microchip Technology Inc.) offers a flexible, abstracted, fully integrated firmware development platform for PIC32 microcontrollers.

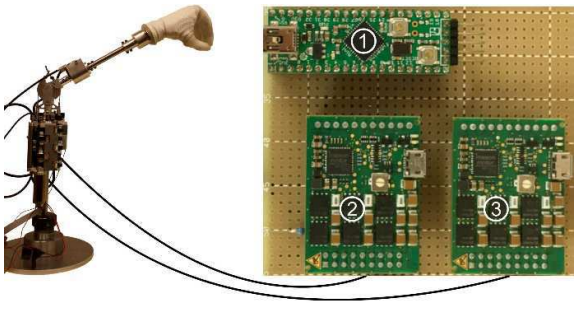

Fig. 3 Actuator control unit. 1 – Fubarino™; 2,3 – servo controller (ESCON module 50/5)

The communication between ADS1299 and the microcontroller is realized via serial peripheral interface (SPI). It offers data rates up to 25 Mbps. To ensure fast and safe data transfer the direct memory access (DMA) module is used to reduce CPU workload.

Using all eight channels and having a sampling rate of 8 kSPS the ADS1299 is producing 216 kB/s, which is within the USB bulk transfer limit of about 1245 kB/s.
It is not possible to transfer the data in real time via USB, therefore, a buffer is needed. Ideally, this is realized with a ring buffer, to ensure data consistency. The ADS1299 writes data in blocks of 27 Bytes but the USB is reading 64 Bytes at once. Therefore, the smallest possible ring buffer size is the least common multiple which is in that case 1728 Bytes. To get the best results, the ring buffer was chosen to be as big as possible. The PIC32MX offers 64 kB RAM, with the space occupied by the program itself, the resulting ring buffer size is around 55 kBytes.

Software

A C# program was developed to process the data packets. It allows digital filtering and visualizes the recorded signals per channel. The software detects all connected modules and offers the possibility to trace every channel per device. It is also possible to set the configuration of each module, i.e. sampling rate, gain, and other registers of the ADS1299. Furthermore, the data can be recorded and saved in the common Hierarchical Data Format (HDF5), which is particularly useful for managing large amounts of data. It is supported by many commercial and non-commercial software platforms including C#, Java, MATLAB. Data compression is necessary because of a large amount of data. Eight channels sampled with 8 kSPS generate about 13 MB data per minute. Using eight modules, this would produce more than 100 MB per minute. So structured data and especially compression are essential.

Control signal

In a preliminary evaluation, we recorded an input signal of the biceps brachii in a human subject. Therefore, an on/off control signal was generated using the EMG signal. The threshold of activating the actuator was set to 2 mV. Figure 5 shows the data stream of the myoelectric signal during a contraction and the corresponding on/off signal for the actuator control unit.

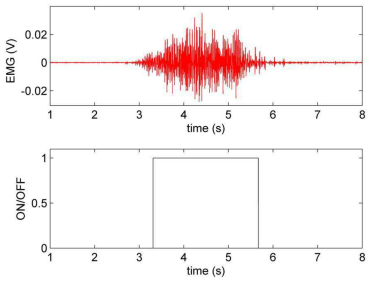

Fig. 4 Exemplary control input based on a myoelectric signal during a biceps brachii contraction. The EMG signal is filtered in a range form 20 to 300 Hz. Sampling rate: 8 kSPS; Gain: 6; Resolution 24-bit

The surface EMG signal is a stochastic signal that displays the overall activity of a muscle and its exertion is primarily related to the amplitude of the signal. By calculating the envelope of the EMG signal, the muscle activity intensity can be measured. One of the most widely used methods is the root mean square (RMS) [15].
Using this envelope signal, it is not only possible to calculate an on/off signal but to control the speed of the actuators based on the intensity of the muscle contraction.

Discussion

The advantage of the system is a flexible design which is essential for advanced control of a prosthetic arm, but keeps it also suitable for other movement rehabilitation applications, as reactivation of a paralyzed arm by FES. The modules are compact enough to be carried e.g. on a belt as a light weight and small experimental recording unit. We intend to use the system wirelessly, so power consumption is essential. The estimated supply current of the acquisition system is below 1 A. Because we use the USB standard for all our devices, it is possible to use commercially available power-banks. By using only one core of the Raspberry Pi 3 the power consumption halves [16].
The presented front-end device, ADS1299, is a versatile component for EMG acquisition. The small size of the chip, the low supply voltage, and low power consumption make it especially suitable for small, battery-powered, portable solutions. The flexible design is of great importance for the intended primary application for advanced real-time control of a prosthetic arm. The modules are compact enough to be carried for mobile use.

Acknowledgement

Collaboration with the Christian Doppler Laboratory for Bionic Reconstruction sponsored by the Christian Doppler Gesellschaft, Austria.

References

[1] M. B. I. Reaz, M. S. Hussain, and F. Mohd-Yasin, “Techniques of EMG signal analysis: detection, processing, classification and applications.,” *Biol. Proced. Online*, vol. 8, no. 1, p. 163, 2006.

[2] S. Boukhenous, N. Meziane, M. Attari, and Y. Remram, “A USB based data acquisition system for EMG signal recording,” *2013 8th Int. Work. Syst. Signal Process. Their Appl. WoSSPA 2013*, pp. 230–232, 2013.

[3] A. Ruvalcaba, A. Altamirano, C. Toledo, R. Muñoz, A. Vera, and L. Leija, “Multichannel EMG acquisition system for arm and forearm signal detection,” *Conf. Rec. - IEEE Instrum. Meas. Technol. Conf.*, pp. 1075–1078, 2014.

[4] B. U. Kleine, J. H. Blok, R. Oostenveld, P. Praamstra, and D. F. Stegeman, “Magnetic stimulation-induced modulations of motor unit firings extracted from multi-channel surface EMG,” *Muscle and Nerve*, vol. 23, no. 7, pp. 1005–1015, 2000.

[5] D. Farina, P. Madeleine, T. Graven-Nielsen, R. Merletti, and L. Arendt-Nielsen, “Standardising surface electromyogram recordings for assessment of activity and fatigue in the human upper trapezius muscle,” *Eur. J. Appl. Physiol.*, vol. 86, no. 6, pp. 469–478, 2002.

[6] S. Morita, T. Kondo, and K. Ito, “Estimation of forearm movement from EMG signal and application to prosthetic hand control,” in *IEEE International Conference on Robotics and Automation*, 2001, vol. 4, pp. 3692–3697.

[7] C. Cipriani, F. Zaccone, S. Micera, and M. C. Carrozza, “On the shared control of an EMG-controlled prosthetic hand: Analysis of user-prosthesis interaction,” *IEEE Trans. Robot.*, vol. 24, no. 1, pp. 170–184, 2008.

[8] M. Asghari Oskoei and H. Hu, “Myoelectric control systems-A survey,” *Biomed. Signal Process. Control*, vol. 2, no. 4, pp. 275–294, 2007.

[9] E. P. Gardner, “Touch,” *Encycl. Life Sci.*, pp. 1–12, 2010.

[10] G. Chai, X. Sui, S. Li, L. He, and N. Lan, “Characterization of evoked tactile sensation in forearm amputees with transcutaneous electrical nerve stimulation,” *J. Neural Eng.*, vol. 12, no. 6, p. 066002, 2015.

[11] M. R. Mulvey, A.-M. Bagnall, M. I. Johnson, and P. R. Marchant, “Transcutaneous electrical nerve stimulation (TENS) for phantom pain and stump pain following amputation in adults.,” *Cochrane Database Syst. Rev.*, no. 5, p. CD007264, 2010.

[12] K. a Sluka and D. Walsh, “Transcutaneous electrical nerve stimulation: basic science mechanisms and clinical effectiveness.,” *J. Pain*, vol. 4, no. 3, pp. 109–121, 2003.

[13] M. R. Mulvey, H. J. Fawkner, H. Radford, and M. I. Johnson, “The use of transcutaneous electrical nerve stimulation (TENS) to aid perceptual embodiment of prosthetic limbs,” *Med. Hypotheses*, vol. 72, no. 2, pp. 140–142, 2009.

[14] R. R. Riso, “Strategies for providing upper extremity amputees with tactile and hand position feedback--moving closer to the bionic arm.,” *Technol. Health Care*, vol. 7, no. 6, pp. 401–409, 1999.

[15] M. Polisiero, P. Bifulco, A. Liccardo, M. Cesarelli, M. Romano, G. D. Gargiulo, A. L. McEwan, and M. D’Apuzzo, “Design and assessment of a low-cost, electromyographically controlled, prosthetic hand,” *Med. Devices Evid. Res.*, vol. 6, no. 1, pp. 97–104, 2013.

[16] S. Macdonald, “Raspberry Pi 3 - First Look,” *Piratical Tales From Pimoroni*, 2016. .

Author’s Address

Christoph Kast
Center for Medical Physics and Biomedical Engineering, Medical University of Vienna, Vienna, Austria
christoph.kast@meduniwien.ac.at

Frequency characteristics of power coils under practical FMS conditions

M. Nalbach[1], J. Vargas Luna[2], M. Krenn[1], H. Gondola[1], W. Mayr[2]

[1]Technical University of Vienna, Austria
[2]Medical University of Vienna, Austria

Abstract: *Over the last years the use of Functional Magnetic Stimulation (FMS) has importantly grown, due to some advantages over conventional electrical stimulation. Unlike electrical stimulation, FMS uses a magnetic field, which bypasses the skin's impedance, to induce depolarization of deeper tissues and subsequently evoke action potentials on targeted nerve fibers.*
These magnetic fields are generated by coils, that are designed for stimulation of specific structures. While the main consideration of coil design is the shape of the magnetic field, it is also important to consider the electric properties, which significantly change with frequency and with the presence of conductive metals within the magnetic field—implants and coil cores—which can heat up.In this work we compare the electrical characteristics of three different coils, one with a laminated magnetic core and two air coils. Each coil was characterized by Bode plots in the range of 10Hz to 1.5MHz, whilst there either was no metal or a CoCr hip implant upon the coil's center. The results show that the usage of a laminated magnetic core significantly increases the parasitic ohmic resistance with frequency and overcomes the wire's resistance. In a similar way the presence of the CoCr hip implant near the coil's center increases the parasitic ohmic resistance and resonance frequency. This means that coil designs must consider the presence of metallic parts, e.g.laminated magnetic cores and implants, because they may lead to an important heating process. Moreover the shift of the resonance frequency is a suitable parameter to detect metals near the magnetic field.

Keywords: *Connectors, cables, electrodes, Functional Magnetic Stimulation (FMS), Safety*

Magnetic field induced heating of metal implants during FMS on the example of an artificial hip joint

Gondola H[1,2], Nalbach M.[1,2], Vargas Luna J.L.[2], Mayr W[2]

[1] Vienna University of Technology, Austria

[2] Center for Medical Physics and Biomedical Engineering, Medical University of Vienna, Austria

Abstract: *Magnetic stimulation can be defined as a technology that applies a time varying magnetic field applied to produce useful body function. [1] Despite many advantages such as stimulation of deep muscle structures, sensible comfort, no direct skin contact, there is one main safety concern relating to performing functional magnetic stimulation (FMS) on a patient who has a metal implant inside his/her body, namely: there is a potential of heating of metal objects by induced eddy currents that can lead to several unwanted and dangerous side effects in the body. [2] The aim of this study was to monitor the temperature dependence of the hip prostheses during the functional magnetic stimulation. The measurements were carried out on prosthesis with different geometry and material that are in commercial use in order to get a clearer picture about this issue.*

Keywords: *FMS, hip joint prosthesis, temperature measurements*

Introduction

In magnetic stimulation, a time-varying magnetic field is created by a short electric current I(t) pulse, that is driven through a stimulation coil. The strong magnetic field pulse induces an electric field (E) in the underlying biological tissue. The high magnetic field strength is achieved by discharging a capacitor charge of more than one kilovolts through the application coil. The resulting current pulse, with the peak current in the coil up to kiloampers, is usually one decaying sine wave cycle. The strength of E is proportional to dI(t)/d(t) and decrease significantly with the distance from the coil. This field causes ionic current flow in the intra- and extracellular spaces, depolarizing or hyperpolarizing the cell membranes. The efficiency of the stimulation has a dependence on the duration of the stimulus, because the cell membrane behaves as a leaky integrator. [3]

Heating problem

One possible safety hazard during FMS is the heating of the metal objects by the induction of eddy currents. Eddy currents are electrical currents induced by changing magnetic field.

These eddy currents cause Joule heating of the metal object. This heating is particularly severe if a train of stimulating pulses is delivered at a higher frequencies (in practice up to 100 Hz), so that the metal object does not have time to cool down between pulses. [2]

Material and Methods

In this study in vitro measurements were carried out with a Tesla functional magnetic stimulator (Iskra Medical Ltd., Slovenia). The implant component was placed on a wooden desk. Before each magnetic stimulation the initial temperature of the implant was measured with a thermometer (Fluke 51, Fluke Corp,Walled Lake, USA) . The magnetic coil was fixed axially above the prostheses with a constant hight of 6.4 cm. In order to facilitate the reproducibility of the temperature measurements, there was always the same spot on the implant surface measured. After the optimal coil placement was established, each measurement was carried out under constant conditions but with varied stimulation parameters (frequency, intensity of the stimulation). During the measurements the temperature changes under magnetic stimulation were monitored. The goal was to measure the time that is needed to induce a six degree temperature difference on the implant surface. The increase was continuously monitored between the initial and the maximum temperature during the active mode of the magnetic stimulation. The duration of the measurements was set to 15 minutes in the stimulating device, but in case the desired change of the temperature was reached earlier, the measurement was stopped. In every measurement the ON and the OFF time of the magnetic stimulation was 4 seconds. The experiments were performed with selective osteosynthesis and joint implants as provided by B.Braun Austria (B. Braun Meissungen AG, Germany).

Results

Stem measurements

The first part of the experiment was carried out with three different prostheses stems, the two with the product

numbers of 1-4627G and NH011 were made of titanium and covered with a dioxide layer, and the one with the product number of NA462 was made of uncoated titanium. The time to reach the 6°C temperature increase varied between 2-8 minutes.
Although the geomerties of the implants were similar, the measurements showed very different behaviours. At the implant NA462, the measurement duration was 1 minute at 100% at 35 Hz, while in a repetition with an intensity of 90%, it lasted 15 minutes to reach the same temperature increase. Finally at 80% intensity the plus 6 degrees were achived after only 15 seconds. Big differences occured also in the tests at the frequency of 30 Hz: At 100% intensity the heating time was 15 minutes, while at 80% only 40 seconds.

Nail measurements

The measurements were carried out with titanium and titanium alloy nails. The protheses with the product numbers 51485922 and 427.376 were made of titanium alloy and the one with the number of 12-440L was made of pure titanium. There was a significant difference between the implant geomerties, the lenght of the 472.376 implant was only half of that of the others.
The implant number 51485922 showed a measurement curve at 35 Hz that is independent of the change of intensity within the range 80 to 100 Hz, the same was observed for implant 472.376 at 25 Hz.

Head measurements

The temperature characteristics of two head parts (ball shaped) were investigated. The one with the product number NK544K was made of a CoCrMo-stainless steel alloy, the product number of 249AJ was made of oxyde ceramics (Al_2O_3/ZiO_2). Both implants had similar geomertries. The measurements at 25 Hz and 30 Hz showed, that the heating process occured faster at the metal implant, which can be explained with the fact, that metal has generally higher thermal conductivity, than ceramics. Furthermore, it can be seen, that the implant showed less cool down during the OFF time of stimulation, than observed in stem or nail parts. It was also obvious, that the cool down process at the ceramics prothesis was slower than in similar metal parts. At 35 Hz with the intensity of 80% the temperature difference between ON time and OFF time of stimulation was less than 1°C.

Cup measurements

The measurements were carried out on three different joint cups, two with the product numbers 32-1244L+4 and 51025853 were made of titanium and one with the product number NA882 was made of titanium alloy. The duration of the heating processes was quite similar in each case, the protheses components needed 1-4 minutes to reach a temperature increase of 6° C. In only one case was the heating time appeared significantly longer, taking 12 minutes to heat up the implant.

Table 1: Stem measurements at 35 Hz

Product number	**Intensity (%)**	**T_{max} (°C)**	**T_{min}(°C)**	**Time**
1-4627G	100	30.4	23.4	45sec
	90	29.3	24.4	3min50sec
	80	28.4	24.1	6min20sec
NA462	100	30.4	22.7	1min
	90	27.6	25.2	15min
	80	29	26.5	15sec
NH011	100	31	23	14sec
	90	29.4	24.1	2min25sec
	80	29	24.9	12min45sec

Table 2: Nail measurements at 35 Hz

Product number	**Intensity (%)**	**T_{max} (°C)**	**T_{min}(°C)**	**Time**
51485922	100	29.1	22.9	1min30sec
	90	30	28.6	1min50sec
	80	31	26.8	1min30sec
12-440L	100	31	22.9	40sec
	90	29.8	24.2	1min
	80	29.5	25.4	9min10sec
472.376	100	29.5	23.2	1min50sec
	90	29.3	25.1	6min40sec
	80	28.8	25	15min

Table 3: Head measurements at 35 Hz

Product number	Intensity (%)	T_{max} (°C)	T_{min}(°C)	Time
NK544K	100	31	25.8	2min40sec
	90	30	28	1min40sec
	80	30.6	30	2min
249AJ	100	29.7	26	40sec
	90	29.4	27.8	1min
	80	30	29.5	2min

Table 4: Cup measurements at 35 Hz

Product number	Intensity (%)	T_{max} (°C)	T_{min}(°C)	Time
NA822	100	28.6	25.1	2min
	90	29.5	27.6	1min50sec
	80	29.2	27.3	4min40sec
32-1244L+4	100	29.2	24	6min50sec
	90	29.4	27.8	1min
	80	29.9	24.8	12min40sec
51025853	100	30	24.7	20sec
	90	30	28.6	1min50sec
	80	31	26.8	1min50sec

Discussion

The measurements were carried out on eleven different hip joint protheses and osteosynthesis parts in order to survey a first order of magnitude of induced temperature changes in medical implants during magnetic stimulation. The experiments were carried out with different frequencies, intensities and implant possitions in relation to the application coil for magnetic stimulation. Despite all limitations of the set-up that the risk of heat induction in medical implants by FMS cannot be neglected as a potential serious treatment complication. A temperature rise of 6° C at implant surfaces, which may already result in protein denaturation in living tissue, was observed in every measurement in significantly lower time periods than usual application imes of 20 to 30 minutes.

Conclusions

These preliminary observations need to be verified in a more realistic in vitro or in vivo model, where the implant components are embedded in artificial are living tissue, to support guidelines for save application of this novel and growingly used therapy option.

Acknowledgments

I would like to kindly thank Prof. Dr. Winfried Mayr for providing me place at his research group and for the great supervision.

References

[1] Spinal cord medicine principles and practice, V. W. Lin, ISBN 1-888799-61-7, 2010

[2] Bradley J. Roth, Alvaro Pascual-Leone, Leonardo G. Cohen and Mark Hallett, 1991, Electroencephalography and clinical Neurophysiology, 85(1990) 116-123

[3] Jarmo Ruohonen, Paolo Ravazzani, Ferdinando Grandori, Bioelectrochemistry and Bioenergetics 47 213-219, 1998

Author's Address

Hajnalka Gondola
Vienna University of Technology
gondolahajni@gmail.com

Authors Index

DR. SCHUHFRIED
MEDIZINTECHNIK GMBH
a-1090 wien . van swieten-gasse 10
fon: (+43-1)405 42 06 . fax: (+43-1)405 44 64
info@schuhfriedmed.at . www.schuhfriedmed.at

Stimulette den2x

High performance 2-channel electrotherapy stimulator; specialized to be used for activating flaccid paralyzed denervated muscles.

Functional Electrical Stimulation (FES) of denervated muscles - a novel therapeutic option after peripheral nerve lesion. The Stimulette den2x represents a major breakthrough in FES.

Stimulette den2x - the RISE stimulator manufactured by Schuhfried.

The RISE-Project

The EU Project RISE demonstrates that home based FES of denervated muscles is a secure and effective home treatment.

Benefits of stimulating denervated muscles:

- Recovery of muscle mass and fibre size
- Recovery of tetanic contractility
- Restoration of muscle fibre structure
- Long-lasting, increased perfusion
- Better skin condition
- Reduced risk of pressure sores

If standing upright is accomplished:

- Improved cardiovascular fitness
- Unloading of seating surface

The conclusion of the RISE project was, that there is an high need for an electrotherapy device for home based FES.

Our Stimulette den2x is the first device, which delivers the needed power (up to 300mA per channel) and technical requirements to fullfil these steps.

For more information please don't hesitate to get in contact with us:
Phone: +43 1 405 42 06 or Mail: info@schuhfriedmed.at

PELVIPOWER

1. Bewegliche Lichthaube mit integrierter Lichttherapie
2. Verstellbare Rückenlehne
3. Therapiebedieneinheit
4. Chipkarteneinheit
5. Integrierter Sauerstoffkonzentrator
6. Verstellbarer Wirkfeldapplikator
7. Verstellbare Fussanlage

IHR ANSPRECHPARTNER:

PONTEMED INTERNATIONAL

ÖSTERREICH

PONTEMED GMBH
BIBERSTRASSE 3
1010 - WIEN
+43 660 685 70 72
austria@pontemed.com

SCHWEIZ:

PONTEMED AG
HAUPTSTRASSE 17
9053 - TEUFEN
+41 71 333 60 77
office@pontemed.com

HASOMED

RehaMove® Pro

Functional Electrical Stimulation

RehaMove Pro with ScienceMode offers advanced communication for higher scientific FES performance.
(Low-Level and Mid-Level stimulation / 2-channel EMG measurement / C-Library for simplified integration)
RehaMove Pro is available with a Science Adapter, which enables the usage of a demultiplexer for an electrode array with up to 61 elements. This option for DEMUX application has to be ordered initially as a system combination.

Science Adapter for DEMUX / ARRAY Support

RehaMove Pro + Science Adapter = DEMUX application

Performance:

· 4 stimulation channels · 2 EMG channels (1, 2 and 4 kHz) · frequency 1-500* Hz · pulse width 10 µs - 4 ms (1 µs steps)
· amplitude 0-130 mA (0,5 mA steps) · adjustable stimulation waveform (16 characteristic points)
· compatible for Demux/Array applications · MatLab/Simulink library
· pre-compiled library for several compiler (e.g. MSVC, GCC)

* full load on 4 channels

www.rehamove.com +49 391 6107-650

Official Journal of the Vienna FES Workshop:

Edited by:
Paul S. Malchesky, D. Eng.
http://www.wiley.com/bw/journal.asp?ref=0160-564X

Sponsors and Exhibitors (in alphabetic order):

Dr. Schuhfried
Medizintechnik GmbH
Van Swieten-Gasse 10
A-1090 Wien
Austria

Hasomed GmbH
Paul-Ecke-Str. 1
39114 Magdeburg
Germany

Inerventions AB
Ankdammsgatan 35
171 67 Solna
Sweden

MED-EL
Fürstenweg 77a
6020 Innsbruck
Austria

PonteMed GmbH Austria
Biberstraße 3
1010 Wien
Austria